Treatment of a multicomponent mining effluent using calcium hydroxide in a fluidized bed crystallizer

Chiara Maharaj, Jemitias Chivavava and Alison Lewis
Crystallisation and Precipitation Research Unit
Department of Chemical Engineering
University of Cape Town
Private Bag, Rondebosch, 7701
Cape Town
www.crystal.uct.ac.za

I know the meaning of plagiarism and declare that all the work in the document, save for that which is properly acknowledged, is my own.

Chiara Maharaj	Signed by candidate
Date	31 March 2016

Acknowledgements

To Prof. Alison Lewis, thank you for the opportunity, all the motivation, encouragement and guidance throughout this project. Most importantly, thank you for inspiring me to think outside the box and discover my strengths. You are an inspiration.

To Jemitias Chivavava, I cannot begin to describe the impact you have had on my development as a researcher and as a person. I will always be grateful for all you have done, your advice, encouragement and support. Thank you for always understanding and helping me to exceed my potential.

To Robert Gaertner, thank you for the opportunity, all your feedback and your involvement in this project, it is much appreciated.

To Lhoist, thank you for the financial support and supply of reagents. To Spyridon Karamoutsos and Chris Duplessis, thank you for your time and input.

To the crystallization and precipitation unit, Sarah Adam and Prof. Jochen Peterson, thank you for all the assistance, input, advice and contribution. It has made my time as a research student an enriching and enjoyable experience, thank you.

To Hayley, thank you for all your support and all that you have done. It is greatly appreciated.

"The arrival time of a space probe travelling to Saturn can be predicted more accurately than the behaviour of a fluidised bed chemical reactor"- Geldart

Abstract

Wastewater which primarily emanates from mining operations and manufacturing industries, has the potential for re-use if treated effectively. These wastewaters, which are typically characterized by high concentrations of dissolved inorganic salts are often disposed in evaporation ponds, which promotes the risk of ground water pollution and land wastage. Moreover, this forfeits the potential benefits of valuable salts recovered. The aim of this project was to investigate the treatment of multicomponent saline wastewater rich in sodium and magnesium sulphates, since these salts are prevalent in most wastewater streams. The intention was to treat the wastewater with a calcium hydroxide ($Ca(OH)_2$) suspension in a laboratory scale seeded fluidised bed crystallizer, thereby precipitating gypsum and magnesium hydroxide. The objectives of this study were to investigate how the chosen reactor configuration, feed stream and reagent characteristics affect the conversion and recovery of gypsum and magnesium hydroxide over a range of wastewater concentrations. Particular focus was on reducing the formation of fines through the use of seeds and to get an insight into the possible precipitation mechanisms. It was important that the resulting precipitate product quality favoured effective separation from the treated water stream for re-use.

Preliminary experiments were conducted over a feed concentration ranging from 1.5 g/L – 120 g/L (total sulphate salts) which was contacted with a stoichiometric amount of calcium hydroxide with respect to the sulphates in the the stream, that is a $Ca:SO_4$ ratio of 1:1 in the fluidised bed crystallizer. These experiments identified a feasible feed concentration range for operation (8 000 -35 000 mg/L). High inlet concentrations (≥ 50 000 mg/L) were not feasible due to rapid formation of a large mass of precipitates which disrupted fluidisation and caused the reactor contents to be elutriated. These high concentrations resulted in high rates of accumulation which necessitated the need for frequent intermittent product removal. The fluidised bed crystallizer using silica seeds was found to be effective at reducing the formation of gypsum and magnesium hydroxide fines by almost half. The study also found that feed concentrations of 35 g/L of total sulphate salts yielded better conversions (± 75%) of sulphates to gypsum, compared to a feed concentration of 8 g/L yielding a sulphate conversion of around 30%, due to the higher driving force and thus faster rate of crystallization. A $Ca:SO_4$ molar ratio of 1:1 did not yield equilibrium sulphate conversions, as a result of the incomplete dissolution of calcium hydroxide for the given residence time of the reactor and calcium hydroxide suspension PSD. However, it was possible to remove 99% of the magnesium in the wastewater stream under these conditions for each concentration investigated, since the Mg:OH molar ratio was effectively in excess. Excess calcium hydroxide (a $Ca:SO_4$ molar ratio greater than 1) improved the supply of calcium ions for reaction and thus sulphate conversions, and the equilibrium conversion of 88% was achieved at four times the amount of calcium to sulphates in the feed stream, based on the characteristic suspension used. Residual sulphate concentrations (2200 ppm at 15 g/L to 1400 ppm at 35 g/L), even after equilibrium conversions were achieved, did not meet the maximum sulphate discharge levels (200-600 ppm). A crude separation of magnesium hydroxide and gypsum could be initiated in the fluidised bed at 35 g/L. Gypsum crystals formed as needles and progressed to plates at higher feed concentrations. Magnesium hydroxide produced nano-agglomerates that were elutriated out of the bed or were imbedded in the product grain at higher concentrations. Overall the ratio of product, both magnesium hydroxide and gypsum, retained in the bed increased as the concentration increased.

An alternative treatment process was also explored to recover products in separate stages. The process involved two stages. The first step involved precipitation of magnesium hydroxide with caustic soda, since the stream is rich in magnesium sulphate. The next step treated the sodium sulphate generated in the first stage, by forming gypsum when dosed with a calcium hydroxide suspension. The second stage also regenerates caustic soda that could potentially offset reagent costs in the first stage. Thermodynamic modelling found that a 99% magnesium conversion was obtainable in the first stage. Only 18% sulphate conversion was attainable in the second stage, due to the electrostatic effects of sodium that shield sulphate ions which would otherwise react with calcium to form gypsum. This shielding effect resulted in a significant amount of sulphate ions in solution that are unable to react, resulting in low sulphate conversions. In addition, this hindered the consumption of calcium ions which drives the dissolution of calcium hydroxide, resulting in a large amount of undissolved calcium hydroxide as predicted by thermodynamic modelling. Another process alternative to explore is the use of cooling crystallization, which could potentially remove more sulphates than precipitation with calcium hydroxide can.

Contents

List of Tables

List of Figures

Nomenclature

a	Activity (mol/L)
A	Pre exponential factor (nuclei per m^3/s)
B	Nucleation rate (nuclei/cm^3.s)
c_i	Concentration of species i (kg/dm^3)
d	Particle diameter (m)
e	Bed voidage
g	Gravitational acceleration (m/s^2)
G	Gibbs free energy (J/mol)
Ga	Galileo Number
k	Rate constant (mol/kg H_2O.min)
K	Boltzman Constant (J/K)
k_d	Mass transfer coefficient by diffusion (m/s)
K_{sp}	Solubility product
k_r	Surface reaction rate constant (m/s)
l	Height of bed at rest (m)
m	Mass (kg)
n	Number of growth sites
p	Pressure (Pa)
r	Growth rate (mol.kg/H_2O.min)
R	Gas Constant (J/mol.K)
Re	Reynolds number
s	Crystal surface area (m^2)
S	Supersaturation ratio
T	Temperature (K)
u	Minimum fluidisation velocity (m/s)
v	Number of moles of ions in 1 mol of solute
V	Molar volume (m^3)
x, y	Stoichiometric coefficients
X	Conversion (%)

Greek symbols

β	Rate of collisions/ agglomeration (m^3/s)
γ	Activity coefficient
δ	Distance (m)
ζ	Chemical potential (J/mol)
η	Gypsum removal efficiency (%)
θ	Contact angel (°)
μ	Fluid viscosity (cP)
ρ	Density (kg/m^3)
ζ	Interfacial tension (J/m^2)
φ	Percentage of fines (%)
Ψ	Efficiency coefficient
ϕ	Wetting angle correction factor

1 Introduction

1.1 Background

Industrial operations such as mining, metal plating, smelting and pigment manufacturing produce wastewater rich in magnesium, calcium and sodium sulphates. Discharging these wastewaters without pre-treatment is detrimental to the environment and substantial investment has been made towards developing effective treatment methods. Figure 1.1 shows conventional methods used in the treatment of such wastewaters (Baysal et al. 2013).

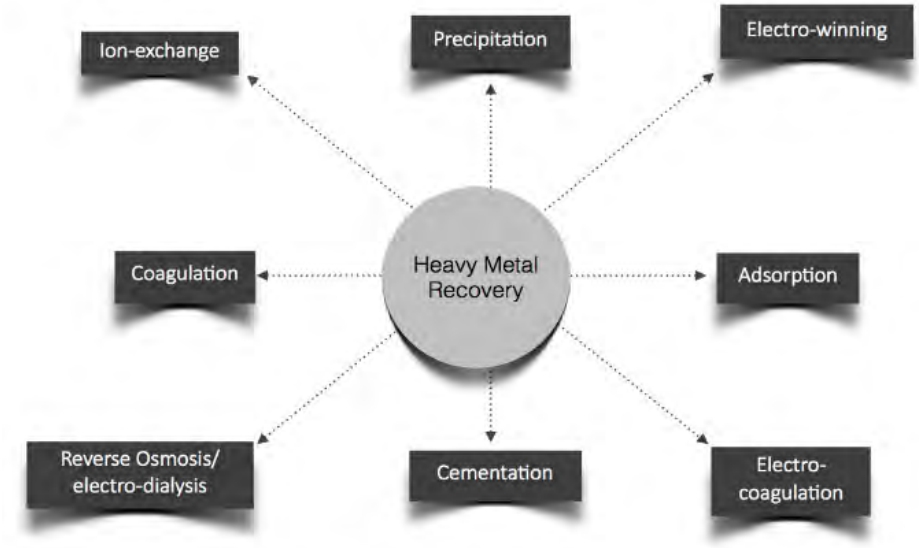

Figure 1.1: Heavy metal recovery technology (Adapted from: Baysal et al. 2013)

Chemical precipitation is the most common method of wastewater treatment because it is cost effective and can remove ions from relatively large volumes of water to ppm levels (Baysal et al. 2013). Precipitation, also termed reactive crystallisation, is the formation of a compound of low solubility, typically of the range 10^{-3} to 1 kg/m^3 (instead of 10-300 kg/m^3 in crystallisation) (Söhnel and Garside, 1992; Kind, 1999).

Alkaline addition via lime or caustic is the most common precipitation method for metal removal from wastewaters (van Hille et al., 2005). However, this results in the generation of large quantities of sludge with poor dewatering characteristics (Fajtl et al., 2002). Thus, separation of the precipitate from the residual stream is difficult, which increases handling and disposal costs (van Hille et al., 2005; Fajtl et al., 2002; Karidakis et al., 2005). Additionally, the presence of other components in solution leads to a mixed precipitate which limits its applicability for reuse. These disadvantages have led to further research into more efficient precipitation processes. A particular technological innovation is the use of seeded precipitation in a fluidised bed crystallizer.

Crystallization in fluidized bed reactors have been extensively used in industry for the softening of drinking water (Aldaco et al., 2007) as well as heavy metal, phosphate and fluoride removal from wastewaters (Seckler,1994). The use of fluidised bed crystallizers allows for controlled precipitation and has many advantages over conventional stirred tank crystallizers. Fluidised bed crystallizers use seeds to minimise the generation of fine particles by providing a large surface area for crystal growth or deposition and act as a site for crystal attachment. This avoids large volumes of sludge streams and facilitates the separation process (Guillard and Lewis, 2001; Heffels and Kind, 1999).

1.2 Problem statement

In the treatment of saline wastewaters, rich in sodium and magnesium sulphate (Karidakis et al., 2005), with calcium hydroxide, a mixed precipitate of magnesium hydroxide and gypsum is formed according to the reactions below, with each solid having different structural characteristics.

$$Mg^{2+}{}_{(aq)} + 2OH^{-}{}_{(aq)} = Mg(OH)_{2(s)} \qquad \text{Equation 1}$$

$$Ca^{2+}{}_{(aq)} + SO_4^{2-}{}_{(aq)} + 2H_2O_{(aq)} = CaSO_4.2H_2O_{(s)} \qquad \text{Equation 2}$$

It is desired to remove as much of the precipitating compound as is possible, while producing crystals that allow for efficient separation from the residual solution. At concentrations typically encountered in industrial wastewaters result in very small needle-like gypsum particles (Karidakis et al., 2005; Zhang et al., 2013) and and magnesium hydroxide forms agglomerates of nano-particles (Karidakis et al., 2005). Gravitational separation and filtration of these crystal structures is difficult. Fine particles remain suspended and recovery through gravitational separation is not possible. On the other hand, separation through filtration is difficult because fine particles induce filter fouling and create a high pressure drop across the filter. Furthermore, in multicomponent systems, where a mixed solid product is formed, it is advantageous to influence separation of the different solid products as well.

1.3 Scope

This project focused on investigating the treatment of saline wastewaters which are rich in sodium and magnesium sulphate, using calcium hydroxide ($Ca(OH)_2$) as a precipitating reagent, thereby precipitating gypsum and magnesium hydroxide. The first part of the project involved carrying out a modelling exercise to predict the aqueous chemistry of the system, followed by experimental work using a laboratory scale fluidised bed crystallizer. The calcium hydroxide reagent used and the relevant wastewater compositions have been provided by Lhoist. The obtained precipitate was characterised in terms of chemical composition, morphology and particle size distribution. The residual magnesium and sulphate content of the treated water, as well as the amount of fines elutriated was analysed to determine gypsum recovery, fines generation and removal efficiency.

The second part of this project involved investigating process alternatives. In this case, the aim was to avoid the formation of a mixed, unusable product since the use of calcium hydroxide in a single stage co-precipitated magnesium hydroxide and gypsum. The focus was to investigate options that recovered the products separately. Aqueous chemistry modelling was conducted, followed by a preliminary cost estimate of the process.

2 Theory

2.1 Precipitation Theory

Precipitation is extensively used in hydrometallurgical processes for solution purification, product recovery and effluent treatment (Al-Othman, 2004). Precipitation is the formation of a sparingly soluble solid compound from a supersaturated solution. It is a sub-class of crystallization in which the driving force for solid formation is induced by a chemical reaction between precursor reagents (Giulietti et al., 2001).

2.1.1 Supersaturation

When the concentration of a solute exceeds its solubility concentration, the solution becomes supersaturated with respect to that compound. Supersaturation is the driving force of crystallization and can be induced in a number of ways. These include solvent removal, heating or cooling a solution beyond its saturation point, introduction of a miscible reactant and formation of a sparingly soluble compound through a chemical reaction (Mullin, 2001). For the purpose of this study, reaction crystallization resulting in the formation of a product of low solubility is considered.

Supersaturation is necessary for precipitation and it is the main factor that influences nucleation and crystal growth. Figure 2.1 shows the correlation between supersaturation and the phenomena of precipitation.

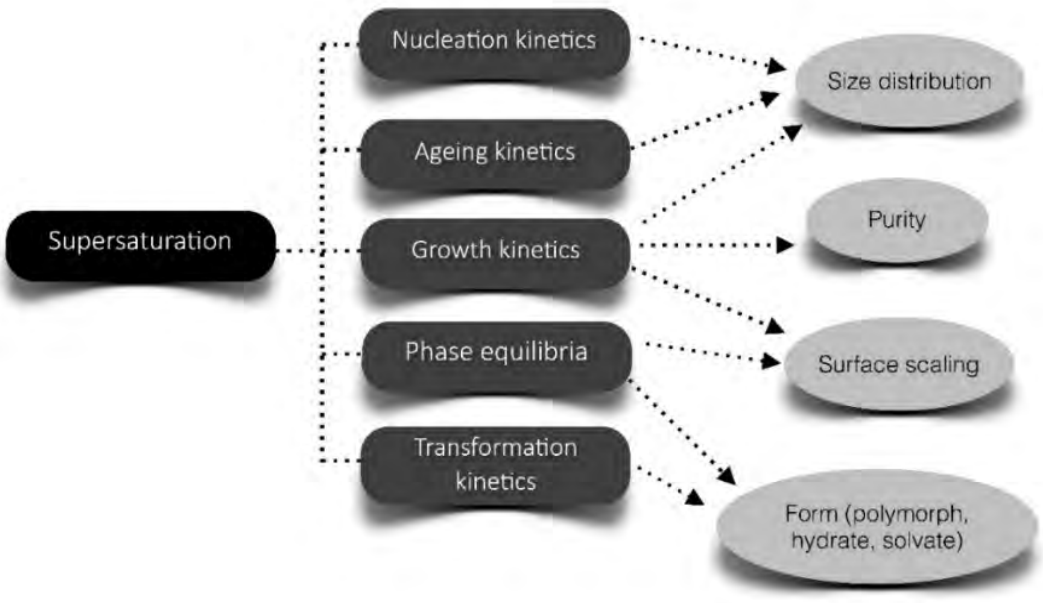

Figure 2.1: Influence of supersaturation on the precipitation process (Söhnel and Garside, 1992)

Precipitation is directly driven by the difference in the chemical potential between the molecule in solution and that in the solid phase defined by equation 3 below (Söhnel and Garside, 1992):

$$\Delta\xi = RTln\left(\frac{a}{a_{eq}}\right) = RTln\left(\frac{\gamma c}{\gamma c_{eq}^{*}}\right) \qquad \text{Equation 3}$$

Where: $a = \gamma . \mathrm{C}$

a= Activity (mol/L)

R= Gas Constant (J/mol.K)

T= Temperature (K)

$\Delta\xi$ *= Difference in chemical potential (J/mol)*

γ*= Activity coefficient*

However, the absolute driving force is difficult to measure and is usually expressed in terms of the supersaturation ratio (S) which is defined according to equation 4 (Söhnel and Garside, 1992):

$$\mathrm{S} = \frac{\prod_i a_i^{vi}}{K_{sp}} \qquad \text{Equation 4}$$

Where: $v = \sum_i v_i$

v *= number of moles of ions in 1 mol of solute*

K_{sp} *= Solubility product*

For aqueous solutions of sparingly soluble salts, the supersaturation ratio is expressed as shown in Equation 6 (Mullin, 2001).

$$A_xB_y = xA^{y+} + yB^{x-} \qquad \text{Equation 5}$$

$$S = \frac{IAP^{\left(\frac{1}{v}\right)}}{K_{sp}} \qquad \text{Equation 6}$$

Where: $K_{sp} = (C_{Aeq+}\gamma_+)^x\ (C_{Beq-}\gamma_-)^y$

IAP = Ion Activity Product (mol/L)

x, y = Stoichiometric coefficients

γ^+, γ^-*= activity coefficient of cation and anion, respectively*

2.2 Solubility

The solubility of a substance in a solvent is the maximum amount that can be dissolved at a given set of conditions (Mullin, 2001). The term solubility thus indicates the extent to which different substances can be recovered from a solvent, in other words, the less soluble a compound, the more of it can be recovered. For a substance to dissolve in a liquid, it must be capable of disrupting the solute structure and permit solvation by the solvent molecules. The forces binding the ions, atoms or molecules in the lattice oppose the tendency of a crystalline solid to enter solution. The solubility of a solid is thus determined by the resultant of these opposing effects (Mullin, 2001).

Solubility of metal ion salts is influenced by pH, temperature and the presence of other species in solution. Figure 2.2 shows metal solubility as a function of pH.

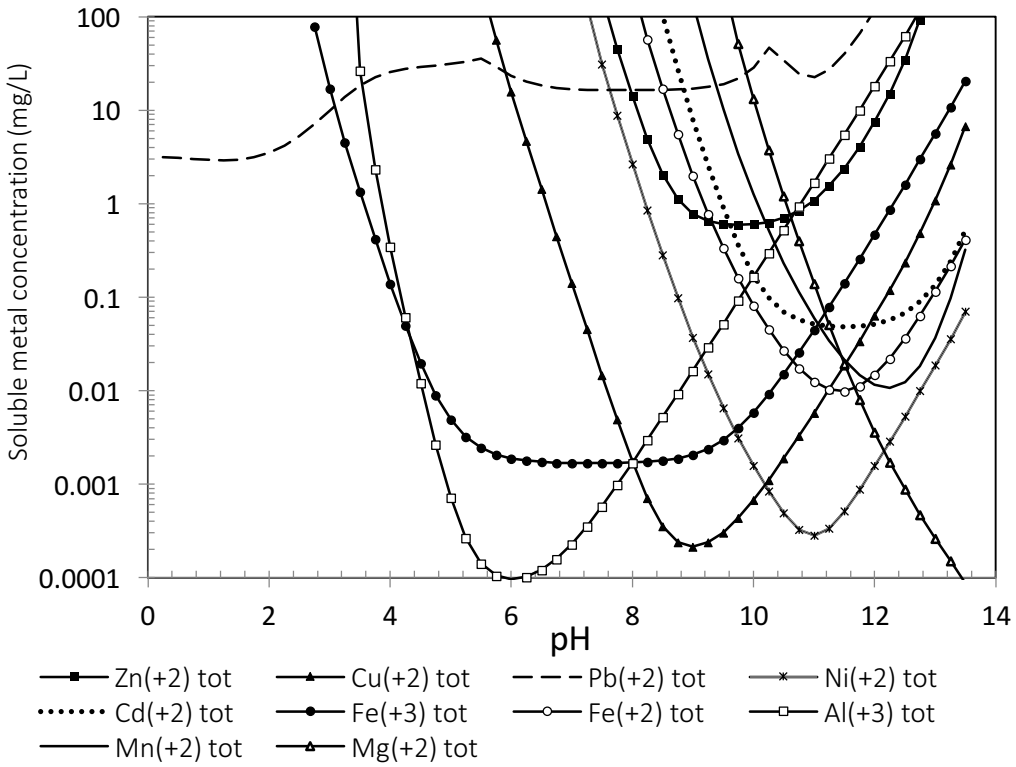

Figure 2.2: Metal ion solubility as a function of pH (Lewis, 2010)

Solubility, curves such as that shown in Figure 2.2, can be conveniently generated using thermodynamic simulation packages such as OLI Stream Analyser™ (OLI Manual, 2015). Thermodynamic packages account for the reactivity of solids for various modifications of a particular compound and accounts for species that influence the solubility equilibrium when defining the K_{sp} (Theonen, 1999). Solubility information obtained from thermodynamic modelling predicts the formation of the solubility limiting solid, that is the first solid to precipitate, under the appropriate composition, temperature and pressure.

Solubility determines the maximum yield of the precipitating solid at the specified conditions. Thus, it is an indication of the minimum residual ion concentration, below which further recovery using precipitation becomes thermodynamically unfeasible.

2.3 Nucleation

Crystallization and precipitation phenomena can be categorised into two stages, namely, nucleation and crystal growth. The first step, nucleation, involves the formation of the first embryonic clusters which subsequently grow to produce crystals. This occurs when ions or molecules in a supersaturated solution aggregate and cluster until a crystal of a critical radius has been formed, after which the crystal either continues to increase in size, or re-dissolves (Jones, 2002).

Nucleation controls the number of crystals and their size (Mersmann, 2001). It is broadly divided into primary and secondary nucleation. These are further sub-divided into several specific classes according to mechanisms through which nucleation occurs within each category summarised in Figure 2.3.

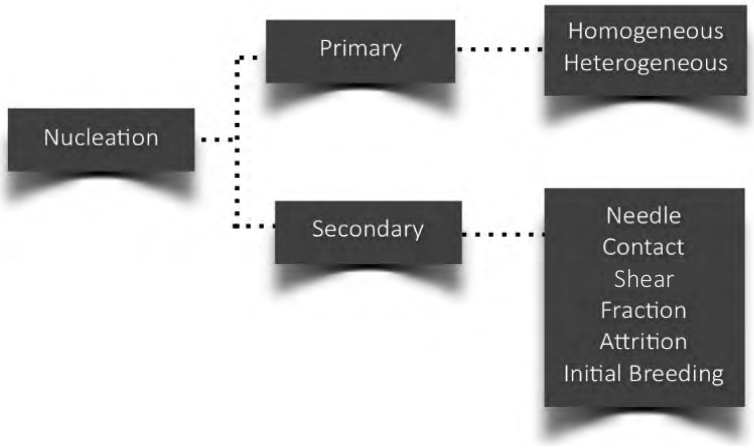

Figure 2.3: Nucleation principle (Randolph and Larson, 1988)

2.3.1 Primary nucleation

Primary nucleation is the formation of a new phase from a solution in the absence of the precipitating solid. The kinetics of primary nucleation are highly non-linear and are found to be very slow at low supersaturation (Mersmann, 2001). Very high levels of supersaturation can be achieved when mixing reactants and this results in high rates of primary nucleation.

Primary nucleation can be further classified as either homogeneous or heterogeneous. Homogeneous nucleation is the formation of stable nuclei in a supersaturated solution in the absence of any solid, which is described by equation 7 (Mullin, 2001):

$$B^0_{hom} = A_{hom} \exp\left[-\frac{16\pi\zeta^3 v^2}{3k^3T^3(\ln S)^2}\right] \qquad \text{Equation 7}$$

Where: ζ = interfacial tension (J/m^2)
A = pre exponential factor (nuclei per m^3/s)
v = molar volume (m^3)
k = Boltzman Constant (J/K)
T = temperature (K)
S = degree of supersaturation

Homogeneous nucleation does not occur in the metastable zone, which is the region bounded by the solute solubility and the metastable limit. The metastable limit is the maximum supersaturation of the precipitating component, beyond which, spontaneous nucleation occurs.

Heterogeneous nucleation on the other hand, is initiated by the presence of foreign particles suspended in the solution, that is, dust particles or reactor walls. Heterogeneous nucleation is described by equation 8, a relationship similar to homogeneous nucleation, with factor $f(\phi)$ correcting for the decreased nucleation energy barrier in the presence of a foreign solid.

$$B_{het}^{0} = A_{het}\exp\left[-\frac{16\pi\zeta^{3}v^{2}f(\phi)}{3k^{3}T^{3}(\ln S)^{2}}\right] \qquad \text{Equation 8}$$

An important parameter in heterogeneous nucleation is the wetting angle of the substrate surface θ in Figure 2.4. It is the angle between the tangent to the nucleus interface and the substrate surface. The wetting angle indicates whether or not the presence of the substrate will lower the nucleation barrier and to what extent (Mullin, 2001).

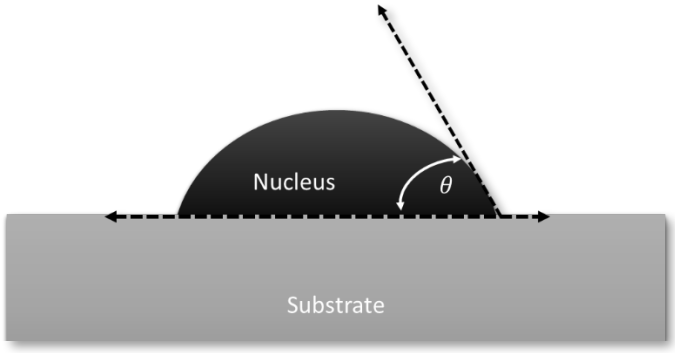

Figure 2.4 Nucleation on a foreign substrate (adapted from Peterson, 2002).

The critical Gibbs free energy relationship between homogeneous and heterogeneous nucleation is shown in Equation 9 below:

$$\Delta G^{*}_{Het} = \phi \Delta G^{*}_{Hom} \qquad \text{Equation 9}$$

The relationship between θ and ϕ is presented in Equation 10 (Mullin, 2001):

$$\phi = \frac{(2 + cos\theta)(1 - cos\theta)^{2}}{4} \qquad \text{Equation 10}$$

In the case where there is complete incompatibility of the crystalline solid and the seeding material, that is, complete non-wetting, f(ϕ) = 1 and the energy required for nucleation is equal to that of homogeneous nucleation. When there is complete affinity or complete wetting, f(ϕ) = 0 and $\Delta G^{*} = 0$. When there is partial wetting, then 0 < f(ϕ) < 1 and the energy required for heterogeneous nucleation is lower than for homogeneous nucleation (Mullin, 2001).

2.3.2 Secondary nucleation

Secondary nucleation is the formation of nuclei induced by pre-existing units of the precipitating solid. It occurs at much lower levels of supersaturation compared to primary nucleation. Secondary nucleation can be further sub-categorised, as shown in Figure 2.3, with the most common type being attrition breeding in stirred tank crystallizers (Lewis et al., 2015). Attrition results from particle-particle collisions, particle-reactor and or particle-impeller collisions.

It is possible for different nucleation mechanisms to dominate in different regions within the reactor. This is usually caused by inhomogeneity in the level of supersaturation within the reactor volume. Thus, the scale of mixing in the reactor influences the precipitation phenomena and ultimately product characteristics. The scale of mixing is the average distance between centres of maximal difference in properties (Uhl, 1966) and is categorised as being macro, micro or meso-mixing. Macro-mixing takes place at a scale equivalent to the size of the reactor, meso-mixing at the scale equivalent to size of the reactant feed pipe and micro-mixing at the Kolmogorov scale, which is the size of the smallest eddy in the fluid (Torbacke and Rasmuson, 2001). All three mixing scales have an effect on precipitation characteristics through the degree of supersaturation resulting from mixing effects. Figure 2.5 shows the effect of mixing two species (A and B) on precipitation phenomena. Each numbered zone indicates a supersaturation level and its corresponding precipitation phenomena. Apart from different crystal size distributions, various crystal modifications can take place depending on the level of supersaturation.

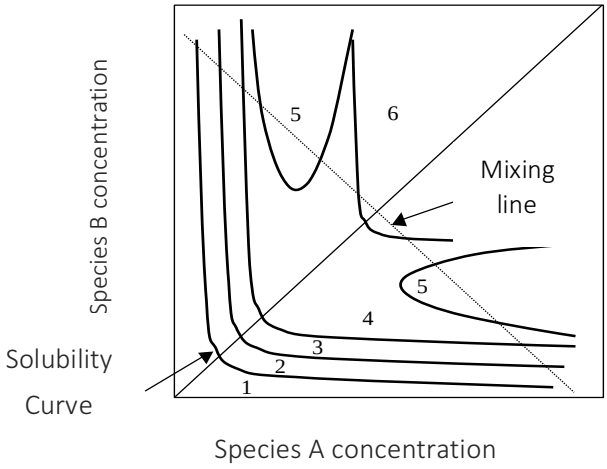

Zone	Precipitation phenomena
1	Undersaturated
2	Secondary nucleation
3	Heterogeneous nucleation
4	Homogeneous nucleation
5	Colloidal precipitation
6	Gel formation

Figure 2.5: Mixing and precipitation zones (Nielsen, 1979)

Zone 1 represents an undersaturated region within the reactor where precipitation is not possible. High rates of primary homogeneous nucleation are dominant at reagent inlet points where the local supersaturation is high. Figure 2.5 also illustrates the mixing effect on the supersaturation profile of a solution of two equi-molar solutions or reactants. The "mixing line" represents the supersaturation values that can be obtained upon mixing, where the prevailing supersaturation zone is determined by the nature of mixing. It is difficult for perfect mixing of reagents to be present throughout the reactor. Zone 2 represents a region in which

secondary nucleation is favoured, and zone 3 represents the region in which heterogeneous nucleation is favoured. Zone 4 is the region in which spontaneous nucleation is observed, while zones 5 and 6, being at very high supersaturation, favour the formation of colloids and gels; products with poor dewatering characteristics.

2.4 Induction time

In some cases, a period of time lapses between the attainment of supersaturation and the appearance of crystals or nuclei (Mullin, 2001). This is known as the induction period, and is made up of several lag stages. The first stage is the relaxation time, which allows for the quasi-steady state distribution of molecular clusters. The stage that follows accounts for the lag time required for the formation of a nucleus, and finally the last stage accounts for the nucleus to grow to a detectable size. The induction period is influenced by the level of supersaturation, viscosity of the system, mixing and presence of impurities (Mullin, 2001). The presence of seeds generally decreases the induction period, however it may not necessarily completely eliminate it (Mullin, 2001).

2.5 Growth

After nucleation, precipitation proceeds via crystal growth, which involves the addition and organisation of molecules or ions onto the space lattice of the crystal surface in a supersaturated solution (Jones, 2002). This results in the overall increase in crystal size and mass of the precipitating solid.

2.5.1 Crystal Growth Kinetics

The growth rate is expressed as the rate of displacement or the mass flux of crystallising material of a particular crystal face in a direction perpendicular to its surface (Söhnel and Garside, 1992). The rate of crystal growth determines the shape, structure and purity of the precipitate (Mullin, 2001). Growth is usually modelled as a two stage process comprising of a diffusion step and surface integration step (Randolph and Larson, 1988).

2.5.2 Diffusion-Reaction Model

The diffusion- reaction model describes crystal growth as a series of diffusion and reaction steps shown in Equation 10 and Equation 11 (Mullin, 2001). Crystallization is considered to be the reverse of dissolution and both rates are influenced by the concentration gradient between the interface and bulk solution.

$$\frac{dm}{dt} = k_d s(c_b - c_i) \qquad \text{(Diffusion)} \qquad \text{Equation 11}$$

$$\frac{dm}{dt} = k_r s(c_i - c^*) \qquad \text{(Reaction)} \qquad \text{Equation 12}$$

Where: *m= mass of deposited solid (kg)*

s= crystal surface area (m^2)

c_b=solute concentration in supersaturated solution (kg/dm^3)

c= equilibrium saturation concentration (kg/dm^3)*

c_i= concentration of solute at the solution-crystal interface (kg/dm^3)

k_d= mass transfer coefficient by diffusion (m/s)

k_r = surface reaction rate constant (m/s)

Figure 2.6 illustrates both diffusion and surface reaction driving forces. It should be noted that the forces are by no means equal and the concentration drop across the stagnant film is not necessarily linear (Mullin, 2001).

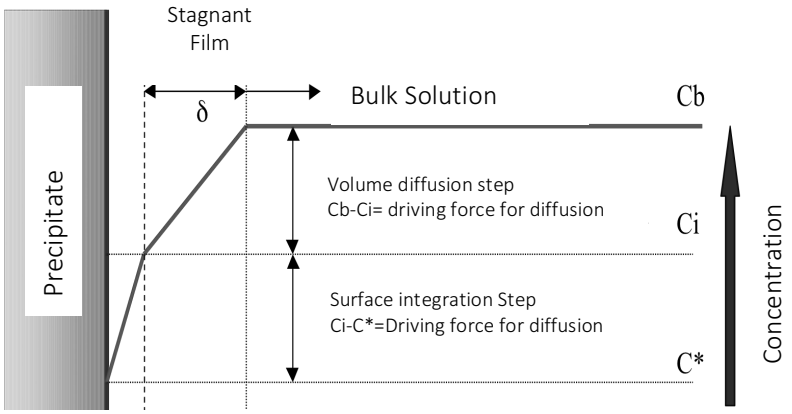

Figure 2.6: Concentration profile perpendicular to crystal surface during growth (adapted from Mullin, 2001)

2.5.3 Adsorption Layer Theory

The adsorption layer theory is based on thermodynamic reasoning and follows the process of a growth unit adsorbing on to the crystal surface. The units of the crystallizing substance are not immediately integrated into the lattice, but migrate over the surface acting as a loosely adsorbed layer of integrating units. Molecules, atoms or ions will incorporate into the lattice at points on the crystal surface at active centres, that is, where attractive forces are the highest (Mullin, 2001). Under ideal conditions, this build up continues until the whole surface plane is covered. The process then repeats itself when a new 'crystallization centre' comes into existence (Mullin, 2001). The process is illustrated by Figure 2.7.

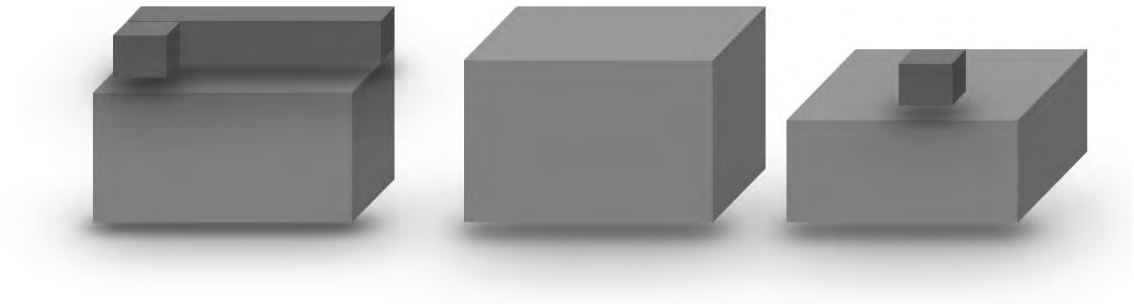

Figure 2.7: Crystal growth model a) migration towards desired location; b) completed layer; c) surface nucleation (Mullin, 2001)

The growing crystal surface can be described by the Kossel model (Mullin, 2001) depicted in Figure 2.8. The model assumes that a crystal surface is made up of moving layers of monatomic height which contain one or

more kinks, loosely adsorbed growth units, vacancies and steps. Growth units attach onto the crystal at a kink, after which the kink moves along the step which eventually completes the face. New steps are initiated by surface nucleation at surface corners.

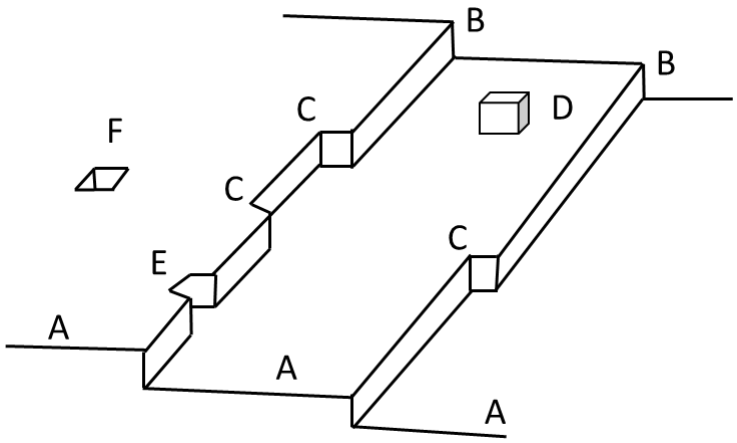

Figure 2.8 Kossel's model of a growing crystal surface A) flat surfaces, B) step, C) kinks, D) surface adsorbed growth units, E) edge vacancies and F) surface vacancies. (Mullin, 2001).

The nature of the growing crystal surface is influenced by several factors mentioned above, but the driving force or supersaturation is of particular significance. The driving force is responsible for the dominant growth mechanism, presented in Figure 2.9.

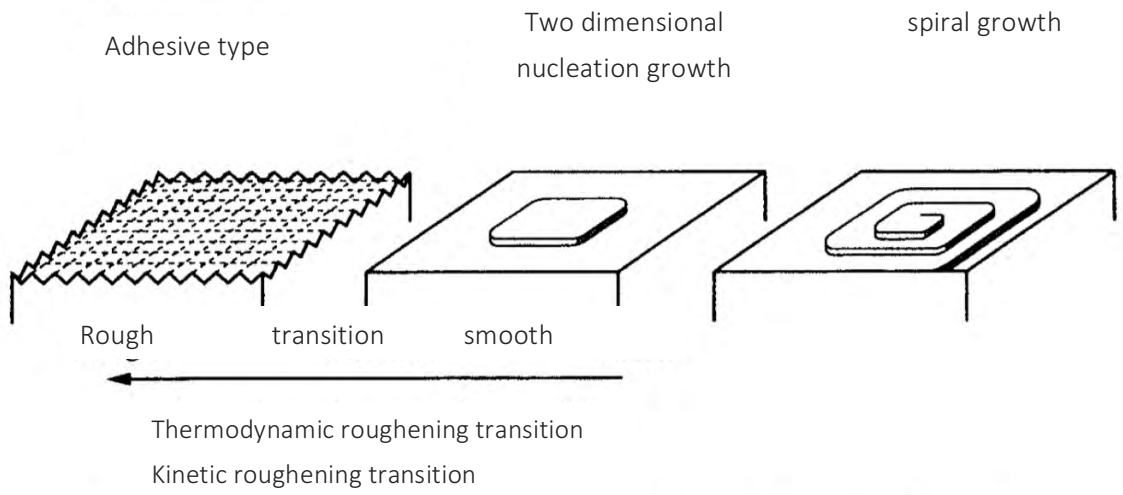

Figure 2.9: Effect of driving force on crystal growth mechanisms (Sunagawa, 2005).

At low levels of driving force, the growth mechanism tends to be smooth, while at higher levels of supersaturation, rough growth mechanisms dominate.

Smooth growth of crystal faces occurs when successive growth layers are orderly deposited on the crystal (Lewis et al., 2015). In order for growth to occur under these conditions of low supersaturation, a permanent step source is required, such as a screw dislocation or a screw component present on the crystal surface. The step becomes a preferred growth site, and growth units curve around the defect, eventually forming a spiral hill with the defect still present (Mullin, 2001 and Lewis et al., 2015). Such a mechanism is known as the spiral growth model. Intermediate levels of supersaturation induce what is termed two-dimensional nucleation or the birth and spread model (Sunagawa, 2005; Lewis et al., 2015). In this case, the step source as discussed above, is in fact the formation of two-dimensional nuclei on the crystal surface, which grows into islands by spreading across the crystal surface. This mechanism requires sufficient supersaturation to overcome the critical size barrier of the two dimensional nuclei (Lewis et al., 2015). High levels of supersaturation induce rough growth on crystal surfaces. The absence of preferential growth sites on the crystal surface forces the growth rate to depend simply on the flux of growth units from the bulk onto the growth position (Lewis et al., 2015).

2.6 Morphology

The external appearance of a crystal, also known as the morphology, shape or habit, is determined by both internal, that is, the crystal structure and external factors such as the crystal growth conditions and processes (Sunagawa, 2005). Another way of understanding morphological influences is to consider thermodynamic and kinetic factors such as (Lewis et al., 2015):

- The periodic structure of the crystal lattice imposed by the bonding energies between atoms, ions and molecules that make up the lattice (thermodynamic)
- The conditions under which the crystal is grown (kinetic)

It is possible to predict the morphology of a known crystal; however, this is only practically valid if thermodynamics prevail over kinetics. In other words, if the growth kinetics are relatively slow (Lewis et al., 2015). The study on crystal morphology is of particular interest in industry due to its influence on product handling and downstream processing. Crystal habit will affect the rheological properties, filtration and centrifugation efficiency and the bulk density of the solid (Mersmann, 2001).

The type of reactor, hydrodynamics and temperature are some of the factors that influence morphology (Jones, 2001 and Sunagawa, 2005). For the purpose of this study, temperature and pressure effects are will not be investigated. However, flow patterns within the reactor influence primary particle morphology by influencing supersaturation levels at certain crystal faces as discussed below.

2.6.1 Supersaturation on the growing faces

While supersaturation affects the growth rate of crystal surfaces, its effect on each face of the same crystal may not be the same. In the case of a polyhedral crystal bounded by corners, edges and faces, the concentration difference at the corner is expected to be larger than at the edges and, to a larger extent, at

the faces. This state of varying concentration creates surface diffusion and thus different growth rates on a single crystal depending on the bulk supersaturation (Sunagawa, 2005).

2.6.2 Solvents, additives and impurities

The presence of additives or impurities may have a significant effect on the crystal structure. Strong surface interactions on a crystal surface will either retard or accelerate the growth rate, however, if the interaction is strong on a particular face and non-existent on other faces, the shape of the crystal will be altered (Jones, 2002; Mersmann, 2001 and Lewis et al., 2015) as illustrated in Figure 2.10. Foreign species may also alter the growth of crystals by adsorbing along the steps of growth layers on the crystal face (Sunagawa, 2005). It should be noted that some impurities may in fact promote the growth of a particular face (Sunagawa, 2005).

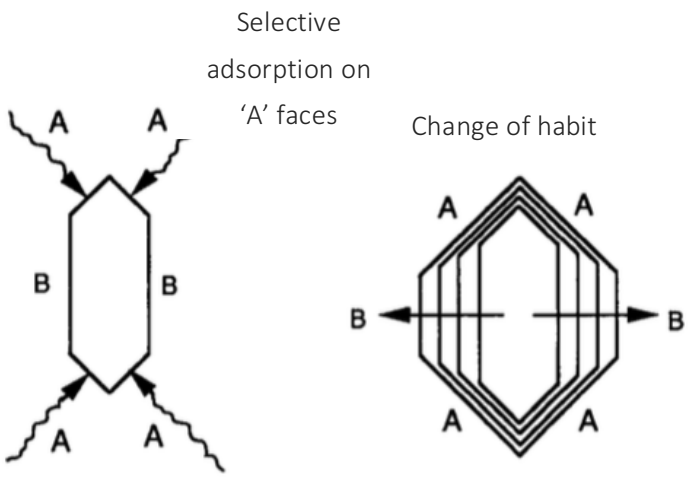

Figure 2.10: Effect of impurities on crystal growth habit. (Sunagawa, 2005)

2.7 Agglomeration

Agglomeration occurs when particles collide, adhere and eventually cement together to form agglomerates (Söhnel and Garside, 1992). This phenomenon occurs in most precipitation processes and has a significant impact on precipitate properties. Agglomeration and crystal growth occur simultaneously and the former is responsible for rapid particle size enlargement. Like crystal growth, agglomeration is also strongly influenced by supersaturation and solution composition, with agglomeration being favoured at certain levels of supersaturation. The process leading to agglomeration is illustrated in Figure 2.11.

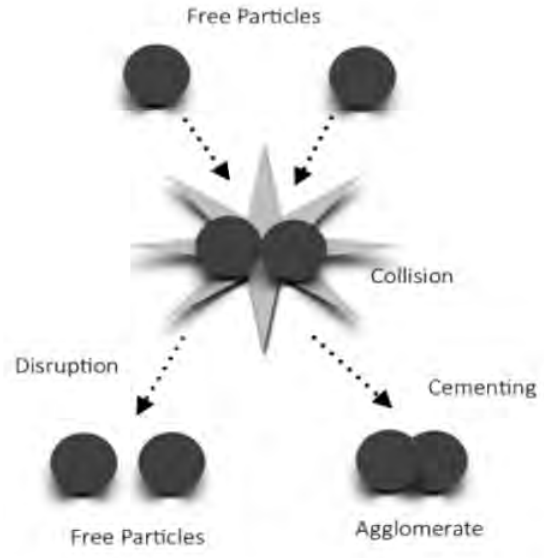

Figure 2.11: Mechanism of agglomeration (Guillard, 2001).

Particles that have collided are then joined or cemented together by the formation of solid inter-particle bridges. The rate of cementing is related to the growth rate of the precipitate (van Hille et al., 2005).

The overall rate of agglomeration is a combination of the collision and cementing rate, and the breakage rate. This is often summarised as shown in Equation 13.

$$\beta_{agg} = \psi\beta_{coll} \qquad \text{Equation 13}$$

Where: Ψ= *efficiency coefficient*

β= *rate of collisions/ agglomeration* (m^3/s)

2.8 Fluidisation

Fluidisation is the process whereby a granular material is converted from a static solid state to a dynamic fluid-like state when a fluid is passed through the granular material (Coulson and Richardson, 1991). The granular bed remains fixed at velocities below the incipient velocity (point A, Figure 2.12), that is, the velocity at which the drag force exerted by the flowing fluid is equal to the apparent weight of the particles (Coulson and Richardson, 1991). At this point, the bed begins to expand and exhibit fluid-like properties, with increasing bed voidage. As the fluid flows in the upward direction, it experiences an increase in pressure loss due to the frictional resistances of the bed, as shown in Figure 2.12 (Rhodes, 1998).

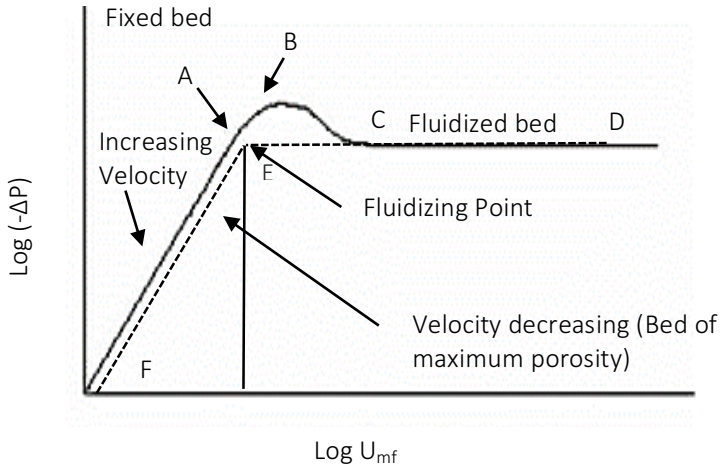

Figure 2.12 : Pressure drop in a fluidised bed reactor as a function of velocity (Coulson and Richardson, 1991)

Figure 2.12 shows the linear relationship between the pressure drop and velocity at zero flow until point A. Upon increasing the velocity, the bed expands and the pressure drop reaches a maximum at point B. The straight line CD indicates a stabilization of the pressure drop which is independent of the velocity. Reducing the velocity causes the bed to contract to point E, the maximum stable voidage of a fixed bed where particles are just resting on one another (Coulson and Richardson, 1991). Further decreasing the fluid velocity until point F results in a lower pressure drop across the bed compared to initial conditions, that is, from rest to point A.

The total pressure drop across the packed bed can be calculated using Equation 14 (Coulson and Richardson, 1991):

$$\Delta p = (1 - e)(\rho_s - \rho)lg \qquad \text{Equation 14}$$

Where: Δp= *pressure drop across bed (Pa)*

e *= bed voidage*

ρ_s*= solid density (kg/m^3)*

ρ*= fluid density (kg/m^3)*

g*= gravitational acceleration (m/s^2)*

l*= height of bed at rest (m)*

Upon increasing the velocity, the point of incipient fluidisation is reached where the particles are just suspended by the fluid. The corresponding velocity at this incipient point is known as the minimum fluidization velocity and can be calculated using the equations below (Coulson and Richardson, 1991):

$$\frac{\rho d^3(\rho_s-\rho)g}{\mu^2} = 150\frac{(1-e_{mf})}{e_{mf}^3}\frac{u_{mf}d\rho}{\mu} + \frac{1.75}{e_{mf}^3}\left(\frac{u_{mf}d\rho}{\mu}\right)^2$$ Equation 15

Substituting the Reynolds number and Galileo at incipient velocity:

$$Ga = 150\frac{(1-e_{mf})}{e_{mf}^3}Re'_{mf} + \frac{1.75}{e_{mf}^3}Re'^2_{mf}$$ Equation 16

$$\mathrm{Ga} = \frac{\rho \mathrm{d}^3(\rho_\mathrm{s}-\rho)\mathrm{g}}{\mu^2}$$ Equation 17

$$\mathrm{Re}'_{\mathrm{mf}} = \frac{\mathrm{u_{mf}}\mathrm{d}\rho}{\mu}$$ Equation 18

Where: u_{mf} *= minimum fluidisation velocity (m/s)*

e_{mf} *= bed voidage*

d *= particle diameter (m)*

μ *= fluid viscosity (cP*)

Practically, the bed voidage at the point of incipient fluidisation is not known, but is estimated to be 0.4. The maximum fluidisation velocity, that is, the point at which the particles are swept out of the reactor is determined from equation 19:

$$u_{max} = \frac{d^2 g}{18\mu}(\rho_s - \rho)$$ Equation 19

Fluidised bed crystallizers are typically modelled as plug flow reactors (Wojcik, 1999). Physical phenomena are accurately described by the axial dispersion model (Toyokura *et al.,* 1973 and Wojcik, 1999).

3 Literature review

This section of the dissertation reviews previous and current developments in the application of fluidised beds in precipitation, followed by a survey of literature and ideas developed. The problem statement is then presented, followed by the aim, objectives, hypotheses and key questions.

3.1 Introduction

Treatment of saline wastewater using precipitation methods is well established and widely implemented across industry (van Hille et al., 2005). Some of these precipitation methods employ calcium hydroxide as a source of hydroxyl and calcium ions, hence as a precipitation reagent. Examples of such processes include the precipitation of magnesium hydroxide from wastewater using calcium hydroxide (Karidakis et al., 2005) and reactive crystallization of calcium sulphate dihydrate (gypsum) from acid wastewater and lime (Zhang et al., 2013). The added calcium ions react with sulphate ions, which are commonly present in wastewater streams, to produce a gypsum precipitate. It is important that the characteristics of the resulting precipitates are such that the solids can be removed from the residual water stream, either for re-use in mining processes or other applications. It has been found that gypsum forms very small particles during precipitation, (Karidakis et al., 2005) which are difficult to separate from the treated liquid through gravitational separation or filtration.

Fluidised bed crystallizers have been identified as an effective reactor configuration for products that are difficult to separate from the residual stream (Guillard and Lewis, 2001), like gypsum. This allows concentration and separation of dissolved components in the form of reusable crystals. Fluidised bed crystallizers have been extensively used in the water treatment industry with applications in the softening of potable water (Aldaco et al., 2007) and in the removal of heavy metals, phosphates, as well as fluorides from wastewater (Seckler, 1994). Aqueous waste streams generated from acid mine drainage, electroplating and base metal refining operations, with dissolved metal concentrations varying from 10 to 10 000 ppm, have been successfully treated using precipitation in fluidised bed crystallizers (Wilms, 1988; Zhou, 1999).

3.2 Fluidised bed crystallizers

Fluidised bed crystallizers provide ideal conditions for controlled precipitation as discussed in this section, and as a result present many advantages over other reactor configurations. Figure 3.1 illustrates the working principle of the fluidised bed crystallizer.

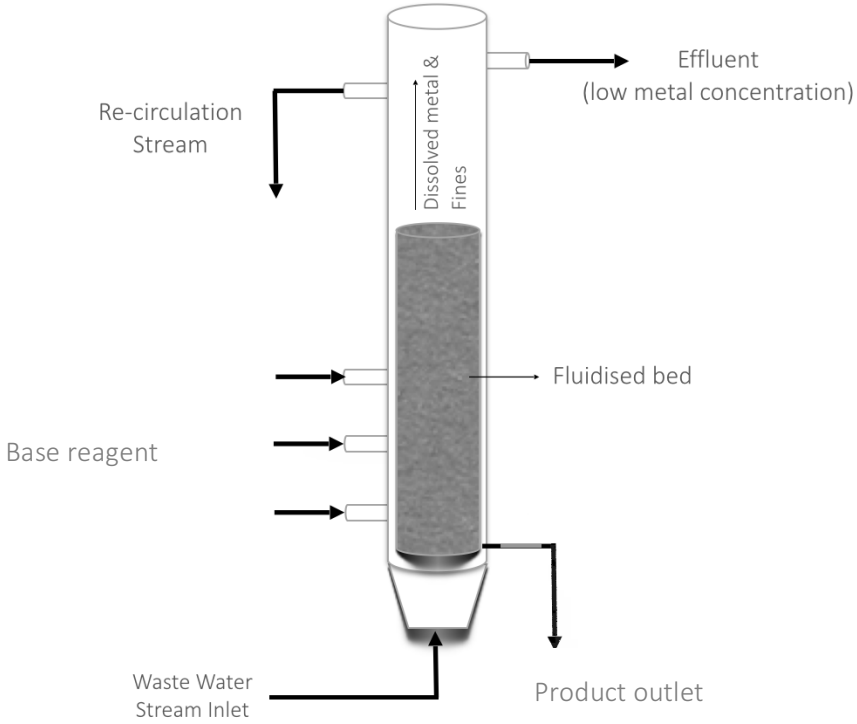

Figure 3.1: Schematic of a fluidised bed crystalliser (adapted from Seckler, 1994)

Before operation, the reactor is charged with a batch of pre-characterised seeds, which is subsequently fluidised by the saline stream that enters the reactor from the bottom. The alkaline reagent, in this case calcium hydroxide, is fed through an inlet port situated on the side of the reactor. As precipitate is deposited on the seeding material, the particle size distribution along the height of the column changes. Larger, denser particles migrate to the bottom of the reactor where they are removed as a product, while the lighter particles remain suspended higher up in the bed and fines being elutriated. In continuous processes, new seeding material is introduced at the top of the reactor, while large particles are removed at the bottom to maintain a constant bed height (Guillard and Lewis, 2001; van Hille, 2005). The remaining mother liquor exits the top of the reactor. In some cases, the effluent stream is recirculated to increase conversion of unreacted ions in excess of equilibrium concentrations or to lower the supersaturation in the reactor. Key parameters of operation are the reactant feed rates, recirculation rate, initial height of the bed at zero flow and size and type of seeds.

An advantage of using fluidised bed crystallizers is that it allows for good mixing of reactants on both the macro and meso-scale, so that local supersaturation levels can be controlled (Guillard, 2001). Fluidised beds also give rise to conditions of good mass transfer (Geldart, 1973). Fluidized beds are optimized for crystal growth by providing low shear, low energy and minimum impact between crystals (Nienow et al., 1997). Further to this, the reactor allows for more seeds to be used per unit volume compared to stirred tanks, while maintaining good mixing. The reactor configuration also eliminates crystal-impeller collisions experienced in a stirred tank reactor, which result in attrition and therefore fines generation. However, crystal-crystal and crystal-wall collisions are inherent to this system and may become significant in the dense solid environment.

Fluidised bed crystallizers allow for gravitational separation of products from the treated water, as large crystals migrate to the bottom of the bed where they are harvested, as mentioned in studies by Guillard and Lewis (2001), Al-Othman (2004) and van Hille (2005). However, this is not limited to fluidised bed crystallizers only and is also evident in reactor configurations where solids are suspended until they reach a certain size and subsequently migrate to the bottom of the reactor. Another separation feature of fluidised bed crystallizers is its ability to classify crystals according to size, where the upward flow of the fluidising stream elutriates very small particles. This particle size depends on the velocity of the upward flowing stream. These small particles would otherwise be classified as a product in an MSMPR. This separation feature may be advantageous when product quality is very important. Fines generated during precipitation, which would otherwise exit the reactor, can be recycled and allowed to agglomerate, thus forming larger particles which can be recovered to increase the solid-liquid separation efficiency (Guillard and Lewis, 2001; Heffels and Kind, 1999). While this can be implemented in many other reactor configurations, fluidised bed crystallizers allow for recycle streams to enter in specific locations along the reactor, for example, in regions of supersaturation along the bed that promote agglomeration. The recycle stream will not be explored in this study.

Another advantage of fluidised bed crystallizers presented in literature is the ability to control supersaturation through the use of multiple reagent inlet ports (Guillard and Lewis, 2001). However, this is not characteristic of fluidised bed crystallizers only, and may be implemented in other reactor configurations as well.

3.2.1 Supersaturation control in fluidised bed crystallizers

The control of supersaturation is one of the most important aspects in precipitation processes, however, it is very difficult to obtain uniform supersaturation in any reactor. High local supersaturation zones lead to spontaneous primary nucleation (Seckler, 1994; Guillard and Lewis, 2001; van Hille, 2005) that form unfavourable fine particles which are lost with the effluent stream. The supersaturation profile in a fluidised bed crystallizer in particular, forms a gradient with a high degree of supersaturation closer to reagent inlet ports in the lower region of the reactor, and decreases along the height of the reactor as a result of the progressing precipitation reaction (Seckler, 1994). On the other hand, zero supersaturation inhibits the precipitation process and agglomeration of fine particles. It is therefore vital to control the level of supersaturation in the fluidised bed crystallizer (Söhnel and Garside, 1992) to promote growth or crystal attachment on to seeds while minimizing fines.

In an attempt to control supersaturation, feeding the alkaline reagent through multiple inlet ports along the side of the reactor has been found to be effective in studies conducted by Seckler (1994), Guillard and Lewis (2001) and van Hille (2005). These studies attributed process inefficiencies to high levels of supersaturation at reactant inlets and attempted to alleviate this by distributing the reagent flow through 3 inlet ports along the bed. These studies did not however discuss the implications of introducing more zones of high supersaturation at these additional inlet points. The number of inlet ports used would have an effect on the extent to which supersaturation is distributed, with more ports leading to a better distribution. This strategy may also fail when the reagent requires some time for dissolution or an induction period for the reaction.

Other techniques to control supersaturation during continuous operation include stepwise addition of the precipitating agent and solvent dilution (Al-Othman, 2004). Stepwise addition of the alkaline solution allows

for the reagent to be consumed before being replenished so that the concentration of reagent ions in solution, and thus supersaturation, does not exceed a certain amount. This was shown to grow large crystals by favouring growth instead of nucleation and is successfully applied to acid neutralization and precipitation processes (Karidakis et al., 2005; Tai et al., 1999; Bond and Veerapaneni**,** 2007; Villa Gomez, 2013). Solvent dilution on the other hand, allows for a lower concentration of the alkaline solution and better control over reaction components (Mullin, 2001), but dilutes the system which may adversely affect precipitation kinetics, such that maximum conversions of the desired components are not attained within a given residence time. The use of dilute solvents also presents a problem when the reagent to be used has a low solubility and thus requires large volumes of water. If the intention is to treat wastewater to recover water, diluting the reagent stream may defeat the purpose altogether.

Another method to control supersaturation involves controlling the release of the reagent ion, by feeding a suspension of a sparingly soluble compound into the system. The effectiveness of using a suspension to control supersaturation in a fluidised bed reactor in this way has been studied by Seckler (1994). The investigation compared process inefficiencies, that is the formation of fines due to high supersaturation when using a calcium hydroxide suspension and a sodium hydroxide solution. The study found that the calcium hydroxide suspension produced less fines than when using sodium hydroxide, due to the controlled release of hydroxyl ions. A study by Karidakis and co-workers (2005) employed the same method of supersaturation control by adding the base reagent, calcium hydroxide, as a solid in the precipitation of magnesium hydroxide and gypsum in a stirred tank reactor. The study further revealed that calcium hydroxide fed in excess produced better magnesium hydroxide conversions compared to stoichiometric amounts. This reveals that the implications of adding a suspension to a precipitating process may present challenges regarding dissolution. For the control of supersaturation to be effective, the dissolution of the reagent must not be hindered by inefficient mixing or armouring of the solids before they dissolve.

The method of supersaturation control is very important to influence product characteristics and process efficiencies like conversion and recovery and each presents its own advantages and disadvantages depending on the system to be treated. A calcium hydroxide suspension has been chosen as the base reagent in this study, and is discussed further below.

3.2.2 Dissolution of $Ca(OH)_2$

In the treatment of acidic wastewaters, lime neutralization is preferred over ion exchange, adsorption, reverse osmosis and electrochemical methods, due to its significant economic advantage (Zhang et al., 2013). However, the disadvantage of using lime (calcium hydroxide) is that it often requires large dosages to be effective and the dissolution kinetics are not well understood. Despite this, the use of calcium hydroxide is still the most widely used treatment method because of its high efficiency (Matlock et al., 2002) and economic benefits.

Calcium hydroxide is a sparingly soluble compound, which when added to water, becomes a source of calcium and hydroxide ions as shown by Equation 20 and Equation 21 (Bates et al., 1959):

$$Ca(OH)_{2(s)} \Leftrightarrow CaOH^{+}{}_{(aq)} + OH^{-}{}_{(aq)} \qquad \text{Equation 20}$$

$$CaOH^{+}_{(aq)} \Leftrightarrow Ca^{2+}_{(aq)} + OH^{-}_{(aq)}$$ Equation 21

The solubility of calcium hydroxide in water at 25 °C is 1.8 g/L. Due to this slight solubility, calcium hydroxide is typically used as a suspension in industry. The nature of the suspension presents inherent advantages and disadvantages. The benefit of using a calcium hydroxide suspension, compared to a solution, is the smaller volume to be handled (Rademacher et al., 1999). In addition, a calcium hydroxide solution would contain a large volume of water due to its low solubility, and would dilute the system and alter supersaturation levels. Moreover, in precipitation processes where controlling supersaturation is important for desired product characteristics, the concentration of calcium hydroxide in solution remains constant at 1.8 g/L as the equilibrium concentration is maintained by replenishing ions used up in reactions. On the other hand, the dissolution kinetics of calcium hydroxide plays a significant role in precipitation reactions (Rademacher et al., 1999), and can be a limiting factor. Thus, attempting to control supersaturation to avoid primary nucleation by adding a calcium hydroxide suspension may in fact aggravate the problem. The presence of solid surfaces, in this case calcium hydroxide, lowers the activation energy for primary nucleation, which promotes the formation of fines.

Factors that affect the dissolution rate of calcium hydroxide are the purity, pH, particle size distribution, that is, the total surface area of the solids in the suspension, as well as the dosed amount of solids which also increase the exposed surface area. A study by Kadambi and co-workers (1998) conducted an experimental investigation on the effect of particle diameter on the dissolution of rate of a single calcium hydroxide particle in water.

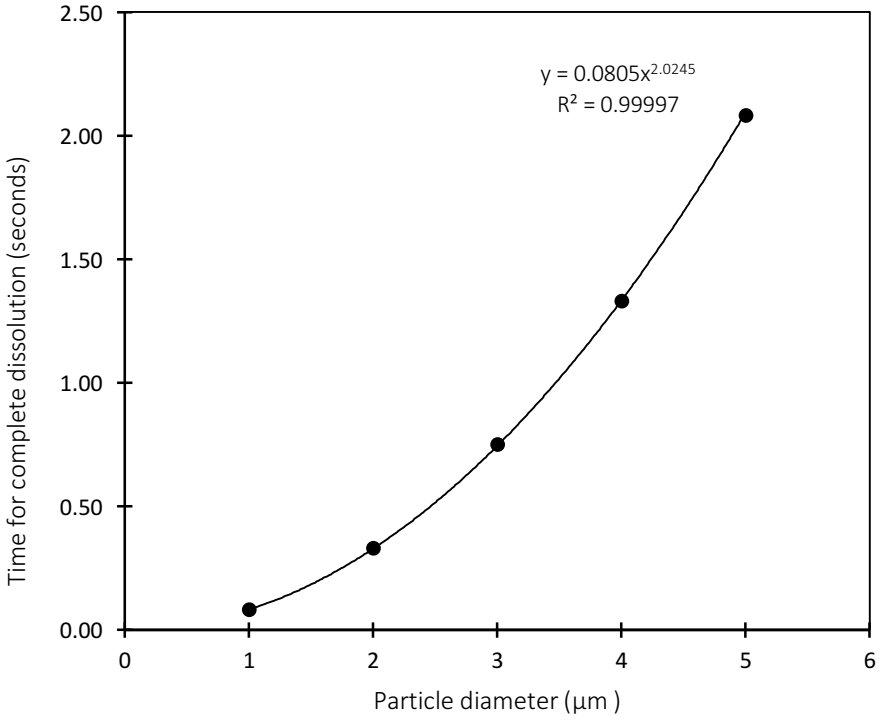

Figure 3.2: Dissolution time of calcium hydroxide in water (Kadambi et al., 1998)

The dissolution time of a calcium hydroxide particle of a given purity will follow a second order power trend with respect to particle diameter. Figure 3.2 shows that the time taken for a particle to dissolve varies significantly with particle size. This may hinder processes in which fast reactions that require fast dissolution of reagents occur.

3.2.3 Superficial velocity

For a given supersaturation and seed PSD, the expected growth rate of crystals increases with increasing superficial velocity in a fluidised bed crystallizer (Aldaco et al., 2007). The increase in superficial velocity improves mass transfer, and thus nucleation and crystal growth. However, high superficial velocities increase the porosity of the bed, resulting in regions that favour primary nucleation and thus fines. Moreover, the increased superficial velocity may promote abrasion and attrition of seeds with low hardness factors that further contribute to inefficiencies.

3.3 Seeding

According to Mullin (2001), the best method for inducing crystallisation is to seed a supersaturated solution with small particles of the crystallizing material. This decreases the activation energy required for homogeneous nucleation because the wetting angle of the crystallizing material is zero. In the presence of other solid material, the activation energy is decreased to a lesser degree, but still promotes heterogeneous nucleation over homogeneous nucleation. Figure 3.3 illustrates the four possible conditions for precipitation processes.

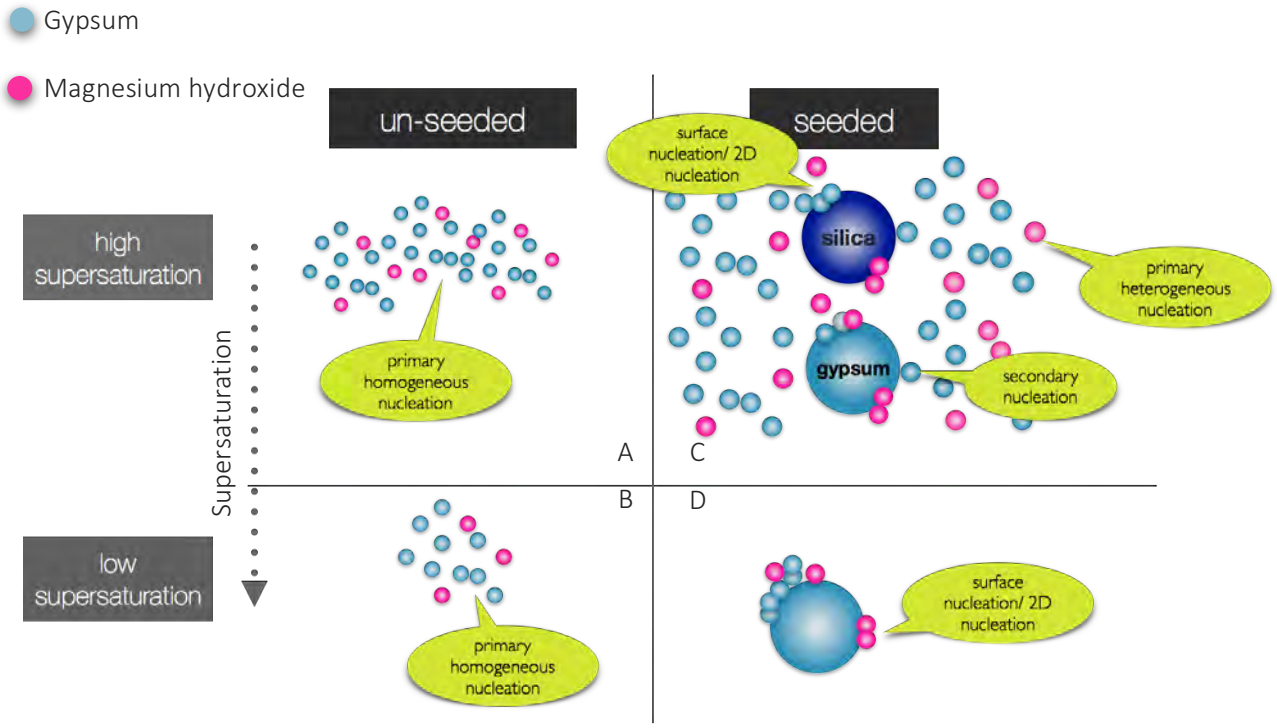

Figure 3.3: Mechanisms for seeded and unseeded precipitation scenarios

Homogeneous nucleation is expected in scenario A, where conditions of high supersaturation exist in the absence of seeds. This means that the activation energy for nucleation is high, but is countered by the high energy possessed by the system due to its supersaturation. Under these conditions, a large number of very small particles form. At low levels of supersaturation, in the absence of seeds (scenario B), provided that the system possesses enough energy to overcome the requirement for nucleation, a small number of crystals form and subsequently grow. Scenario A may eventually end up as scenario B if supersaturation is decreased or consumed. As mentioned above, the presence of seeds lowers the energy requirement for heterogeneous nucleation and under high levels of supersaturation (Scenario C), it promotes heterogeneous nucleation. If the seeds are the same as the crystallizing material, nucleation proceeds via secondary nucleation in the bulk, and the energy requirement is even lower. There may also be two-dimensional nucleation on the surface of the seed, irrespective of the type of seed, which is classified as a growth mechanism. Finally, in scenario D, conditions of low supersaturation promote surface nucleation (2D nucleation) or growth onto the seed surface. Here, the energy possessed by the system is just enough to deposit onto the seed but not enough to overcome the nucleation energy barrier.

A study of gypsum precipitation kinetics in a stirred tank batch crystallizer by Halevy and co-workers (2013) found gypsum to be a viable seeding material, whereby size enlargement proceeds via crystal growth for solutions of low supersaturation (S = 2 - 3.5). As a result, this would minimise fines formation and enhance gypsum recovery. The study also concluded that silica was a viable seeding material for gypsum precipitation, where the mechanism of crystal formation was through growth and heterogeneous nucleation and that results obtained using silica seeds were comparable with those of gypsum seeds. The use of silica as seeding material has been supported by other work. Guillard and Lewis (2001) successfully grew nickel carbonate on silica seeds for solutions of low supersaturation (solution concentration of 50 – 150 ppm), while van Hille and co-workers (2005) precipitated copper sulphide on silica seeds at conditions of very high supersaturation ($S > 10^{14}$). In this case the method of attachment of the precipitate on the seed surface was hypothesised to be through agglomeration, which is expected given the high degree of supersaturation. Other work includes the coating of silica with a compact layer of calcium phosphate by Seckler (1994) using solutions of low phosphate concentrations (5 – 100 mg/L). It is therefore important to consider the level of supersaturation in the presence of seeding material, given that certain mechanisms prevail over others at different conditions.

3.3.1 Seed type

Using silica allows for good fluidisation but requires a higher activation energy for the first layer of crystal formation in comparison to that of the crystallizing substance. This higher activation energy results from the wetting angle differences in gypsum and silica seeds. In the precipitation of gypsum, gypsum seeds are expected to have a smaller wetting angle compared to silica seeds. In the case where silica seeds are used, gypsum removal from solution occurs through primary heterogeneous nucleation in the bulk and primary heterogeneous nucleation followed by growth on the silica surface. Recovery requires an additional step to separate the product from silica. This allows silica to be reused after re-dissolving the resulting product.

When gypsum seeds are used, the transfer of ions from the aqueous solution into the solid phase occurs through crystal growth and secondary nucleation in the bulk. The product may be milled and healed for seed generation, which leaves the gypsum in a solid state as opposed to dissolving it as is in the case of silica seeds.

Another factor to consider when choosing the type of seeding material is the amount of fines generated through attrition, that is, crystal breakage as a result of particle collisions. Gypsum seeds are expected to produce more fines through this process compared to silica because silica has a higher hardness factor (hardness = 7 according to Moh's Hardness scale) than gypsum (hardness = 3). It should be noted that mixed precipitate products have further implications if used as a seeding material due to the presence of magnesium hydroxide deposits on regenerated seeds. Table 3.1 summarizes the advantages and disadvantages associated with each seed type.

Table 3.1: Advantages and disadvantages of seeding material choice

	Advantages	Disadvantages
Gypsum seeds	• Lower activation energy required for gypsum growth • Product can regenerate seeds (implications of using mixed precipitate as product to be investigated)	• Crystal morphology (needles) is difficult to fluidise • Prone to a larger amount of fines generation through attrition due to the difference in hardness (Pritchard, 1998)
Silica seeds	• Seeds can be reused • Easily fluidised	• Induction period and higher activation energy compared to gypsum seeds (Halevy et al., 2013) • Gypsum and magnesium hydroxide need to be dissolved for recovery

3.3.2 Specific surface area and seed size

The specific surface area of the seeding material has an influence on the efficiency of the entire precipitation process, since mechanisms such as nucleation, growth and agglomeration are all surface dependent (Wang and Anderson, 1992). These mechanisms are therefore sensitive to the nature of the surface, the specific surface area, as well as the number of active sites available (Randolph and Larson, 1988).

The specific surface area provided by the seeding material is initially very large, but declines as seeds increase in size and are subsequently harvested from the reactor. The specific active surface area of seeds needs to remain sufficiently large to promote crystal growth, hence coated seeds should remain relatively small, that is, diameters less than 1 mm (Seckler, 1994). Large particles hinder fluidisation and cause inefficiencies in mixing, which further compromise the effectiveness of the fluidised bed configuration. It is also important to ensure that seed sizes remain small, since larger crystals tend to generate more secondary nuclei in agitated systems than smaller crystals (Mullin, 2001). A study by Kubota and Fujiwara (1990) found that potassium sulphate crystals less than 500 μm did not produce secondary nuclei, with conditions sensitive to agitation rate and seed type. However, its hardness or morphology were not taken into consideration.

It is also important to note that at high levels of supersaturation, when nucleation mechanisms prevail in the bulk, newly formed nuclei increase the specific surface area in the bed as well. This may be advantageous as the larger surface area promotes growth, but the problem arises when these fine particles are elutriated from the fluidised bed and no longer take part in the crystallization process. In this sense, a fluidised bed configuration may not be as beneficial as a reactor that can retain these fines, such as an MSMPR. However, if it was possible to recirculate these fines back into the reaction zone, this may improve efficiencies as described above.

In addition to fines, using a calcium hydroxide suspension also increases the specific surface area in the system. The solid calcium hydroxide particles that are yet to be dissolved promote surface dependent mechanisms and may serve as a site for growth and subsequently become armoured, that is, coated by precipitates undesirably. While this increase in surface dependent mechanisms may increase conversion efficiencies, the armouring of calcium hydroxide decreases the supply of hydroxyl and calcium ions to their respective reactions as unreacted calcium hydroxide particles leave the system with the product. A study by Hammarstrom and co-workers (2003), which investigated the treatment of acid mine drainage using lime neutralization, found that gypsum tends to attach or form on the surface of lime particles shown in Figure 3.4.

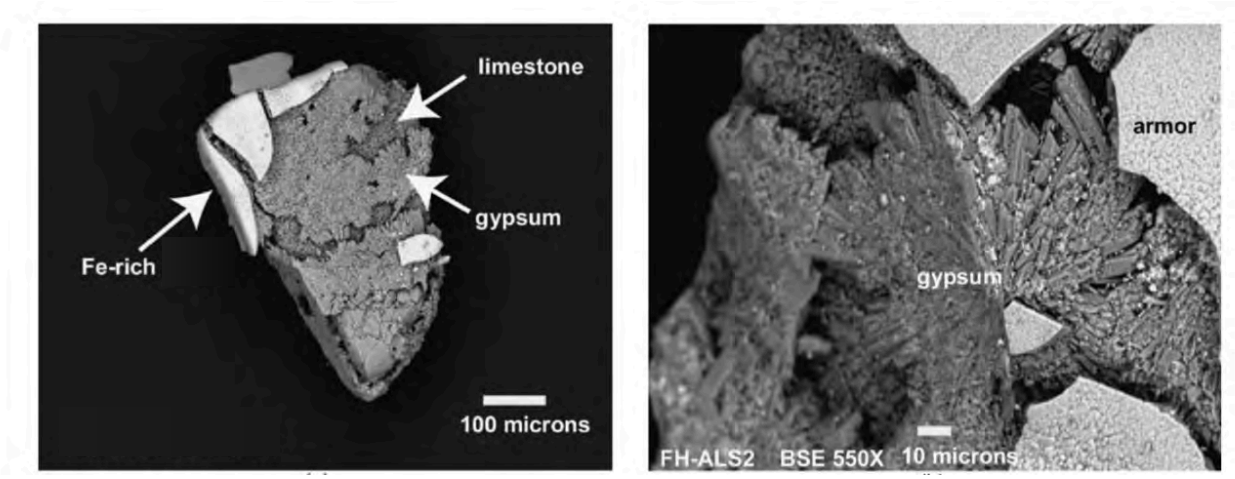

Figure 3.4: Gypsum on the surface of lime particles (Hammarstrom et al., 2003).

Another important factor to consider with seeding material is the fluidisation behaviour of particles, which is affected by both particle and fluid properties. A bed consisting of particles of diameter 100 μm will expand far less than particles of diameter 30 to 80 μm, because fluid flows easily through the larger inter-particle spaces created by larger particles, and is less likely to fluidise the bed. Moreover, the shape of particles is equally important, as non-spherical particles are difficult to fluidise, while irregular (i.e. needles or flakes) are not inclined to fluidise at all (Coulson and Richardson, 1991). The Geldart classification of particles (Figure 3.5) categorises the fluidisation behaviour of particles according to their size and density.

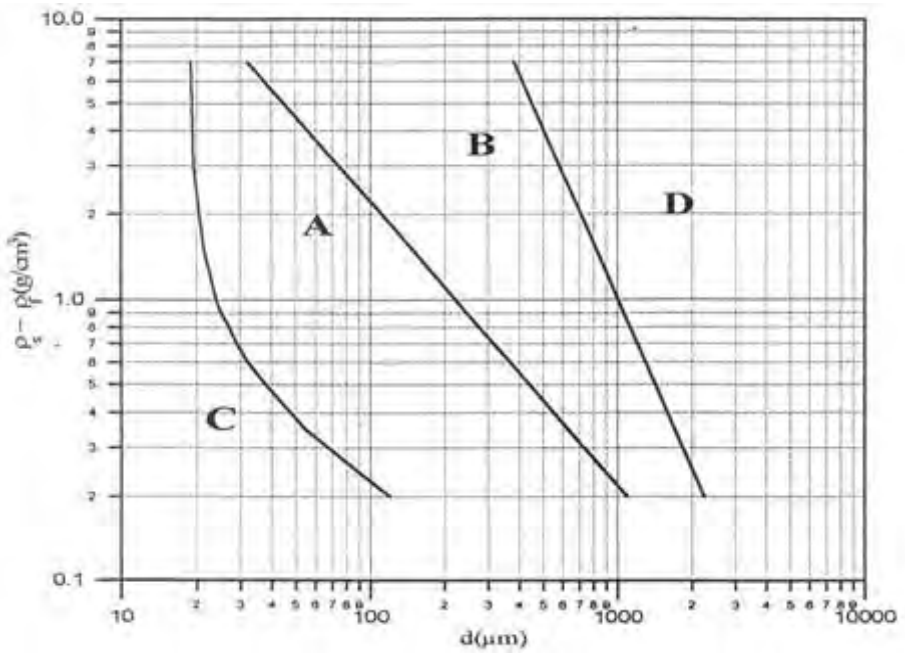

Figure 3.5: Geldart classification of particles (Geldart, 1973)

Particles that are categorised as group A and B particles are easily fluidised and are unlikely to induce channelling in the bed. Group A particles have a mean particle diameter of 30 μm and low particle densities (<~1.4 g/cm^3). Particles in this group fluidize easily, with smooth fluidization at low fluid velocities. Group B particles, described as sand-like particles, are of the size range 150 μm to 500 μm with densities ranging from 1.4 to 4 g/cm^3. Group C and D particles on the other hand, are difficult to fluidise. Group C particles are described as cohesive or very fine powders and have diameters less than 30 μm. Particles that fall in this group are very difficult to fluidise because they exhibit strong inter-particle forces. These particles give rise to channelling in bed. Group D materials are either very large or very dense, which make them difficult or unlikely to fluidise (Geldart, 1973). While both sand and gypsum seeds have been studied previously, the choice of seeding material has not been evaluated for fluidisation experiments. Silica seeds are categorised as group B particles that fluidise well, while gypsum seeds tend to coagulate and could possibly be categorized as a group C powder depending on its size.

3.4 $MgSO_4$-$CaSO_4$-Na_2SO_4-H_2O system

It is uncommon for industrial wastewaters to exist as simple binary streams, but occur rather as multicomponent systems. Wastewaters particularly emanating from mining processes have varying concentrations and compositions of dissolved salts. Waste streams with magnesium, sodium and calcium sulphates in particular, are very common (Randall, 2010). The presence of many components in an aqueous system can introduce many complexities. According to Mullin and co-workers (2001), these additional components alter solution properties, diffusion coefficients or the structure of the solution. A study by Popovic and co-workers (2011) predicted the solubility data for the $CaSO_4$ + Na_2SO_4 + H_2O at T = 298.15 K

using the Extended Pitzer's Ion Interaction Model in the ionic strength range of 0.0616–10.9062 mol/kg, as shown in Figure 3.6.

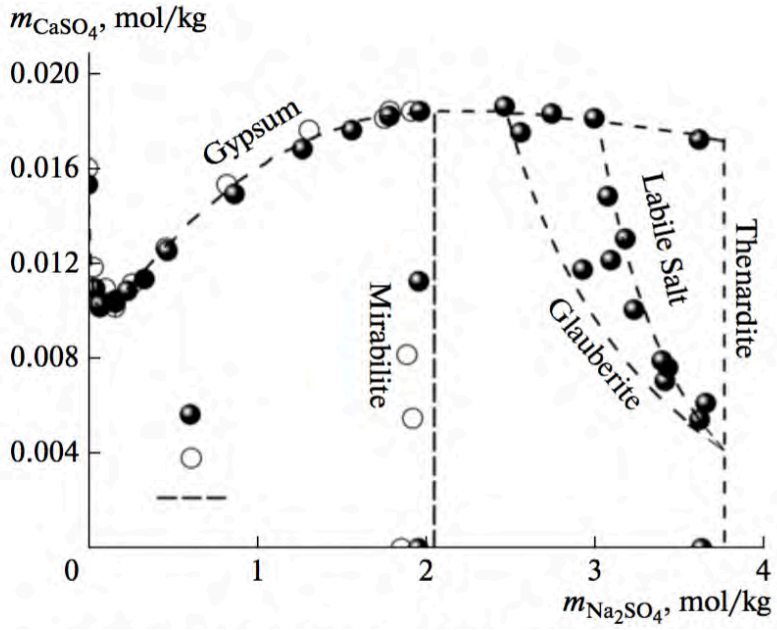

Figure 3.6: Solubilities of salts in the system $CaSO_4$+Na_2SO_4+H_20 (Popovic et al., 2011)

The solubility of gypsum decreases sharply at low concentrations of sodium sulphate, passes through a minimum at 0.08 mol/kg molality of Na_2SO_4, and then increases gradually with increasing sodium sulphate concentration, until it reaches a maximum at approximately 2.0 mol/kg, where it begins to decrease slightly again. This behaviour is due to electrostatic effects, speciation and the common ion effect.

3.4.1 Electrostatic effects

Of particular importance is the behaviour of calcium sulphate in multicomponent systems, particularly its solubility, because of its tendency to scale in most water treatment systems. The solubility of calcium sulphate is known to be influenced in a number of ways in the presence of certain ions. The solubility of sparingly soluble salts, like calcium sulphate, is three times higher in 0.1 molal solutions of monovalent salts, like sodium and up to ten times higher in 0.1 molal solutions of divalent ions, like magnesium (Spiegler et al., 1980). The reason for this increase in solubility is due to electrostatic effects (Murray, 2004). Sulphate and calcium ions tend to hydrate in solution, which induces a shielding effect (Figure 3.7).

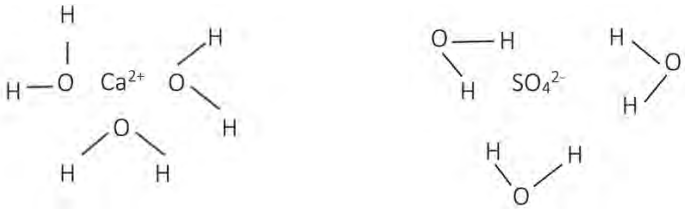

Figure 3.7: Shielding of calcium and sulphate ions (Murray, 2004)

However, in the presence of other ions like magnesium and sodium, which are attracted to ions of the opposite charge, the electrostatic shielding effect illustrated in Figure 3.7 is amplified, shown in Figure 3.8. This hinders the ability of calcium and sulphate ions to meet and react.

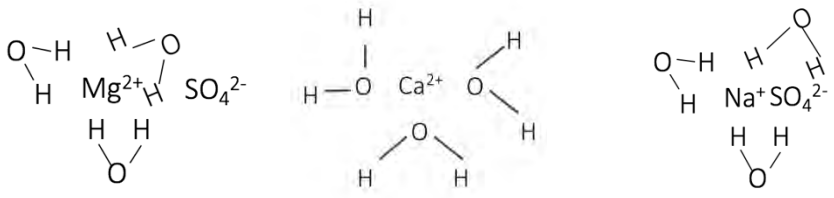

Figure 3.8: Shielding of magnesium, sodium and calcium sulphate system (Murray, 2004).

The extent to which magnesium is hydrated is larger than sodium due to magnesium's higher charge density. The hydrated magnesium ion is thus shielded from sulphates and calcium, which allows for calcium and sulphate ions to effectively meet and react relatively easier than in the presence of sodium-sulphate ion pairs. Therefore, sulphate ions are not able to take part in the reaction forming gypsum, resulting in a lower solid recovery.

3.4.2 Ion complexing or speciation

Multicomponent systems also undergo ion complexing, where interactions between ions and solutes are strong enough to allow for the formation of a new species, complex or ion pair. The ions in these pairs are in fact not bonded, but are separated by water molecules and share their first hydration shell (Murray, 2004). Similar to the effects of shielding, these complexes are unable to react, so their formation lowers the effective concentration or activity in solution. In some cases, complexes dominate to such a large extent, that the free ion population is only a fraction of the total (Murray, 2004).

3.4.3 Common ion effect

In multicomponent systems containing common ions, these common cations or anions have a cumulative effect on the solubility equilibrium (Spiegler et al., 1980). For example, in a solution of sodium sulphate and calcium sulphate, the solution being saturated with respect to calcium sulphate, the presence of additional sulphate, if more sodium sulphate were to be added, may cause the precipitation of calcium sulphate. This is due to the common sulphate ion shared by both sodium sulphate and calcium sulphate. The common ion effect thus decreases the solubility of a compound in solution. In this particular multicomponent system, calcium is also a common ion between calcium sulphate and calcium hydroxide. This means that the solubility of calcium sulphate is lowered, which results in more gypsum precipitates forming or the solubility of calcium hydroxide being lowered, which would stop its dissolution altogether. This would in turn, would stop the precipitation of gypsum due the absence of calcium ions.

The solubility of gypsum in the presence of magnesium sulphate and sodium sulphate was predicted by Ahuja and co-workers (2000) to account for the common ion effect. Figure 3.9 shows the predicted and the experimentally obtained solubility of gypsum. The deviation from the solubility of gypsum in pure water is

significant for both magnesium and to a larger extent, sodium sulphate. The deviation becomes even larger with increasing salt concentration.

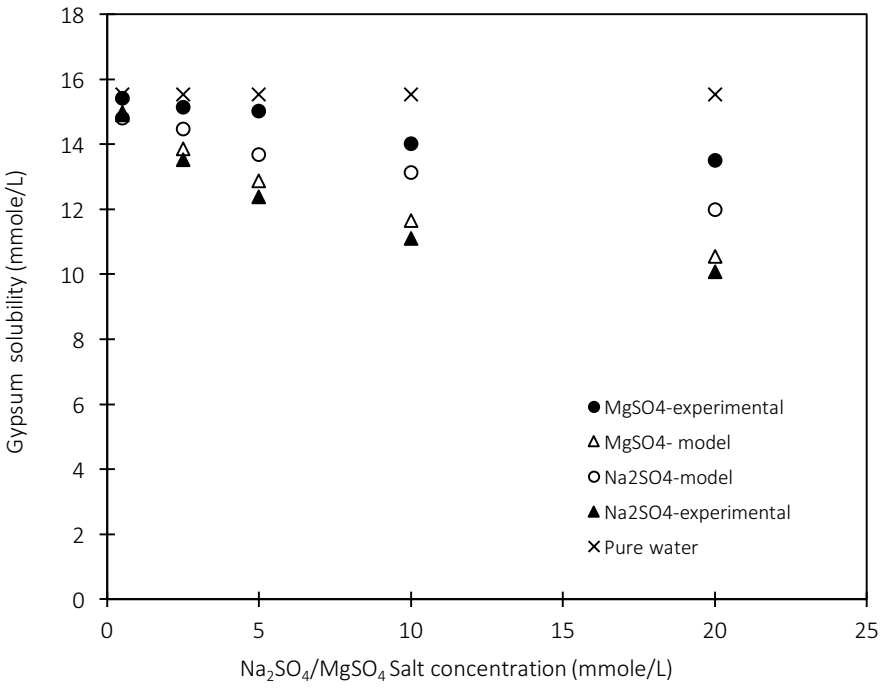

Figure 3.9: Gypsum solubility in the presence of magnesium and sodium sulphate salts (adapted from Ahuja and co-workers (2000)).

3.4.4 Mixed precipitates

Another implication of multicomponent precipitation is the formation of co-precipitates that result in a mixed product, if not treated sequentially. A study by Karidakis and co-workers (2005) investigated the removal of magnesium from a binary magnesium-water system by adding calcium sulphate. The resulting precipitate was magnesium hydroxide and gypsum which was impossible to recover separately. Further implications may be changes in precipitate morphology, where components are adsorbed on certain faces of crystals and alter the shape of crystals.

3.5 Precipitation mechanisms

3.5.1 Precipitation mechanisms of gypsum

The crystallization of gypsum is controlled by two mechanisms: nucleation and the subsequent growth of nuclei into larger crystals (Mullin, 2001). Precipitation reactions are characteristically fast, and the nucleation rate is assumed to dominate over the growth rate. The nucleation rate for gypsum depends on the degree of supersaturation, interfacial energy between gypsum and the solution; and the solubility of gypsum in the solution (Reznik et al., 2012). According to the classic nucleation theory discussed in previous sections, the overall nucleation rate for gypsum in a seeded fluidised bed reactor accounts for heterogeneous nucleation

in the presence of silica seeds, homogenous nucleation arising in zones where possible channelling or eddying takes place, as well as zones above the bed in which residual supersaturation allows for precipitation; and finally secondary nucleation in the presence of gypsum accumulating in the bed. It is however, difficult to decouple these mechanisms due to varying conditions in the reactor. A study by Abdel-Aal and co-workers (2015) investigated the nucleation rate of gypsum scale formation in reverse osmosis membranes for varying supersaturation ratios. The investigation found that the nucleation rate for gypsum increased with increased supersaturation ratio. This finding was corroborated by a study conducted by Reznik and co-workers (2012). Uchymiak and co-workers (2008) found that rate of gypsum crystal formation on a reverse osmosis membrane decreased and eventually ceased when the surface of the membrane was covered in crystals. This subsequently led to increased crystal size by diffusion controlled growth, possibly because the available surface area for deposition was large and supersaturation levels were low enough to promote growth rather than nucleation.

Another phenomenon to consider is the associated with gypsum nucleation. In the absence of existing crystal surfaces, some time elapses between the state of supersaturation in a solution and the detection of a new phase in the system. This is known as the induction time and is inversely related to the nucleation rate (Sohnel and Mullin, 1988), where a slow nucleation rate prolongs the induction period. The effect of the different parameters on the induction time for gypsum nucleation was determined in the past under varying conditions (Smith and Sweett, 1971; Keller Douglas Martin and Hileman, 1978a,b, 1980; Liu and Nancollas, 1973; Packter, 1974; Klepetsanis and Koutsoukos, 1991; He et al., 1994; Klepetsanis et al., 1999; Lancia et al., 1999; Linnikov, 1999; Hina et al., 2001; Prisciandaro et al., 2001; Abdel-Aal et al., 2004; Uchymiak et al., 2008). The general trend observed in these investigations confirms that induction time decreases with increasing supersaturation. In a seeded reactor, it is possible for the induction time to be reduced and not completely eliminated. Halevy and co-workers (2013) found that the induction time for gypsum in a stirred tank reactor decreased from 100 min to 40 min for solutions of very low supersaturation (1.8) and 25 g/L of seeds (in a 1L vessel) compared to when there were no seeds. It is expected that at higher supersaturation and more seeds, in other words, larger specific area, the induction time would be significantly reduced. It Is therefore expected that the nucleation rate of gypsum would be very high for wastewaters of high sulphate concentrations, especially in the presence of seeds, and a fluidised bed reactor configuration may be a futile attempt at minimizing the formation of fines for these particularly concentrated streams. However, it is important to fully consider other mechanisms of crystallization such as growth and agglomeration, as well as crystal morphology when evaluating the efficiency of the reactor.

Once nuclei have been formed, crystal enlargement proceeds via growth. The seeded growth rate of gypsum was found to be of second order and is shown by Equation 22 (He et al., 1993):

$$r = kn(C - C_S)^2 \qquad \text{Equation 22}$$

Where: r= growth rate (mol/kg.H_2O.min)

k= rate constant (mol/kg.H_2O.min)

n= number of growth sites

C= concentration of dissolved calcium sulphate

C_s= solubility of gypsum

The work conducted by Halevy and co-workers (2013) is in agreement with a second order growth rate for gypsum in the presence of silica seeds. The growth rate for gypsum has been found to be affected by solution composition and the rate constant is dependent on interfacial tension and solubility (He et al., 1993). The proposed mechanism of diffusion-controlled growth for gypsum crystals is agreed upon by Liu and Nancollas (1973), Klepetsanis and co-workers (1999) and He and co-workers (1994). On the other hand, Halevy and co-workers found that at under hydrodynamic conditions (1000 RPM agitation speed) and low supersaturation (1.8), growth was in fact surface reaction controlled. It is unknown whether growth will be significant in highly supersaturated conditions or rather dominated by nucleation. However, given that there are supersaturation gradients in a fluidised bed, the possibility of growth is likely in regions of low supersaturation.

3.5.2 Precipitation mechanisms of magnesium hydroxide

The mechanism of magnesium hydroxide precipitation is of keen interest in processes that experience scaling of this compound because attempts of inhibiting it have, for the most part, been unsuccessful. Due to the nature of the particles formed, it is difficult to decouple nucleation, growth and agglomeration mechanisms. As the concentration of magnesium hydroxide is increased, the effective kinetic order of the seeded precipitation reaction changes from three to seven at a relative supersaturation degree of one (Chieng and Nancollas, 1982). Chieng and Nancollas (1982) found that the change in concentration of magnesium during precipitation is characterized by an initial fast decline, possibly nucleation, followed by a much slower rate of decrease implying that crystal growth took place. The study also found that the presence of magnesium hydroxide seeds eliminated the induction time. By changing the fluid dynamics (agitator speed of 80 – 800 RPM), the rate of crystallization of magnesium hydroxide did not change, suggesting it is controlled by a surface limiting process. Due to the low Ksp (1.8×10^{11}) of magnesium hydroxide, the supersaturation levels are significantly high at the concentrations for this study (80% of the total salt concentration). This may not corroborate with the findings above, because the supersaturation is orders of magnitude larger, and nucleation mechanisms rather than growth mechanisms are expected.

3.6 Product quality

The quality of precipitates refers to its morphology, size and mechanical integrity. Precipitates that can be separated from the treated stream and are easily handled are considered to be of good quality. The quality of product crystals is influenced by the nucleation, growth and agglomeration rate as depicted in Figure 3.10.

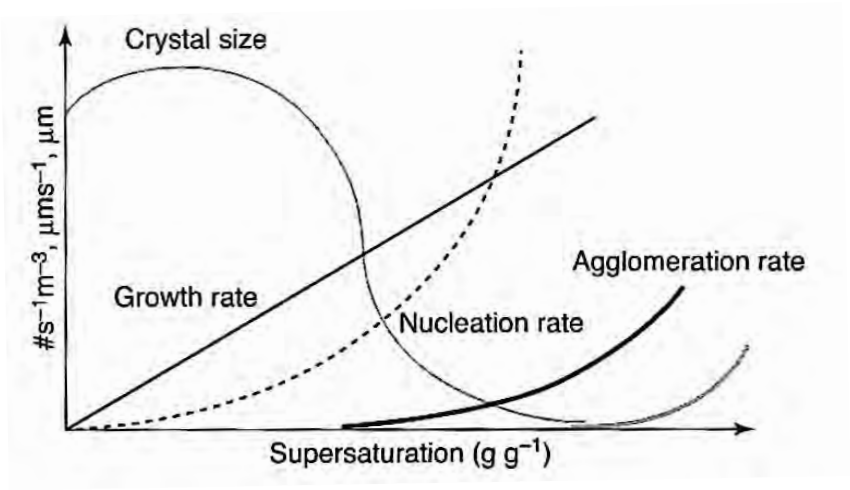

Figure 3.10: Effect of precipitation rates on crystal size (Lewis et al., 2015)

As larger particles are favoured for better product recovery, growth and agglomeration mechanisms are preferred. Nucleation results in smaller particles that are difficult to filter. It is therefore important to control supersaturation to influence product quality. Further to crystal size, the morphology plays a significant role on product quality as well because certain crystal shapes promote mechanical integrity of product grains, elutriation or water retention.

3.6.1 Gypsum morphology

The morphology of gypsum varies and is described as being needle-like crystals, which are more or less ramified with different aspect ratios, to plate-like crystals. The crystals are typically in the micron-size range for precipitation processes. A study by Seewoo and co-workers (2004) investigated the morphology of gypsum and found two distinct morphologies: needles and platelets, depending on experimental conditions. This was further confirmed by Christoffersen and co-workers (1982); Lewis and co-workers (2002). The conditions under which these two morphologies form is however, disagreed upon. While Lash and Burns (1984) produced both needle and platelet forms of gypsum, it was at calcium sulphate concentrations higher than 0.4M that produced needles and platelets formed at calcium sulphate concentrations lower than 0.25M. Lewis and co-workers (2002) focused on producing gypsum crystals of a particular morphology and size distribution, by altering process conditions. Needle-like crystals were formed under conditions of low supersaturation (S_g = 2.27) with average lengths of 100 μm after a significant induction period, however, the residence time is not known and is important factor to consider. The plate-like morphology was formed at high levels of supersaturation (S_g = 10.86), with smaller crystals (25μm) having a relatively larger surface area being formed at a reduced induction time, however, the method of size classification was not explicitly stated. The larger surface area but smaller length is indicative that the axis of growth changed, resulting in morphology change from needles to plates. An observation by Liu and Nancollas (1970) found needle-like crystals 80-120 μm and 30-50 μm in seeded experiments over a concentration range of 0.1 to 0.6 M ,respectively. It is therefore expected that both needles and plates are expected to form, given the range of supersaturation to be investigated.

Another characteristic of gypsum crystals is its tendency to form rosette like structures at high levels of supersaturation, where plates or needles extend radially from a central axis (Shih et al., 2005).

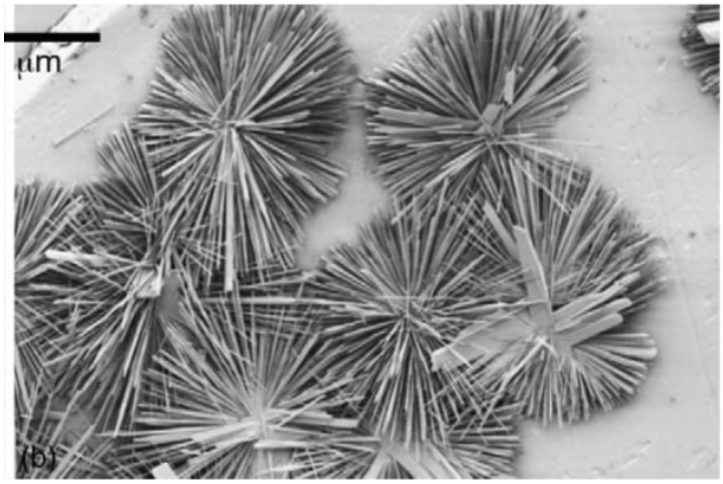

Figure 3.11: Gypsum rosette- like structures (Shih et al., 2005).

The term for these structures is spherulites (Granasy, 2005). They are known to form under highly non-equilibrium conditions, such as high levels of supersaturation. Studies have found that spherulites may be identified by two categories illustrated in Figure 3.12. The first category describes crystals growing radially from the nucleation site, branching out intermittently to fill spaces in the structure. The second category describes threadlike fibres forming new grains at the growth front. The structure proceeds to form a sheath as growth continues (Granasy, 2005). It is possible for both categories to be observed for the same material, under the same conditions.

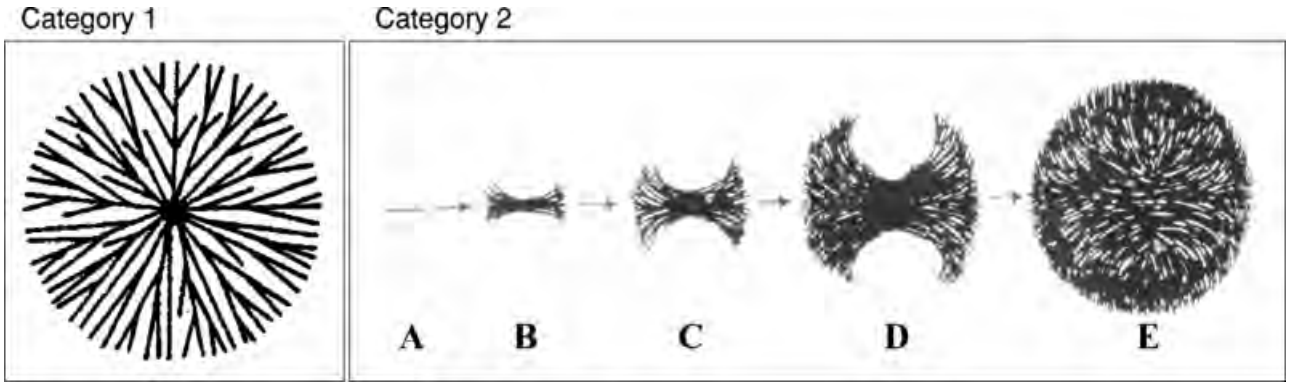

Figure 3.12: Spherulitic growth categories (Granasy, 2005)

These spherulitic structures may lead one to believe that its presence at high levels of supersaturation is as a result of agglomeration, rather than growth mechanisms which are known to occur at intermediate to low

levels of supersaturation (Lewis et al., 2015). It is difficult to predict how these structures behave in a fluidised bed reactor and thus its effect on the recovery and separation of products. Based on their morphology, these spherulites may be elutriated out of the bed because their large surface allows for greater exposure to the upward force of the fluidising stream, or they may in fact just be too heavy to be carried out with the effluent stream. If these crystals are elutriated, the effects on filterability of the fines is of particular interest as well as its tendency to retain mother liquor. If the crystals remain in the bed, it would be interesting to note whether these structures attach onto the seeding material or simply continue to grow as its own structure. Further to this, its mechanical integrity and tendency to break would be of interest during fluidisation, as it may be a source of fines.

3.6.2 Magnesium hydroxide morphology

The morphology of magnesium hydroxide is of particular interest due to its use as a precursor for magnesium oxide synthesis (Henrist et al., 2002). The morphology of magnesium hydroxide at low levels of supersaturation is expected to be hexagonal platelets due to its molecular structure (Figure 3.13a), however due to high supersaturation levels, it is commonly encountered as large aggregates of spherical units, with diameters of around 300 nm, themselves being made up of spherical smaller sub-units (Henrist et al., 2002). This is in agreement with the findings of Wu and co-workers (2014). The study by Henrist and co-workers (2002) further postulated that the morphology of magnesium hydroxide is affected by the supersaturation level and the chemical nature of other ions in solution during the growth phase. At high supersaturation levels, nucleation occurs rapidly, forming a large number of poorly defined nuclei which take the form of a gelatinous colloid (Chieng and Nancollas, 1982). In the presence of sodium ions, their small hydration sphere in solution promotes adsorption on to the nuclei faces, thus hindering the income of new magnesium ions. These small isotropic particles tend to aggregate in an attempt to lower their surface energy, and eventually take the form depicted in Figure 3.13b).

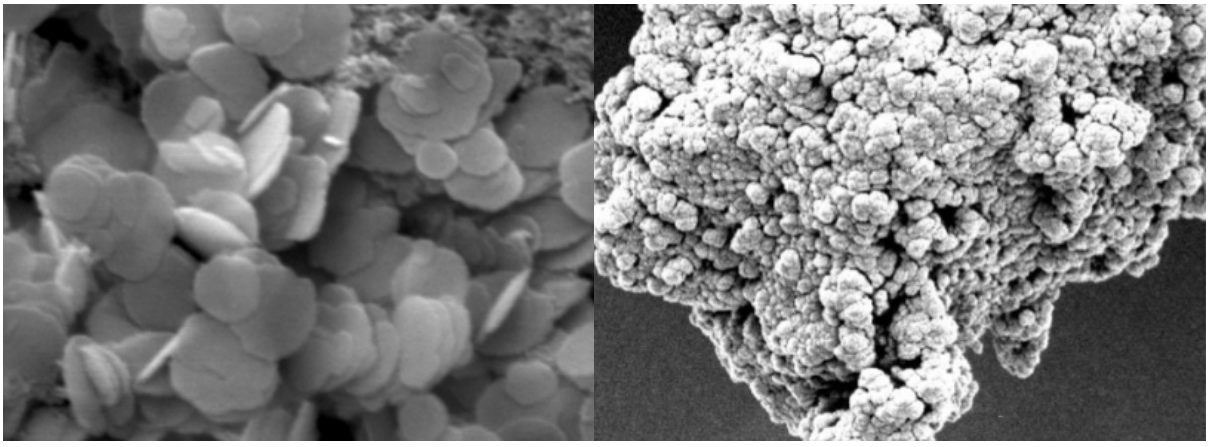

Figure 3.13: a) Hexagonal platelets of magnesium hydroxide crystals, b) magnesium hydroxide nano agglomerates (Henrist et al., 2002).

3.7 Efficiency

The desired product quality of gypsum and magnesium hydroxide is such that these precipitates are easily separable from the residual solution for reuse. The presence of fines makes separation and recovery difficult. In fluidised bed crystallizers, elutriation of fines out of the bed with the effluent stream is the primary factor contributing to inefficiencies (van Dijk et al., 1991; Seckler, 1994; Guillard and Lewis, 2001; van Hille, 2005). The formation of fines is usually avoided by using seeded precipitation, however in the presence of high supersaturation zones at the reactant inlet ports or due to channelling, particularly in the fluidised bed, fines may still form through primary nucleation. At extremely high concentrations the presence of seeds might actually increase inefficiencies by promoting nucleation. Furthermore, high energy dissipation zones, predominantly at the bottom of the reactor and inlet ports, trigger fines formation through attrition when crystals collide. However, maintaining a small average seed size minimises fines formation through attrition. The size of the particles elutriated is dependent on the fluidisation velocity, where larger particles can be elutriated as the fluidisation velocity increases.

In practice, compound removal via precipitation in fluidised bed crystallizers yield good results. Seckler (1994) achieved metal recoveries of between 80 to 95% in phosphate precipitation while Guillard and co-workers (2001) achieved removal efficiencies of greater than 90% in nickel carbonate precipitation using fluidised bed crystallizers. Metal concentrations from 10 up to 10 000 ppm can be treated (van Dijk et al., 1987). The gypsum removal efficiency (η), conversion (x) and fines concentration (φ) can be quantified as (Seckler, 1994):

$$\eta(\%) = \frac{C_{gyp,in} - C_{gyp,out}}{C_{gyp,in}} \times 100 \qquad \text{Equation 23}$$

$$x(\%) = \frac{C_{gyp,in} - (C_{gyp,dis} - C_{gyp,out})}{C_{gyp,in}} \times 100 \qquad \text{Equation 24}$$

$$\varphi(\%) = x(\%) - \eta(\%) \qquad \text{Equation 25}$$

Where: η = gypsum removal efficiency

X = conversion

φ = concentration of fines (%)

$C_{gyp,in}$= Concentration of gypsum in feed stream (g/l)

$C_{gyp,dissolved}$= Concentration of dissolved gypsum in effluent (g/l)

$C_{gyp,out}$= Concentration of gypsum in effluent stream and as fines (g/l)

3.8 Problem development

This section of the report presents a critical synthesis of the current state of knowledge and gap identification. This is followed by the problem statement, aim, objectives, hypothesis and key questions.

3.8.1 Critical synthesis

Neutralization of acidic wastewater streams using lime is one of the most popular treatment methods because of its effectiveness and attractive low cost. In these treatment processes, it is desired to remove as much of the precipitating compound as is possible, while producing crystals that allow for efficient separation from the residual solution. In the case of gypsum, where very small particles form, gravitational separation and filtration is difficult. Fine particles that have not agglomerated remain suspended and recovery through gravitational separation is not possible. On the other hand, separation through filtration is difficult because fine particles induce filter fouling and create a high pressure drop across the filter. In multicomponent systems, where a mixed solid product is formed, it is advantageous to influence separation of solid products as well, in this case gypsum and magnesium hydroxide.

In an attempt to recover products from wastewater treatment, fluidised bed crystallizers have been studied extensively (Guillard and Lewis, 2001; Seckler, 1994; Zhou et al., 1999, van Hille et al., 2005). The reactor configuration makes use of seeds, which eliminates crystal-impellor collisions and provides good mixing to attain homogeneity in the reaction zone. The reactor also initiates separation of product crystals based on crystal sizes. Large particles migrate to the bottom and fines leave the reactor with the effluent stream. This may serve as a disadvantage to the fluidised bed crystallizer because fine particles may improve crystallization rates due to their increased surface area.

The presence of seeds in a precipitation system allows for nucleation to occur at lower degrees of supersaturation, as well as to serve as a site for crystal attachment either through growth or agglomeration. Gypsum was found to be a viable seeding material and size enlargement was through crystal growth for solutions of low supersaturation (2 - 3.5) (Halevy et al., 2013). This minimised fines and enhanced gypsum recovery. Silica was also identified as a viable seeding material for gypsum precipitation, where the mechanism of crystal formation was through growth and heterogeneous nucleation at the same supersaturation levels (Halevy et al., 2013). Silica seeds have also been successful in the precipitation of other compounds in fluidised beds at low concentrations (Guillard and Lewis, 2001, Seckler, 1994). The use of silica seeds in the fluidised bed reactor with high levels of supersaturation has also been successful (van Hille et al., 2005). In this case the method of attachment of precipitate on the seed surface was found to be through agglomeration. Given that the feed concentrations in this study are significantly higher than in previous studies, crystal enlargement might proceed via agglomeration of primary crystals formed through nucleation and subsequent growth. The nucleation rate might in fact be promoted by the presence of seeds, which could defeat the purpose of using seeded precipitation to reduce the formation of fines. However, seeded precipitation becomes viable if agglomeration is promoted at these levels of supersaturation.

In an attempt to control supersaturation, feeding the base reagent through multiple inlet ports along the side of the reactor has been found to be effective (Seckler ,1994; Guillard and Lewis, 2001; van Hille et al. 2005). Process inefficiencies due to high levels of supersaturation at reactant inlets are alleviated by distributing the supersaturation along the height of the bed. However, these studies did not discuss the implications of

introducing more zones of high supersaturation at these additional inlet points. This strategy may fail when the reagent requires some time for dissolution or an induction period before the reaction takes place. It is then expected that using multiple inlet points may in fact be less effective at distributing supersaturation.

A more effective way of controlling supersaturation is the slow release of calcium and hydroxide ions from a suspension (Seckler, 1994). A study by Karidakis and co-workers (2005) employed the same method of supersaturation control by adding the base reagent, calcium hydroxide, as a solid in the precipitation of magnesium hydroxide and gypsum in a stirred tank reactor. The study revealed that calcium hydroxide fed in excess produced better conversions compared to stoichiometric amounts. This implies that adding a suspension to a precipitating process may present challenges regarding dissolution. For the control of supersaturation to be effective, the dissolution of the reagent must not be hindered by inefficient mixing or armouring of the solids before they dissolve.

An important aspect of this project is that the system is at concentration levels that are orders of magnitude higher than that of previous researchers. The concentration levels for this project are between 1 500 and 120 000mg/L (total dissolved salts), whereas previous researchers operated at 150 mg/L Ni (Guillard and Lewis, 2001); 5-100mg/L P (Seckler, 1994); 3000mg/L total metal (Zhou et al., 1999); 3557mg/L $NiSO_4$ (Wilms, 1988) and 5500 mg/L (Tai et al., 1999). This means that the rate of mass deposition onto seed particles is significant compared to those in previous research projects, hence the need for frequent product removal. At these high concentrations, the nucleation and subsequent growth rates are expected to be much higher based on Equation 22, resulting in more precipitate accumulating in the bed at a faster rate. If long operating periods are to be achieved, product removal is required to prevent the product grains from leaving the top of the reactor. Previous studies could operate for longer periods of time due to the low concentrations. Seckler (1994) found that his system (5-100 mg/L of phosphate) could operate for longer than three hours without product removal. Guillard and co-workers (2001) found that their system (50-150 mg/L Ni) could operate for longer than 48 hours for start up, during which silica particles were coated before experiments were even conducted, and for 12 hours during operation.

Another implication of these high rates of crystallization is that the equilibrium conversion of gypsum and magnesium hydroxide is reached faster compared to lower rates over the same residence time. Figure 3.14 illustrates the comparison of crystallization rates as a function of residence time.

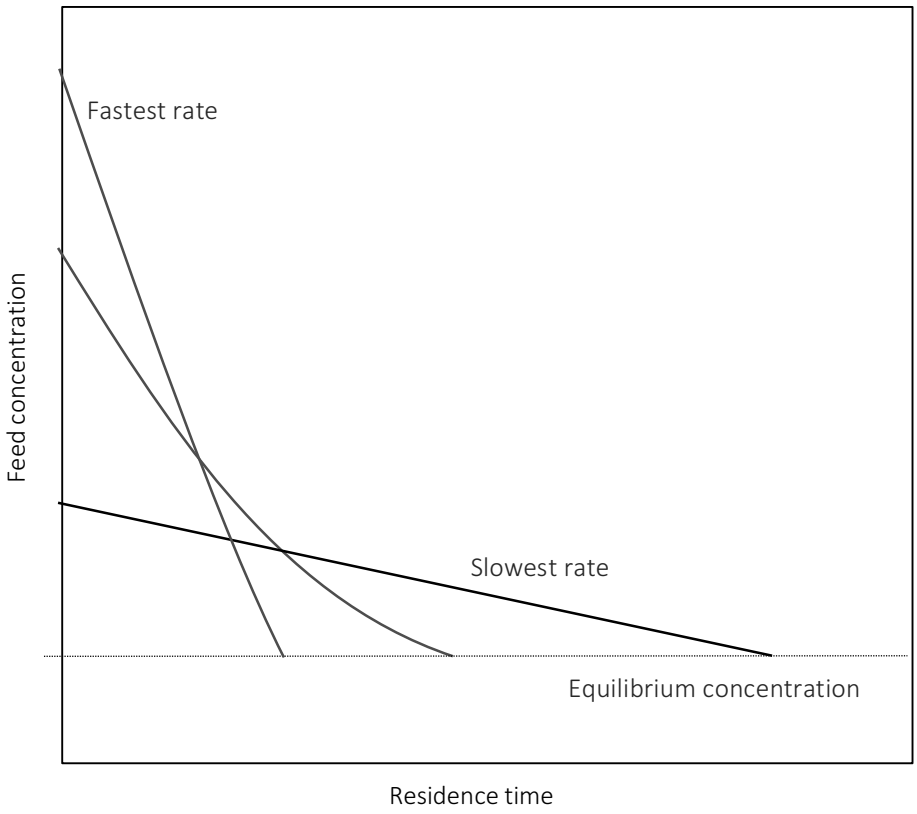

Figure 3.14: Comparison of rates of crystallization as a function of residence time

The rate of crystallisation is related to the feed concentration through the degree of supersaturation. This means that at low concentrations, the rate of crystallization is slower than for higher concentrations. Therefore, it is expected that these higher rates of crystallization translate to higher conversions over the same residence time. However, due to the nature of this multicomponent system, in which competing effects on the solubility of gypsum have been investigated by Spiegler and co-workers (1980), Ahuja and co-workers (2000), Murray (2004) and Popovic and co-workers (2011), it is difficult to predict whether the equilibrium concentration of gypsum will increase through electrostatic effects of sodium and magnesium, or decrease due to the common ion effect or speciation. This will affect the thermodynamically achievable conversion of sulphate and its removal efficiency. The removal efficiency, however, is not only dependent on the conversion of sulphates and magnesium, but also on the amount of fines lost with the effluent stream, where both size and morphology influence a particles' tendency to be elutriated.

3.8.2 Problem statement

In the treatment of saline wastewaters, rich in magnesium and sodium sulphate, with calcium hydroxide, a mixed precipitate of magnesium hydroxide and gypsum is formed, each having different characteristics. It is therefore desired to remove as much of the precipitating compound as is possible, while producing crystals that allow for efficient separation from the residual solution. In the case of gypsum, where very small needle-like particles form, and in the case of magnesium hydroxide where nano-sized agglomerates are formed,

gravitational separation and filtration is difficult. Fine particles remain suspended and recovery through gravitational separation is not efficient. On the other hand, separation through filtration is difficult because fine particles induce filter fouling and create a high pressure drop across the filter. Furthermore, in multicomponent systems, where a mixed solid product is formed, it is advantageous to influence separation of solid products as well.

3.8.3 Aim

This project aimed at investigating the treatment of saline wastewaters of, for example, mining operations, which are rich in sodium and magnesium sulphate. The intention was to investigate the removal efficiency of sulphate and magnesium using calcium hydroxide in a fluidised bed crystallizer.

3.8.4 Objectives

The objectives of this project were therefore to:

1. Predict the species and amount of precipitate expected in the system using thermodynamic modelling (OLI systems Inc.).
2. Investigate the effectiveness of fines reduction through the use of seeds
3. Investigate the conversion of sulphate and magnesium and the recovery of gypsum and magnesium hydroxide in a seeded fluidised bed crystalliser as a function of pH, seed type and feed composition;
4. Investigate the effect of excess calcium hydroxide on the conversion of sulphate and magnesium and the recovery of gypsum and magnesium hydroxide.
5. Investigate process alternatives which could potentially recover magnesium hydroxide and gypsum separately.

3.8.5 Hypotheses and key questions

1. Seeded precipitation using silica reduces the amount of fines elutriated and thus improves gypsum recovery. This is because silica seeds reduce the wetting angle, thus lowering the activation energy for two dimensional surface nucleation. In addition, the presence of seeds also provides sites for crystal attachment

    - How does the amount of fines compare in the presence and absence of seeds?
    - How does the conversion of sulphate and magnesium compare in the presence and absence of seeds?
    - Do seeds facilitate the precipitation process in any other way other than serving as a site for attachment?
    - Given that precipitation processes occur at fast rates, is growth on the seed surface expected?
    - Does the rate of heterogeneous nucleation increase in the presence of silica seeds given the high feed concentration?

2. Increasing the concentration of total sulphate salts in the wastewater stream increases the conversion of sulphates for a given residence time. This is because supersaturation and thus, the driving force for the nucleation and growth rates increases with an increase in the concentration of sulphate ions.

    Due to the increased nucleation rate, the amount of fines formed increase as concentration increases

- What is the role played by sodium and/or magnesium ions in the nucleation rate of gypsum?
- Is crystal growth favoured at high concentrations?

3. Increasing the calcium hydroxide suspension molar ration to sulphates in the feed stream increases sulphate conversion. Excess calcium hydroxide suspension allows for sufficient supply of calcium ions in solution for conversion into gypsum.
    - Could there be armouring around undissolved calcium hydroxide?
    - Is the rate at which calcium hydroxide dissolves related to its solid content?
    - Is all the calcium hydroxide dissolving within the residence time of the bed?

4 Materials and methods

This section presents details on the experimental equipment, procedure, sampling techniques and reagents used to conduct experiments.

4.1 Thermodynamic modelling

OLI Systems Stream Analyser ™ was used to model the aqueous chemistry and predict the phases expected in the multicomponent system. The software makes use of thermodynamic equations to predict parameters such as activity coefficients using the electrolyte NRTL model, with the extended form of Bromley equation to generate limited or unknown data. Molecule-molecule and ion-molecule interactions are modelled using the Pitzer model, while standard state properties are approximated with the Helgeson-Kirkham-Flowers Equation of State. The Soave Redlich-Kwong Equation of State is used to determine fugacity coefficients of non-ideal states (OLI manual, 2015).

4.2 Experimental and analytical equipment

All experiments were conducted using a laboratory scale fluidised bed crystallizer shown in Figure 4.1. The fluidised bed reactor consists of a 1.5 m high cylindrical perspex vessel with inner diameter 0.025 m, filled with seeding material (Consol silica, 200-300 μm, $\bar{x}$ = 250 μm) to a height of 0.3 m. The bottom of the reactor was filled with glass beads (5 mm diameter) to a height of 5 cm to ensure a dispersed flow of the influent stream and to avoid channelling within the bed, while providing support for the seeding material. Figure 4.1 is a schematic diagram of the experimental set up.

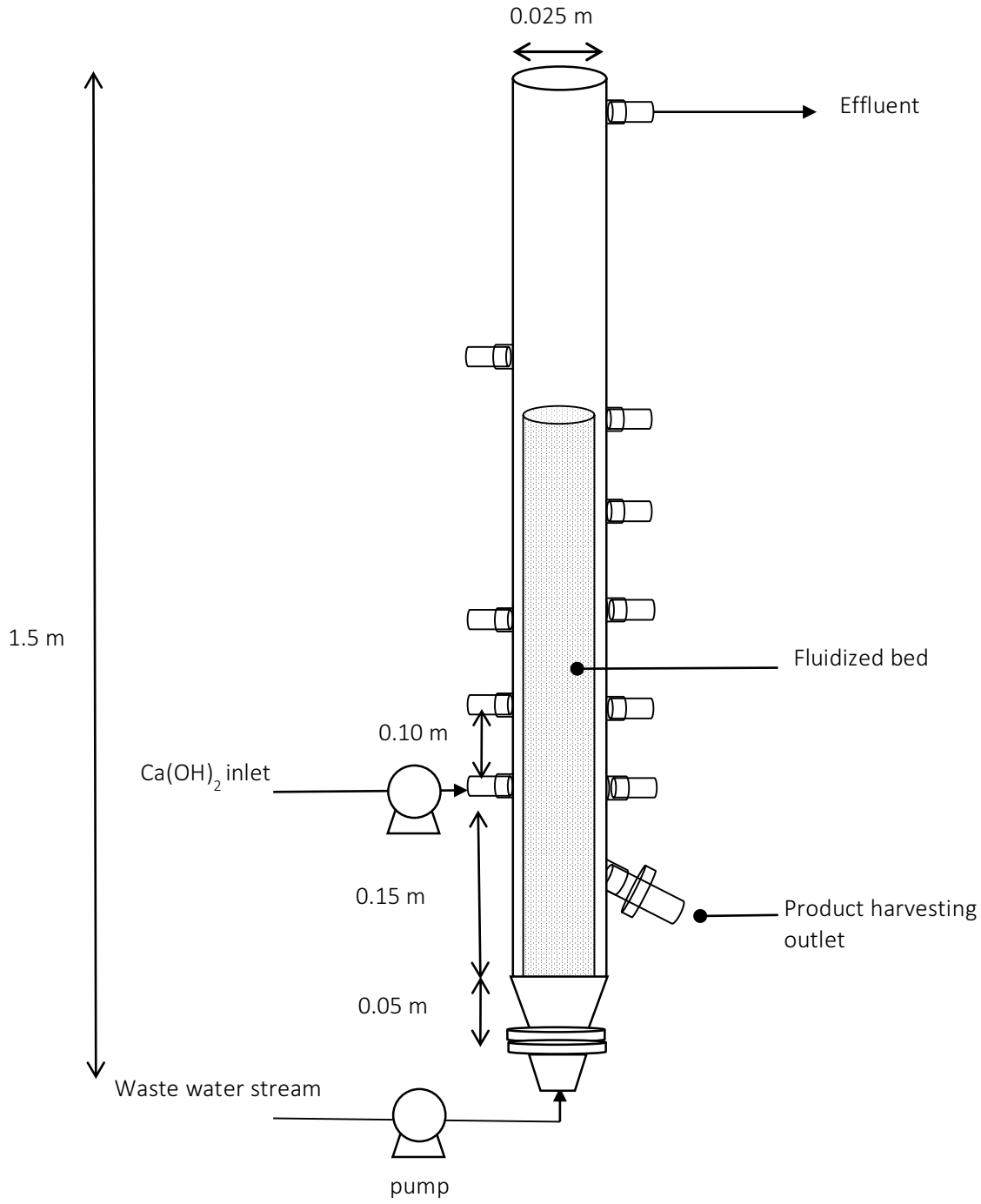

Figure 4.1: Schematic diagram of experimental set up

A rotary gear pump (Micro pump) was used to pump the synthetic saline solution into the bed to attain fluidisation. The pump eliminated a pulsating flow that would otherwise affect the process .The saline solution was stored in a plastic 25 L tank which was continuously agitated to eradicate concentration gradients.

A peristaltic pump (Watson Marlow 505s) was used to pump the calcium hydroxide suspension into the column through an inlet port positioned 15 cm from the bottom of the reactor. The calcium hydroxide suspension was stirred to ensure homogeneity in a 25 L tank.

The product was harvested from the bottom of the reactor from an outlet port situated 5 cm above the reactor inlet just above the glass beads. Harvesting was done by intermittently opening a ball valve through which large particles, that have migrated to the bottom of the bed, exit provided there is sufficient force to keep the bed fluidised. The treated aqueous stream overflowed from the top of the reactor and was collected in waste tanks. Table 4.1 below shows preliminary calculations for the fluidised bed comprised of silica seeds.

Table 4.1: Fluidised bed characteristics

Parameter	Value
Silica particle diameter (μm)	200-300 ($\bar{x}$ = 250 μm)
Silica Density (kg/m^3)	2650
Liquid viscosity (cP)	1
Liquid Density (kg/m^3)	1000
Silica Density (kg/m^3)	2550
Galileo number (see fluidisation section)	1937
Reynolds Number (see fluidisation section)	1.314
Minimum fluidisation velocity (m/s)	0.0026
Maximum fluidisation velocity (m/s)	0.025
Residence time (min)	± 2

Samples were filtered using a Vacutec oil-less piston vacuum pump, Buchner funnel and Whatman™ Cellulose Filter Paper (20 nm pore size). Sulphate, magnesium and calcium ion concentrations were determined using the Spectroquant® NOVA 60A photometer (± 5ppm). Sulphate concentrations were determined through turbidity measurements from the reaction with barium sulphate. Calcium and magnesium concentrations were determined photometrically when the ions react with phthalein purple to form a violet dye (Merck, 2013). The Hannah instruments: pH121 Microprocessor pH meter was used for pH measurements. SEM analysis was also used in this study.

4.3 Design of experiments

4.3.1 Reagents

A varying system composition typically encountered in industry was chosen. Synthetic solutions of total salt concentration varying from 1.5 to 120 g/l were prepared using analytical grade chemicals (Merck). Of the total sulphate salts, 80 %salt was magnesium sulphate, calcium sulphate remaining at its saturation concentration (except when the total salt concentration is below the calcium sulphate saturation concentration), with the remainder being sodium sulphate. The composition of the synthetic streams are presented in Table 4.2.

Table 4.2: Synthetic waste stream composition

	Concentration g/L					
Sulphate salts	**1.5**	**8**	**15**	**35**	**50**	**120**
$CaSO_4$	0.15	1.5	1.5	1.5	1.5	1.5
$MgSO_4$	1.2	6.4	12	28	40	96
Na_2SO_4	0.15	0.1	1.5	5.5	8.5	22.5

A 20 wt.% $Ca(OH)_2$ analytical grade suspension (in water) provided by Lhoist was used. Before use, the suspension was agitated using a pitched blade impeller for 1 hour and diluted to a 4 wt.% suspension using a saturated solution of calcium hydroxide to avoid changes in the solid PSD.

Table 4.3 presents the amount of calcium hydroxide suspension required for experiments conducted across the range of concentrations presented in Table 4.2. The amount of calcium hydroxide is fed in stoichiometric proportion to sulphates in the stream, that is a stoichiometric Ca: SO_4 molar ratio.

Table 4.3: Amount of calcium hydroxide suspension required for each concentration

Feed concentration (g/L)	Feed flowrate (g/min)	$Ca(OH)_2$ required (g/L of feed solution)	$Ca(OH)_2$ flowrate (g/min)
1.5	200	0.90	0.18
8	200	4.81	0.96
15	200	8.99	1.8
35	200	20.9	4.2
50	200	29.9	6.0
120	200	71.6	14.3

Table 4.4 presents the amount of calcium hydroxide suspension required for experiments conducted on the ratio of calcium to sulphates in the feed stream.

Table 4.4: Amount of calcium hydroxide suspension required

Calcium to sulphate ratio	$Ca(OH)_2$ (g/L synthetic stream)
0.5	10.46
1	20.92
2	41.84
4	83.68

The silica seeding material used had an initial PSD of 200-600 μm which was narrowed to 200-300 μm ($\bar{x}$ = 250 μm) using a mechanical sieve (Fritsch Spartan). Table 9.1 in the Appendix lists the composition of the seeding material. All reagents were stored at room temperature and pressure.

4.4 Experimental Procedure

The reactor was loaded with a batch of silica seeds, to make up a bed height of 30 cm. The synthetic solution was pumped into the bottom of the column at a volumetric flowrate of 200ml/min to attain fluidisation of the bed. A flowrate of 200 ml/min was chosen as it provided sufficient fluidisation of the seeds and good mixing, visually. The fluidised bed reached a height of 57±3 cm. Calcium hydroxide suspension was pumped into the reactor at a flowrate that matched the amount required for each experiment as detailed in Table 4.5 above. Table 4.4 Appendix displays the amount of calcium hydroxide required for each concentration investigated. The reactor was run for 3 hours to achieve continuous operation, with intermittent product removal as required per run. Operation for longer than 3 hours is possible, however the laboratory has logistical limitations on the amount of waste that could be generated. Fluctuations in effluent concentration was negligible after 25 min of operation and the system was assumed to be in pseudo-steady state with respect to sulphate and magnesium concentration in the effluent stream.

The effluent was sampled to determine the gypsum conversion, amount of fines and pH. 125 ml of effluent was collected every 30 min during a 3hr operation period. Of the 125 ml, 10 ml was filtered and the amount of fines was quantified by dissolving the filtrate in 10 ml of 0.5 M HCl solution. The concentrations of each of these samples was determined using the Spectroquant as described above. The pH of the effluent was measured every 15 min by taking 50 ml samples and was measured using the pH meter. The harvested product was placed on absorbent paper to dry before being analysed using SEM imaging. Fines were also analysed using SEM after filtration and drying.

4.5 Experimental plan

Table 4.5 presents a summary of experiments conducted.

Table 4.5: Experimental break down

Objective	Variable	Measured parameter
Investigate the effectiveness of fines reduction through the use of seeds	• Silica seeds • No seeds	Residual sulphate and magnesium concentrations. Solid sulphate (gypsum), magnesium (magnesium hydroxide) and calcium concentrations
Investigate the conversion of sulphates and magnesium and the recovery of gypsum and magnesium hydroxide in a seeded fluidised bed crystalliser as a function of pH	pH / amount of calcium hydroxide	Residual and solid sulphate, magnesium and calcium concentrations and pH.
Investigate the conversion of sulphates and magnesium and the recovery of gypsum	• Gypsum seeds • silica seeds	Residual and solid sulphate, magnesium and calcium

and magnesium hydroxide in a seeded fluidised bed crystalliser as a function of seed type		concentrations. Visual observation of fluidisation
Investigate the conversion of sulphates and magnesium and the recovery of gypsum and magnesium hydroxide in a seeded fluidised bed crystalliser as a function of feed concentration	Feed concentration (1.5 – 120 g/L). See Table 4.2: Synthetic waste stream composition	Residual and solid sulphate, magnesium and calcium concentrations
Investigate the effect of excess calcium hydroxide on the conversion sulphates and magnesium.	Calcium hydroxide to sulphate ratio (0.5 – 4) for a solution concentration of 35 g/L	Residual and solid sulphate, magnesium and calcium concentrations
Compare a process alternative which could potentially recover magnesium hydroxide and gypsum separately	Process alternative for a 35 g/L feed solution	Recovery and conversion of sulphates and magnesium

Each experiment was repeated twice at random to ensure reproducibility. The experimental procedure followed is detailed below.

5 Results

This section of the report presents and discusses thermodynamic modelling followed by experimental results.

5.1 Thermodynamic modelling

5.1.1 Solubility diagrams and conversion

The precipitation process was simulated using OLI Systems Stream Analyser ™ to investigate the solubility of compounds and the amount of solids expected in the system as a function of pH for a synthetic multicomponent stream of 3.5 wt. % salts, with the composition described in Table 4.2. (T= 25°C; P = 1 atm) using calcium hydroxide as a base reagent. The results are displayed in Figure 5.1.

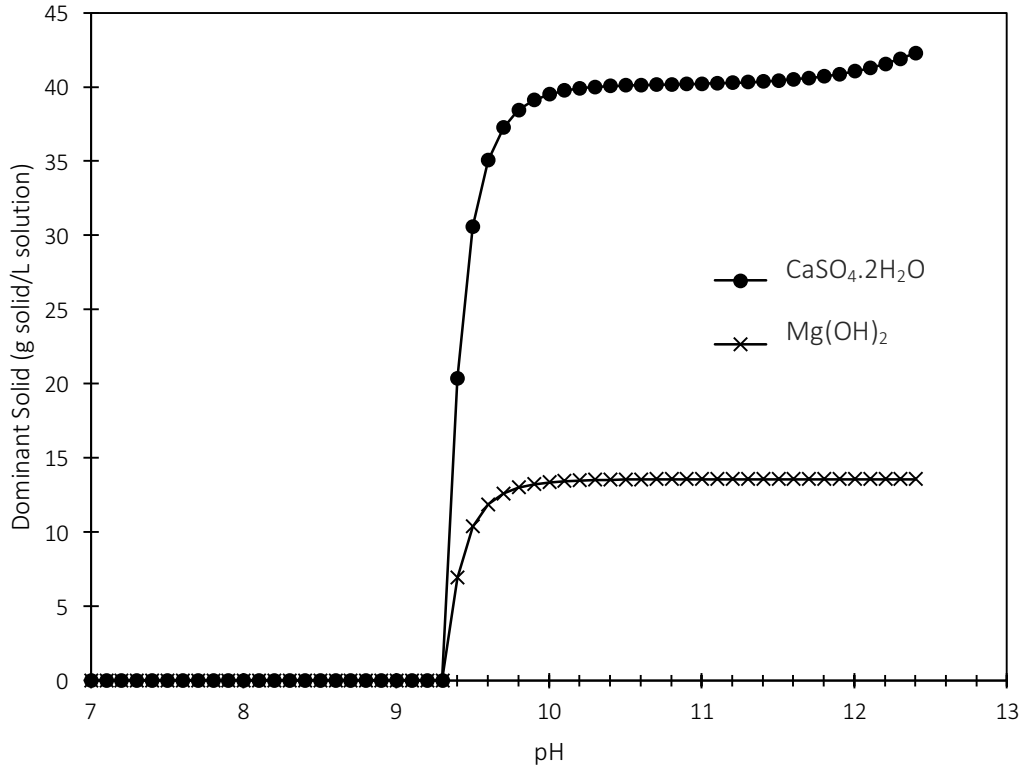

Figure 5.1: Dominant solid prediction for $CaSO_4$-$MgS0_4$-$Ca(OH)_2$-H_2O system as a function of pH

Figure 5.1 above shows that magnesium hydroxide and gypsum start precipitating out at a pH of 9.1. There is a steep increase in the amount precipitated until a pH of around 9.5 for both solids. The amount of gypsum precipitated increases sharply in the range of pH 9 to 10 and follows the same trend as magnesium hydroxide. The reason for the similarity is because calcium and hydroxide ions are released from the same source. After a pH of 10, there is no significant change in precipitate concentration. This is because above pH 10, most of the magnesium in the system has been removed from solution and a very small base addition is sufficient to to promote a pH increase. Therefore, in the pH range of 10 -11.5, a small amount of calcium hydroxide is added with no additional gypsum formation. To increase the pH further, from 11.5 to 12.44, more calcium hydroxide is added, provoking the observed increase in gypsum formation.

For this particular stream composition, the maximum amount of gypsum that can be precipitated is approximately 42 g/L and is 46 g/L for a binary system. In the case of magnesium hydroxide, approximately 14 g/L can be expected for the multicomponent stream as well as a binary system. The maximum amount of a precipitate formed in a multicomponent system may be less than for binary systems of the same initial concentration, due to ion interactions. This means that some ions are unavailable to participate in the reaction and this accounts for the discrepancy between a multicomponent and binary system. When comparing the equilibrium conversion of magnesium hydroxide in a binary system with the theoretical multicomponent conversion, there is no significant difference. However, the expected conversion of sulphate is slightly lower. This lower conversion was investigated with further thermodynamic modelling presented in the following sections of this dissertation.

Thermodynamic modelling was extended to investigate the maximum conversion attainable across a range of concentrations typically encountered in industry (see Table 4.2 in methodology). These results are displayed in Figure 5.2.

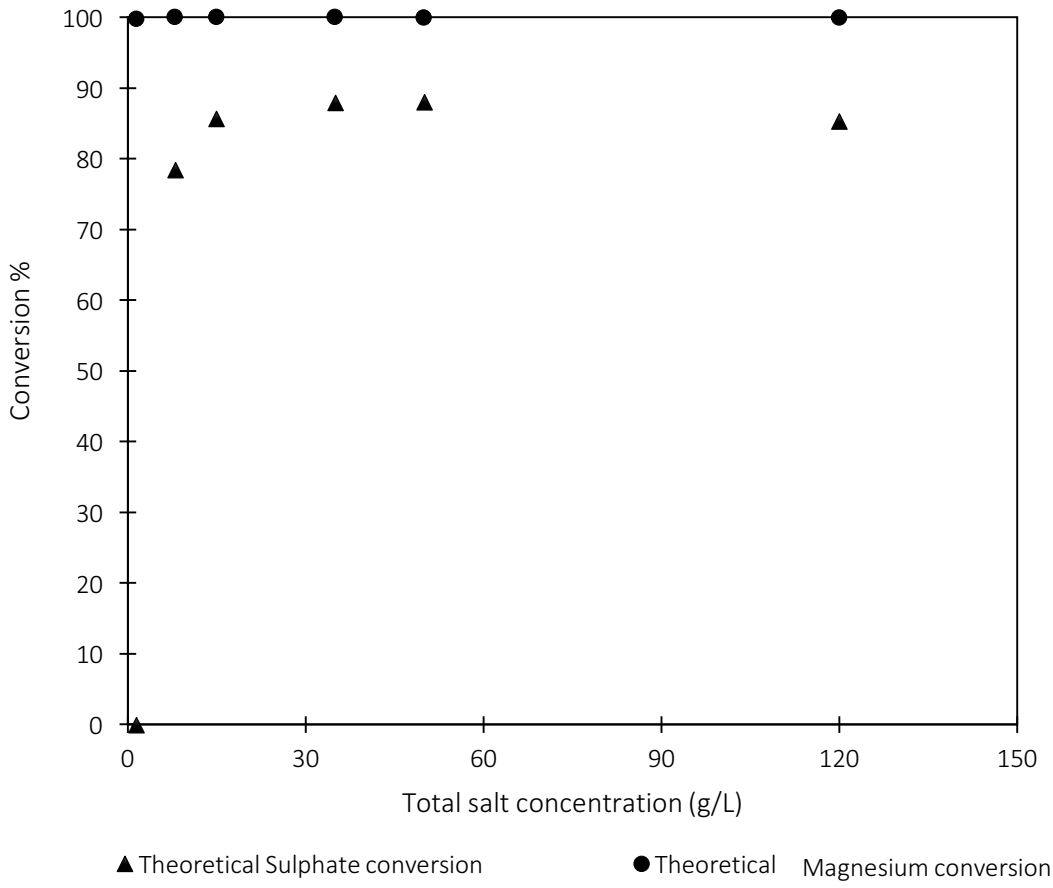

Figure 5.2: Maximum sulphate and magnesium conversion obtained when calcium hydroxide (fixed $Ca:SO_4$ Ratio of 1:1) is reacted with a synthetic stream of varied sulphate salt composition (described in Table 4.2).

As shown in Figure 5.2, the maximum conversion of magnesium remains constant at around 99 %, with no significant deviation across the range of concentrations, because the increase in total salt concentration has

no effect of the solubility of magnesium hydroxide. This high conversion is due to the low K_{sp} (1.8×10^{-11}) value of magnesium hydroxide and its relatively high concentration. The conversion of magnesium is higher than for sulphate because magnesium hydroxide is orders of magnitude less soluble than gypsum.

Sulphate conversion shows an overall increase. At low concentrations (1.5 g/L salts), sulphate conversion is zero because the system is undersaturated with respect to gypsum, resulting in no precipitates forming. At salt concentrations of 8 g/L to 35 g/L, there is an increase in the expected conversion up to 88%, which remains fairly constant at higher concentrations. At 120 g/L, however, sulphate conversion decreases slightly from 88% to 85%. This trend in sulphate conversion is counter-intuitive, because the conversion of sulphates is expected to increase as the amount of sulphates in the system increases, however, the conversion increases slightly and begins to decrease. This reveals that sulphate ions are not available for the reaction forming gypsum.

The reason for this effect on sulphate ions is due to the solution composition. An increase in the total salt concentration in the feed stream means that the relative amounts of magnesium and sodium in the system are also increased. Both these salts are known to affect the solubility of calcium sulphate in a number of competing ways (Spiegler et al., 1980; Murray, 2004). In order to predict the effect of these salts, the activity of calcium and sulphate ions were modelled using OLI Systems Stream Analyser ^{TM}. Figure 5.3 shows the effect of sodium and magnesium on sulphate and calcium activity coefficients.

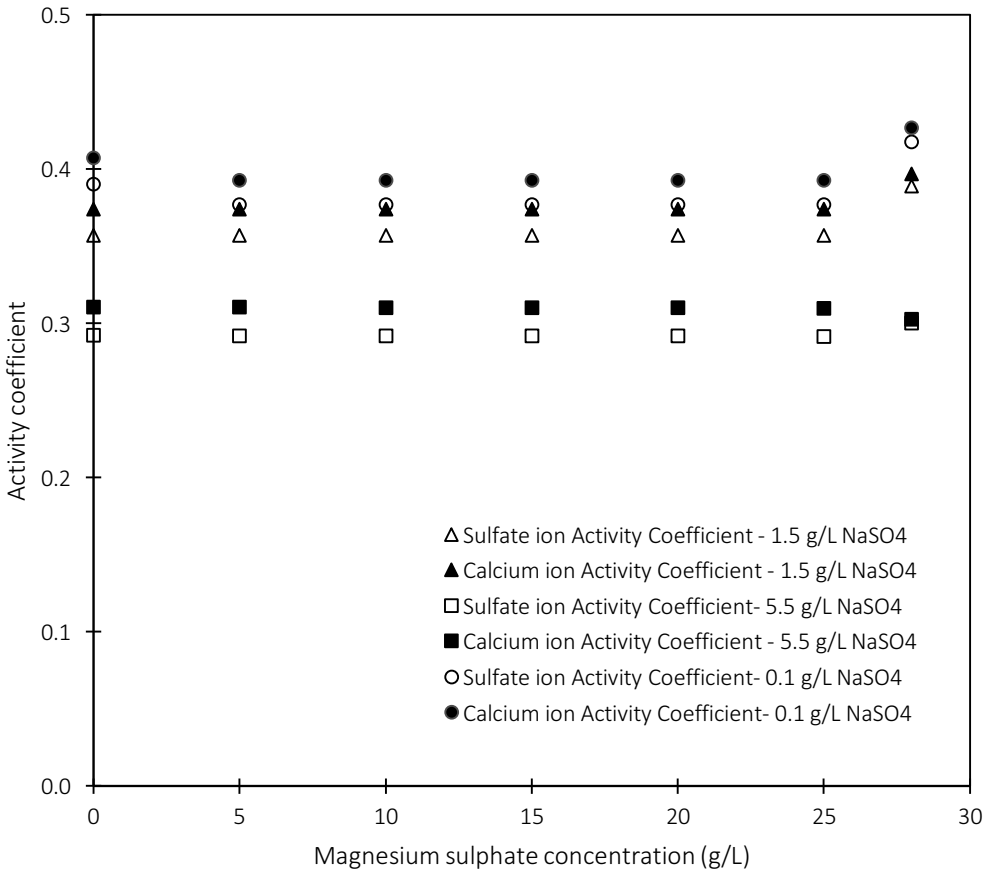

Figure 5.3: Effect of sodium and magnesium on sulphate and calcium activity

The activity coefficients of both calcium and sulphate are significantly lower than one, meaning that a large amount of these ions are not available to react. Figure 5.3 shows that the activity coefficients are not strongly influenced by the presence of magnesium. However, an increase in sodium results in a decrease in the activity coefficient for both calcium and sulphate ions. Sodium sulphate concentrations of 5.5 g/L decrease activity coefficients by approximately 0.1 from 0.4 at 0.1 g/L. This deviation caused by a slight increase in sodium is quite significant and can be induced in a number of ways. A reason for the decrease in sulphate activity is complexing or speciation, that is, the formation of ion pairs in solution. Thermodynamic modelling was used to predict the possible species expected in this multicomponent system and is displayed Table 9.2 in the appendix. It was found that sulphate ions are prone to form ion pairs, particularly in the presence of sodium ions, which is agreement with the trend observed in Figure 5.3.

In addition to complexing, the common ion effect is also known to affect the solubility of gypsum (Spiegler et al., 1980). The presence of the common sulphate ion shared by sodium and magnesium sulphate lowers the solubility of gypsum, thus causing gypsum to precipitate. However, this would result in higher sulphate conversions and contradict the findings in Figure 5.3. This effect may in fact be present in the system, but is instead offset by other stronger effects. Another effect of the common ion is the calcium ion shared between calcium sulphate and calcium hydroxide. The driving force for calcium hydroxide dissolution is the consumption of calcium and hydroxide ions in their respective reactions forming gypsum and magnesium hydroxide. If the dissolution of calcium hydroxide is limited by the calcium in solution as a result of the equilibrium concentration of calcium sulphate, the formation of gypsum is hindered, corresponding to the trend observed in Figure 5.2. Thermodynamic modelling found that this was in fact the case, where the addition of equilibrium concentrations of both calcium sulphate (1.5 g/L) and calcium hydroxide (1.8 g/L) resulted in some calcium hydroxide not being dissolved. The model was then extended to include the effects of magnesium sulphate, which showed that the dissolution of calcium hydroxide was then driven by the consumption of hydroxide ions to form magnesium hydroxide. The effects of sodium sulphate in comparison to magnesium sulphate was then investigated and found that for stoichiometric amounts of sulphate (in the form of magnesium sulphate or sodium sulphate), the amount of gypsum formed in the presence of magnesium (3.5 g/L of gypsum) was higher than in the presence of sodium (1.9 g/L of gypsum). This finding is in agreement with the trend observed for calcium and sulphate activity coefficients in Figure 5.3.

This effect on sulphates caused by sodium in comparison to magnesium is as a result of electrostatic interactions between ions. In the presence of sodium and magnesium ions, the tendency for sulphate and calcium ions to become shielded because of hydration, is amplified. However, due to magnesium's, higher charge density, the extent to which it is shielded from sulphate and calcium ions is higher compared to sodium. This means that sodium readily pairs with sulphate ions and the pair is then hydrated and shielded from calcium ions in solution. Whereas magnesium ions are not readily paired with sulphate ions, leaving calcium and sulphate ions to form gypsum (Murray, 2004). This is in agreement with the thermodynamically modelled and experimental results obtained in a study by Kadambi and co-workers (1998) which predicted the effects of sodium and magnesium on the solubility of calcium sulphate. Figure 5.4 summarizes the mechanism of precipitation for this system.

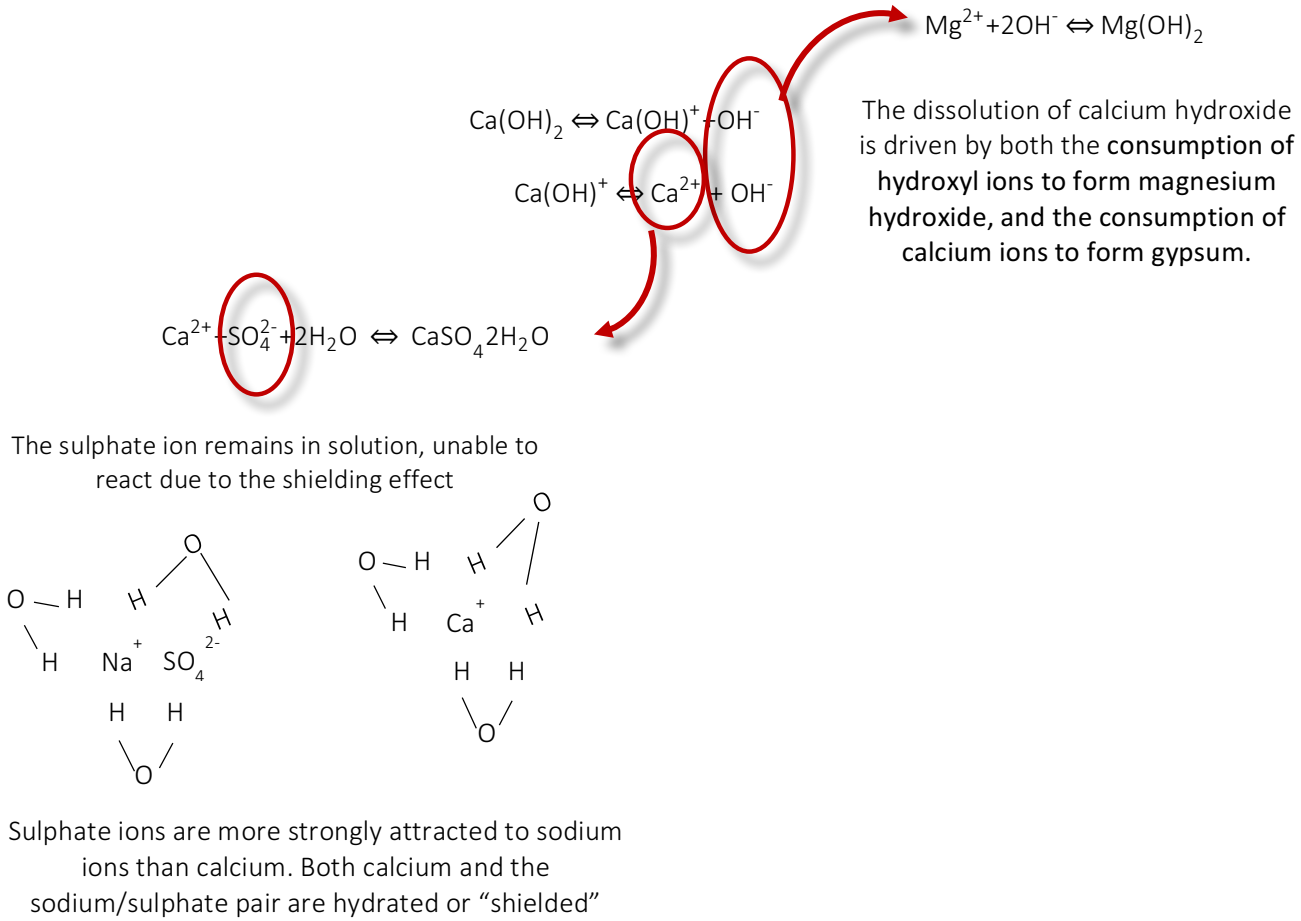

Figure 5.4: Summary of precipitation mechanisms for $CaSO_4$-$Ca(OH)_2$-$MgSO_4$-H_2O system

5.1.2 Supersaturation estimation

Supersaturation estimations were determined as a tool to identify potential crystallization mechanisms occurring in the system. Thermodynamic modelling was used to approximate activity coefficients to calculate global supersaturation values. Table 9.3 and Table 9.4 in the appendix show detailed supersaturation calculations for magnesium hydroxide and gypsum respectively, while Figure 5.5 is a graphical representation of these results.

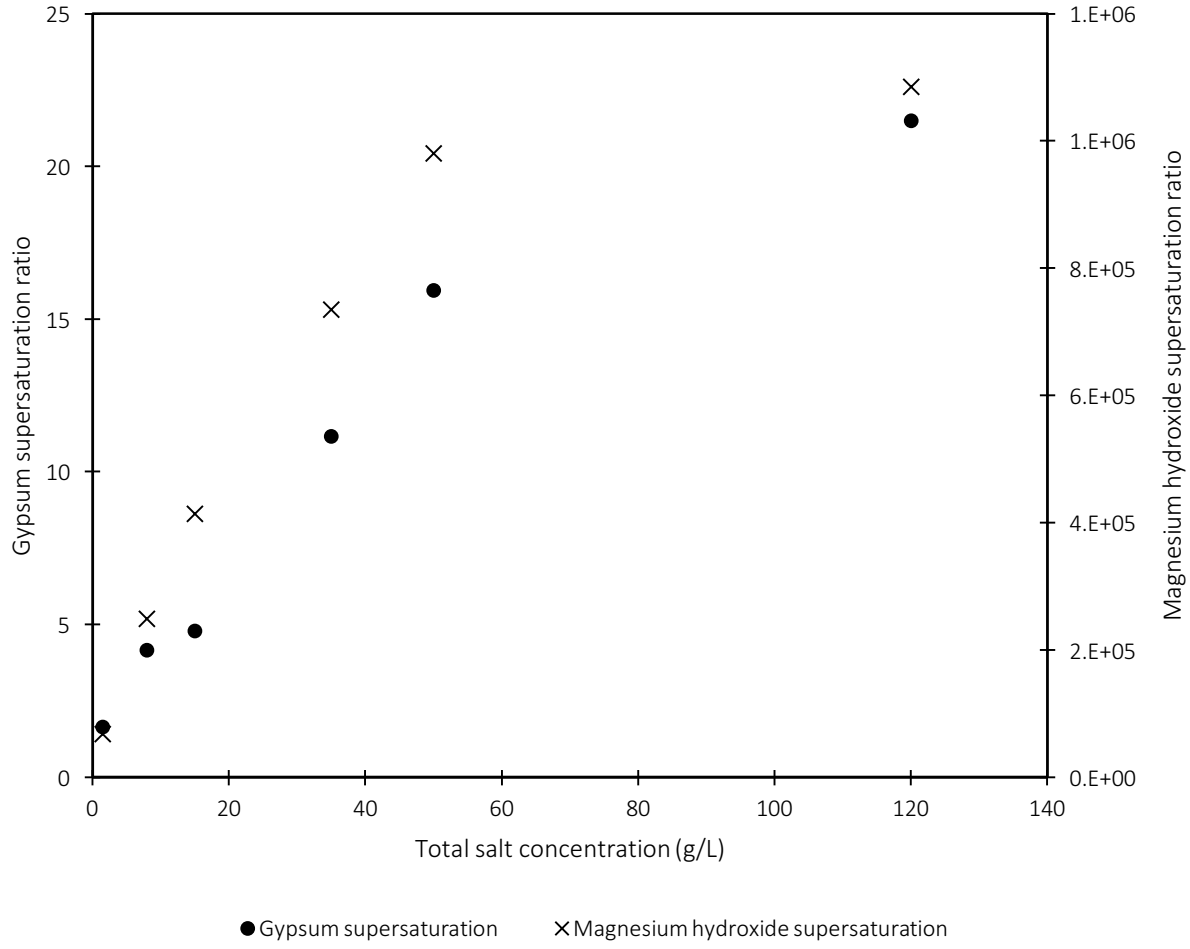

Figure 5.5: Supersaturation of gypsum and magnesium hydroxide at varying feed concentrations with the addition of calcium hydroxide as a base reagent

From Figure 5.5 it can be seen that the supersaturation of gypsum increases with increasing salt concentration, as expected. There is a steep increase from 1.5 g/L to 50 g/L and a gradual increase from 50 g/L to 120 g/L. This trend is a result of the decrease in activity coefficients at higher concentrations investigated in Figure 5.3. The supersaturation of magnesium hydroxide follows the same trend as gypsum, with a steep increase at concentrations 1.5 g/l to 50 g/l and a gradual increase from 50 g/L to 120 g/L. It should be noted that the supersaturation of magnesium hydroxide is 5 orders of magnitude larger than that of gypsum, due to magnesium's lower K_{sp} value. Magnesium hydroxide is therefore expected to precipitate out much faster than gypsum due to its very large driving force, however, this is not always the case because other factors may influence the kinetics as shown in equation 5 and equation 6.

It should be noted that supersaturation estimations are based on the assumption that reactants mix completely without the precipitation reaction occurring. It would therefore represent a hypothetical pre-mixer of the fluidised bed. However, realistically, the precipitation reaction occurs when reactants are contacted, thus lowering the prevailing supersaturation.

5.2 Batch Experiments

Preliminary batch experiments were conducted to establish feasible operating conditions. This section discusses findings on general observations, pH, fluidisation and feasible regions of operation.

Stoichiometric amounts of calcium hydroxide suspension to the amount of sulphates in the feed stream resulted in a pH of 10 when mixed, while excess amounts of calcium hydroxide gave a pH of around 12, which is typically the pH of calcium hydroxide. However, the control of pH was not pursued due to the low solubility of the calcium hydroxide suspension which limit the operable pH range.

The first part of this work was carried out using two different kinds of seeds. Initially, gypsum seeds ($\bar{x}$ = 10 μm) were used, but only partial fluidisation was achieved, with channelling and bed compaction observed at lower regions of the reactor. Fluidisation of this compacted zone was not achieved at higher fluid velocities even, and seeds were elutriated out of the bed. The particle size of gypsum available was found to limit fluidisation. Gypsum seeds were categorised as group C particles according to Geldart's classification of powders (1973). These particles are known to cause channelling in beds due to strong inter-particle forces and are thus unfavourable for fluidisation. Compaction of the bed was attributed to the weight of the seeds that make up the remaining height of the bed, coupled with the tendency of gypsum to coagulate. Channelling of the bed resulted from alternating regions of high and low resistance in the compact bed. This resulted in a non-uniform flow distribution of the fluidising stream attempting to penetrate through the compact bed.

A second attempt at fluidisation involved using silica seeds. Silica seeds of 200-300 μm ($\bar{x}$ = 250 μm), making up a 30 cm bed height, were fluidised. This is as expected, since silica seeds belong to group B of Geldart's classification of particles, in which particles exhibit good fluidisation characteristics. Seeds were coated within a few minutes, as opposed to what was seen in other fluidised bed operations. Seckler (1994) found that after three hours of operation with a system at 5-100 mg/L of phosphate, effluent concentrations were constant and thus removal efficiency increased, due to a complete layer of calcium phosphate covering the silica layer and remained constant thereafter. Guillard and co-workers (2001) found that their system (50-150 mg/L) required a 48 hour 'start up' period in which silica particles were coated, before experiments were conducted. The reason for the difference in time required for silica coating is due to the significant concentration differences compared to the system in this study (1 500-35 000 mg/L). The rate at which mass is deposited is expected to be higher at higher concentrations and the mechanisms of attachment may differ, thus covering the silica surface occurs faster. Previous studies reported a compact mineral layer, while results in this study showed attachment of distinct primary crystals (see Figure 9.17 in appendix), indicating that nucleation is occurring, crystal growth and agglomeration is occurring.

It was found that a 20 wt.% calcium hydroxide suspension caused channelling in the bed and pumping challenges as a result of its solid content and viscosity. A gel like substance, characteristic of hydroxides (Neal and Stanger, 1984) remained fixed in higher regions of the bed (Figure 9.7). The calcium hydroxide suspension was diluted to 4 wt.% to allow for better control of the reagent and easier pumping to avoid blockages.

5.2.1 The effect of seeds on fines formation

Preliminary experiments were conducted to determine what effect the presence of silica seeds had on the formation of fines and the amount lost in the effluent stream. Figure 5.6 shows the results obtained.

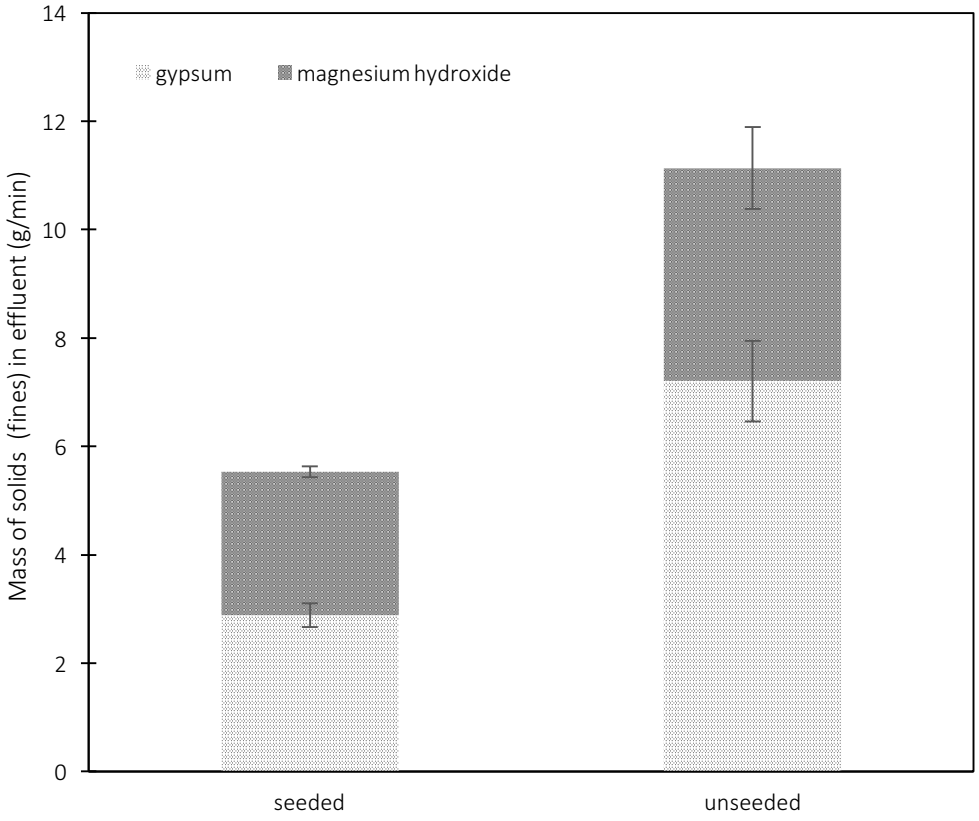

Figure 5.6: Effect of seeds on the formation of fines

The amount of fines exiting the reactor in the presence of seeds is lower (almost half) than when there are no seeds for a 35 g/L synthetic solution (S = 11.2). This is in agreement with literature, which found that the presence of seeds promotes crystal growth on its surface (Seckler, 1994; Guillard and Lewis, 2001), however, this is true for low concentrations and/or low levels of supersaturation. It is also agreed upon that seeds provide a surface for attachment for particles through agglomeration (van Hille et al., 2002), which is the likely mechanism in this case, given that supersaturation conditions favour this (Lewis et al., 2015). Figure 5.6 shows that the amount of gypsum and magnesium fines in the presence of seeds is lower than in the unseeded case, as expected. The formation of fines in the presence of seeds implies that there is in fact heterogeneous, homogeneous and/or secondary nucleation. Nucleation mechanisms are promoted at high degrees of supersaturation because seeds reduce the energy required for heterogeneous nucleation. Another source of fines is through attrition, where crystals break as a result of collisions, however, the morphology of the fines indicate well defined edges (Figure 9.9), as opposed rounded and undefined crystals which is characteristic of crystals that have undergone attrition. The formation of fines is therefore caused by nucleation mechanisms. This means that even though fines are produced, the presence of seeds does in fact decrease the amount of

product lost in the effluent stream. For a complete understanding, the conversion of sulphates and magnesium is presented in Figure 5.7.

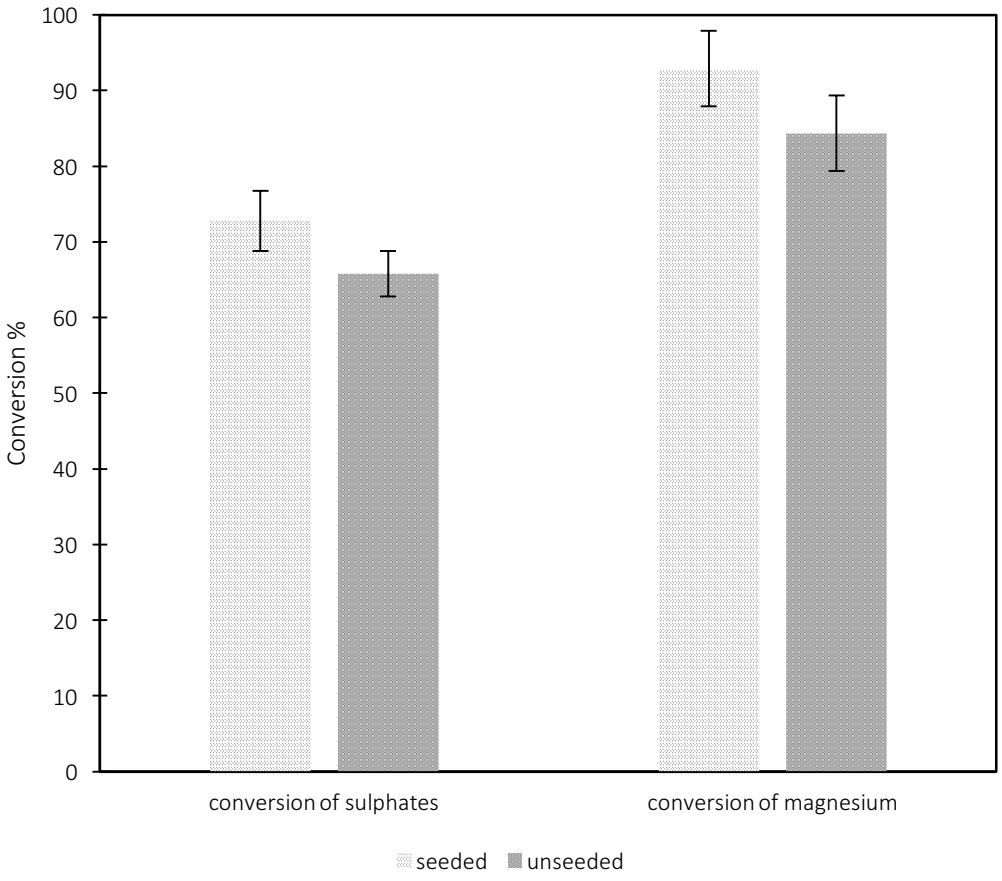

Figure 5.7: Effect of seeds on sulphate and magnesium conversion

Both sulphate and magnesium conversions are higher (7% and 9% increase, respectively) in a seeded fluidised bed than in the absence of seeds. As mentioned above, the presence of seeds themselves may increase conversion due to the lowered energy requirement for nucleation. This means that more nuclei are formed faster compared to the unseeded case, resulting in higher sulphate and magnesium conversions. However, it should be noted that the unseeded case is not entirely unseeded. Calcium hydroxide solids in the suspension used, act as seeding material, which may also lower the activation energy for nucleation by decreasing the surface energy as do silica seeds. Also, the formation of the first nuclei act as seeding material and should in fact lower the activation energy to a larger extent than silica seeds because of a lower wetting angle for gypsum seeds (Mullin, 2001). Further to this, according to Seckler (1994), small particles with large surface areas grow faster. Fines would thus be expected to an ideal seeding material while in the bed. Therefore, the main difference in between the two cases is rather the amount and type of seeds.

The difference in conversions for the two cases is rather due to the residence time distribution in each reactor. The residence time in the seeded case has a wider distribution than that in the unseeded case, due to the

resistance to flow induced by the seeds. The resistance causes the fluidising stream to travel different paths of least resistance, compared to the 'unseeded' case. This varied residence time may account for the increase in sulphate and magnesium conversions simply because some ions spend a longer time in the reactor. on the contrary, seeds assure homogenization of the fluidising stream, and could promote a uniform velocity profile. However, it was also observed that in the presence of seeds, calcium hydroxide was dispersed more thoroughly in the bed by the seeds than in the absence of seeds, where calcium hydroxide remained as a gel without being effectively dispersed. This means that seeds facilitate the dissolution of calcium hydroxide, which would supply hydroxyl and calcium ions for the respective reactions that yield higher sulphate and magnesium conversions.

5.2.2 Operating region

Preliminary batch experiments found that large amounts of precipitate formed at feed concentrations of 50 g/L and higher, making it impossible to operate in this concentration range. Precipitates formed rapidly and carried the silica out of the bed. The resulting highly viscous reactor contents became too heavy and the fluidisation velocity became ineffective. At 1.5 g/L no visible changes to the seeding material was observed in terms of coating. Thus, the "total salt concentration" range for feasible operation has been identified to be between 8 and 35 g/L.

5.3 Morphology

This section presents and discuses the morphology obtained using SEM analysis of the fines elutriated and product grains harvested.

5.3.1 Product grains

The harvested crystals were analysed in order to establish if there was a relationship between the morphology and removal efficiency of the process. Figure 5.8a-e are SEM images of the products harvested for the concentration ranges reported in Table 4.2, with their corresponding supersaturation values presented in Figure 5.5.

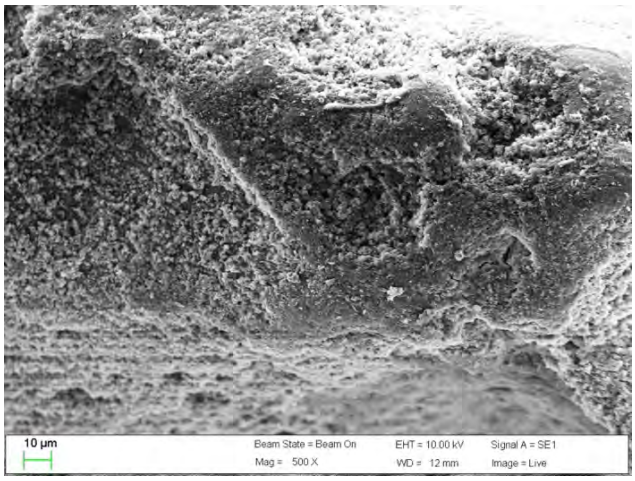

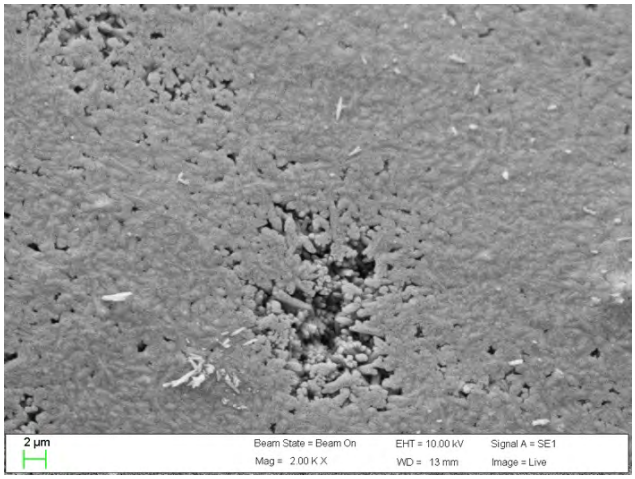

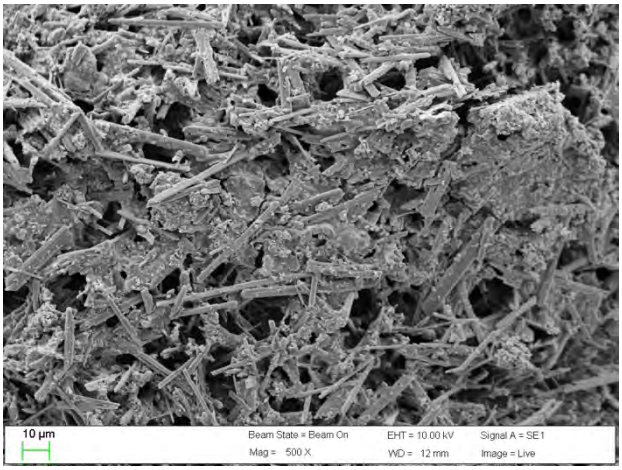

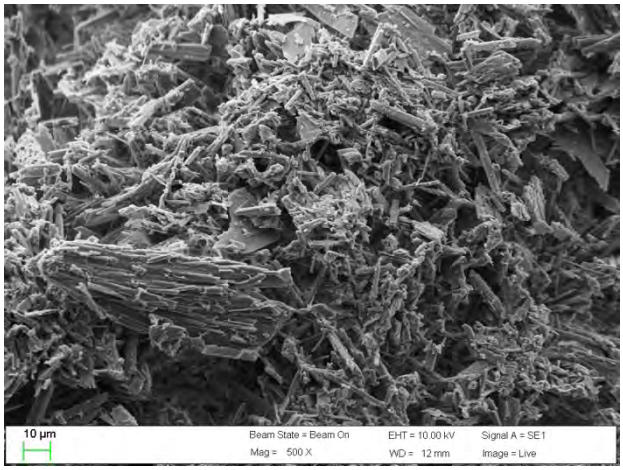

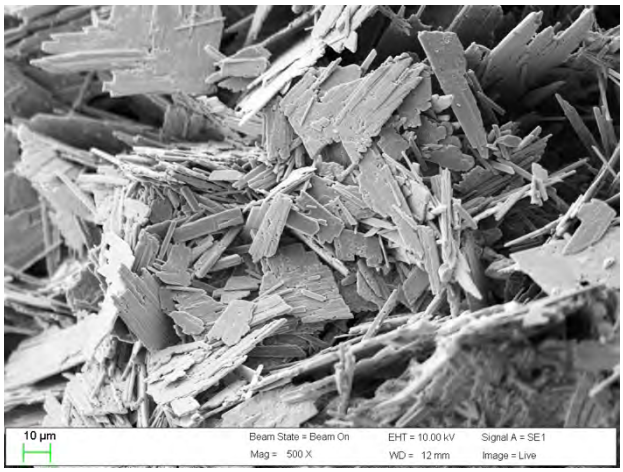

Figure 5.8: a-e: SEM images of product surfaces for 1.5; 8; 15; 35 and 120 g/L

There are distinct differences in product morphology across the range of concentrations investigated. Figure 5.8a shows the silica surface after 2 hours of operation for a feed salt concentration of 1.5 g/L (S_g =1.7). When compared to the surface of the starting seed material (Figure 9.13) there is no significant difference.

The product surface for 8 g/L (S_g = 4.2) showed significant differences from the starting material surface. There appears to be a compact mineral layer of needle shaped crystals arranged in a methodical packing. The crystallographic angle of these crystals may be at 90° to the heterogeneous surface, due to the orientation of the needles in Figure 5.8b which is characteristic of gypsum (Howard et al., 2010). This is most likely an indication of surface nucleation mechanisms, expected in the presence of seeding material at low levels of supersaturation (Mullin, 2001; Lewis et al., 2015). The surface appears to be smooth, which may also be due to abrasion at lower regions of the bed where energy dissipation is the highest. There are a small number of needle-like crystallites (≤ 2 μm in length) scattered on the surface of the particle, which indicates that gypsum nucleation occurred to a small degree. This is not uncommon since zones of high and low supersaturation can exist in a reactor.

At 15 g/L (S_g = 4.8) there are monoclinic prismatic crystals 20 – 40 μm in length, arranged on the surface. There seems to be a thick layer of this arrangement, with irregular shaped agglomerates nested into the structure. There appears to be nano-agglomerates embedded in the crevices of the surface, which may be magnesium hydroxide or undissolved calcium hydroxide. It is expected that calcium and magnesium hydroxide are prone to attachment onto the silica surface because they possess a weak surface charge and have surfaces with a high affinity to hydrogen bonding. When compared to 8 g/L, the product grain surface is significantly different, while the change in supersaturation ratios is only slight (from 4.2 to 4.8). This indicates that the switch over from a growth dominated mechanism to nucleation-attachment mechanism occurs within a narrow supersaturation range. The increase in primary crystal sizes at 15 g/L is due to the influence of supersaturation on the growth rate of gypsum. The rate is second order with respect to supersaturation, due to the dependence on the concentration driving force. In the two step growth model, the increase in supersaturation favours the surface reaction (Equation 12), leading to higher growth rates and thus larger crystals (Aldaco et al., 2007). This increase in growth rate at high concentrations is in agreement with studies on most crystallization systems. (Tai et al., 2001; Hirasawa et al., 1990 and Seckler, 1994). Therefore, at 15 g/L, the nucleation rate and the growth rate have increased.

At 35 g/L (S_g = 11) the product surface is irregular with randomly attached crystallites. Primary crystal lengths have decreased in length (≤ 10 μm) compared to those on the surface of the 15g/L run, however the presence of larger poly-crystalline aggregates of possible gypsum, as well as a few plate-like structures are evident. The decrease in the size of crystals could be due to attrition and abrasion because the amount of solids in the bed has increased through a) the larger amount of solids in the calcium hydroxide suspension required and b) the amount of solids formed due to the faster crystallization rate induced at higher levels of supersaturation. However, the crystals have preserved their structural shapes, which is uncharacteristic of crystals undergoing attrition because crystal abrasion results in rounded edges, rather than sharp defined edges. High supersaturation levels may have promoted nucleation, where a large number of small particles are formed, hence the smaller sized particles. However, despite the decease in primary crystal sizes, the presence of large

polycrystalline structures indicate that agglomeration mechanisms may be favoured at this degree of supersaturation (S_g = 11).

Primary crystal morphology changed from monoclinic prismatic/needles at lower concentrations to platelets at 120 g/L (S_g = 21). Platelets appear to be poly-crystalline agglomerates, or more than one platelet crystal joined together but size enlargement through growth is also possible. This is in agreement with literature, which reported platelets of gypsum crystals forming at high levels of supersaturation (Seewoo et al., 2004; Lewis et al., 2002; Christoffersen, 1982; Liu and Nancollas, 1970). It is difficult to tell if the platelets were formed initially, and by virtue of their morphology, remained entrained in the bed while needle shaped particles were elutriated. The other possibility could be that needles attached on to the seeds and subsequently morphed into platelets because they were exposed to a highly supersaturated environment. However, the presence of both plates and needles are not uncommon in regions with supersaturation gradients. The presence of two different morphologies (plates and needles) for different levels of supersaturation is due to the difference in surface energy requirements of each shape. The energy requirement for needles may be lower along the c-axis, but higher in the a-axis, which promotes growth in the c-direction (Howard et al., 2010). At higher levels of supersaturation, there is enough energy to overcome the requirement for growth in the a-axis, allowing the morphology to change from needles to plates.

Overall, the surface of coated particles moves from being characteristically compact to irregular, with primary particles loosely attached, as the concentration increases. This can be seen in Figure 9.15 to Figure 9.18 (appendix A; Section 3). Product grain sizes do not increase appreciably at low concentrations (1.5 - 15 g/L), however significantly large grain diameters of around 1mm were obtained at 120 g/L. It is important to note that grain sizes depend on how long seeds remain in the bed, and are thus functions of the removal rate. Extremely large grains are difficult to harvest as they do not flow easily. Product grains are round and resemble pellets, implying that they possess mechanical integrity which enables harvesting of intact grains that resist disintegration and hydrodynamic shear forces. The retention of sphericity of the product from the seeding material is remarkable, and implies that the arrangement of primary crystals may not be random, but may in fact be influenced by the crystallographic angle at which gypsum can outgrow from a heterogeneous surface. The typical angles at which gypsum grows from a heterogeneous surface are 5° or 90° or 110° (Howard et al., 2010). However, there appears to be layers of crystals, and thus the mechanism of attachment cannot be concluded with confidence. It could also be possible for the silica surface to be coated with a layer of gypsum, followed by surface nucleation, from which crystals grow out at particular angles.

The presence of primary particles may also be an indication of heterogeneous, homogeneous and/or secondary nucleation mechanisms in the system, even though it is desired to initiate growth on silica through two dimensional nucleation. The presence of seeds lower the activation energy required for heterogeneous nucleation, which may have produced nuclei that grew and agglomerated onto the silica surface. Other sources of primary crystals include homogeneous nucleation; however unlikely it may be in this system due to the high solid density. Furthermore, it is well known that secondary nucleation is initiated at the lowest activation energy when compared to other nucleation mechanisms (Lewis et al., 2015). Therefore, the formation of nuclei in the presence of existing gypsum possibly occurred. These mechanisms are also agreed upon by Costodes and Lewis (2006) and Aldaco and co-workers (2007).

5.3.2 Fines

The morphology of crystals elutriated out of the bed was investigated to determine if there was a relationship between the morphology and the likelihood of elutriation. SEM images of these fines from each experimental run were taken and are presented in Figure 5.9a-e.

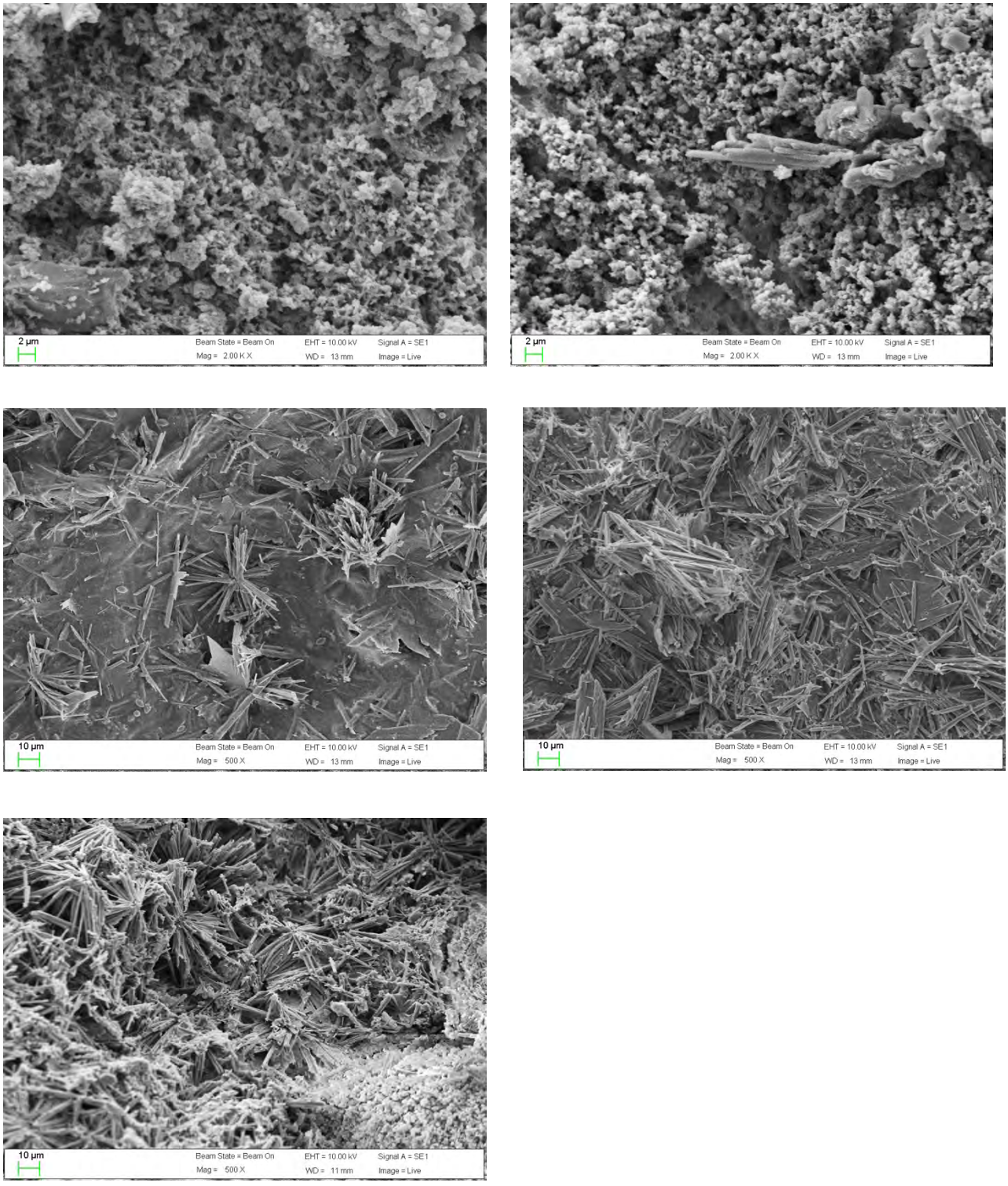

Figure 5.9: a-e: SEM images of fines for 1.5; 8; 15; 35 and 120 g/L

The morphology of fines changes from nano-crystal agglomerates, to needles and plates, across the range of concentrations investigated. Gypsum crystal morphology reported in literature is typically described as exhibiting mostly needle and platelet assemblies with monoclinic, prismatic structures (Shih et al., 2005).

At 1.5 g/L, nano-agglomerates are visible. This is possibly magnesium hydroxide, which is known to form small crystal aggregates (Henrist et al., 2002), due to its high supersaturation (S_m = 6.9 x 10^4). Calcium hydroxide crystals are also known to exhibit this same morphology as magnesium hydroxide. The appearance of crystals of a lighter colour suggests that there was more than one product formed. It is possible for very small gypsum crystals to have formed through nucleation, however, given the low level of supersaturation with respect to gypsum (S_g = 1.7) at 1.5 g/L, there may have been insufficient driving force for growth, resulting in very small gypsum crystals with no distinct shape visible.

At 8 g/L (S_g = 4.2) there is a large amount of nano- agglomerates, possibly magnesium hydroxide and undissolved calcium hydroxide, with a few prismatic agglomerates that is typical of gypsum crystal behaviour. From Figure 5.7, it is expected that gypsum prefers to nucleate onto the sand surface instead of nucleating in the bulk.

At 15 g/L poly-crystalline aggregates that form rosette like structures were visible, as well as monoclinic prismatic crystals of gypsum (Lash and Burns, 1984; Lewis et al., 2002; Shih et al., 2005). There appears to be smaller crystals (± 1μm) scattered amongst larger crystals. The difference in morphologies is quite significant compared to what is observed at 8 g/L even though the change in supersaturation is not significant (S_g = 4.2 at 8 g/L and S_g = 4.8 at 15 g/L).

Fines at 35g/L (S_g = 11) are predominantly plate-like with prismatic agglomerates (10-60 μm). This indicates that plate-like crystals are prone to elutriation due to their surface area compared to needles. However, this is not the only possibility. Crystals may have changed morphology due to high residual supersaturation allowing for crystals to grow above the bed even though they were initially needles.

At 120 g/L rosette structures typical of gypsum crystals are predominant, with regions of nano-agglomerates of magnesium or calcium hydroxide visible (Henrist et al., 2002). Chieng and Nancolas (1982) also reported similar behaviour of magnesium hydroxide in the presence of gypsum and sodium. A study on gypsum scaling in reverse osmosis membranes by Shih and co-workers (2005) found that the morphology of gypsum changed along the membrane from needle like structures to platelets and rod-like structures, forming what is known as spherulites. The reason for this change in morphology is because the membrane experiences a concentration gradient as water is removed. This system is analogous to the changing concentrations investigated and is in agreement with the findings in this study. The formation of spherulites arises from a number of mechanisms that lead to surface nucleation on a 'source' crystal, and is considered to be a growth mechanism. At high supersaturation, crystals nucleate onto a crystal surface, and after exceeding a critical size, can no longer retain the same crystallographic orientation along its perimeter, thus new crystals form along its perimeter and gradually establishes a circular perimeter. Higher levels of supersaturation induce more branches in the polycrystalline aggregate (Granasy, 2005). The presence of these spherulites in the effluent stream may be disadvantageous because their structure may entrain water. Their large diameters

and surface structure may also trap smaller particles, and carry them out of the bed. However, one would expect that crystals of this size (around 60 μm in diameter) would remain entrapped in the bed. It is therefore possible that these crystals form after they have exited the bed through residual supersaturation effects.

Overall, there is an increase in the size of the crystals elutriated, but more importantly, the surface area of individual crystals increase. Needles become longer and morph to plates, with inherently larger surface areas, and finally into large spherulitic structures, 60 μm in diameter. This means that even though crystals are becoming larger and denser and are expected to remain in the bed, their surface structures exposed to the upward force of the fluidising stream is increased, allowing large particles to be elutriated instead. Figure 5.10 summarises these findings.

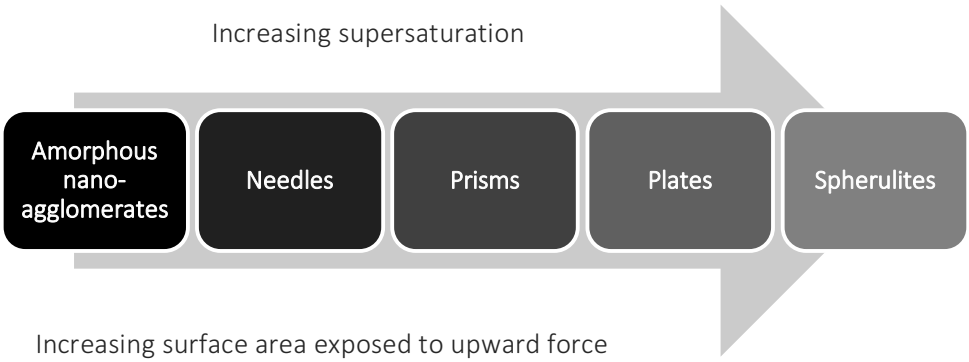

Figure 5.10: Change in morphology of fines elutriated

5.4 Continuous experiments

While batch experiments were helpful in identifying a feasible region of operation, mass accumulated in the column over time and product grains exited the top of the column as expected. Product removal was therefore implemented in order to operate for longer periods of time. The conversion and recovery of sulphate and magnesium during continuous operation of the fluidised bed crystallizer, with intermittent product removal, is presented in this section.

5.4.1 Product harvesting

The fluidised bed was successfully operated in semi-continuous mode with intermittent product removal. At 35 g/L the fast rate of solid accumulation caused the bed to expand rapidly (approximately 6.7 cm/min). Product was harvested at 15 min intervals to avoid elutriation and to continue fluidisation. Steady state with respect to magnesium and sulphate ions in solution was achieved within the first 25 min of operation, after which fluctuations in sulphate and magnesium conversion did not exceed 5%. Operation at concentrations of 15 g/L and 8 g/L did not require frequent product removal as the bed did not expand rapidly and elutriate product grains. It was found that the bed height should remain sufficiently high to disperse calcium hydroxide. An insufficient bed height will cause calcium hydroxide to remain undispersed in the column, because seeds of a certain bed height facilitate mixing. The reactor was operated for three hours, however, it is possible to

operate for longer periods. It should be noted that for longer periods of operation, seeds need to be replenished as they are constantly being harvested.

5.4.2 Feed Concentration

Three synthetic solutions with concentrations of 8, 15 and 35 g/L were chosen to be investigated, based on the feasible range identified in the previous section. The experimental results obtained are presented in Figure 5.11.

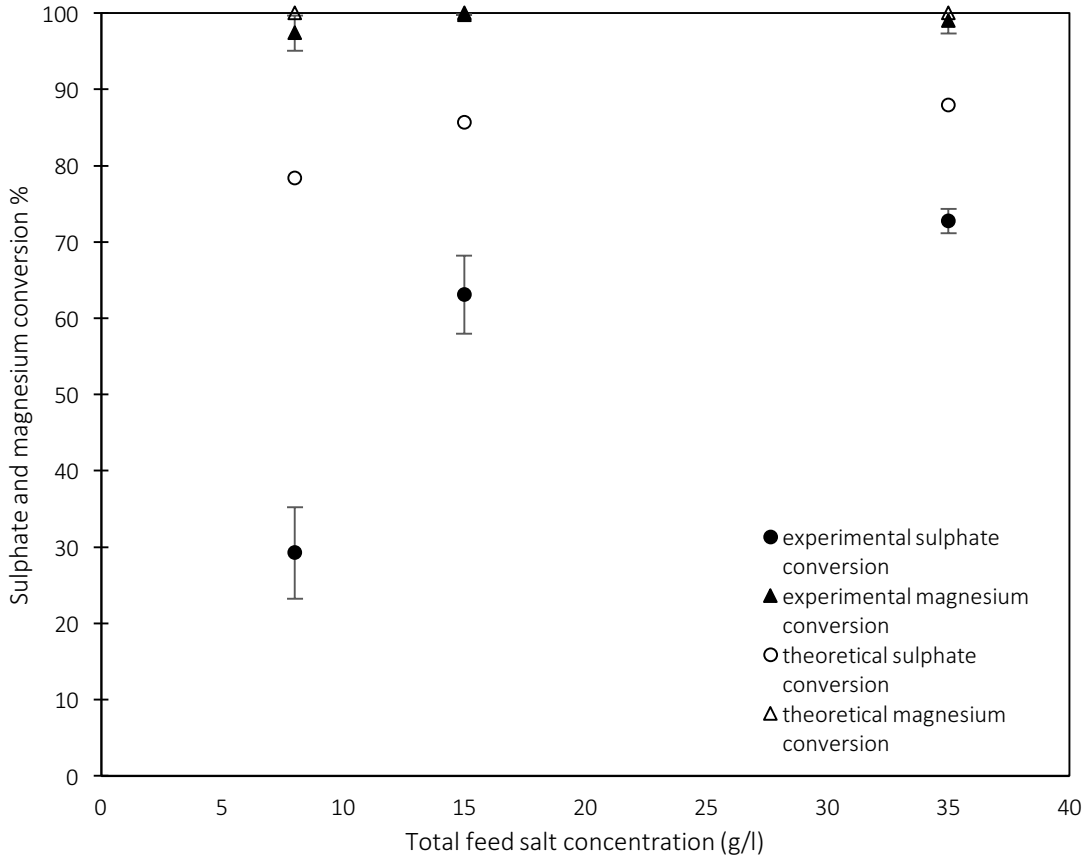

Figure 5.11: Conversion of sulphates and magnesium for a continuously operated fluidized bed reactor

Figure 5.11 shows that the conversion of sulphate increases as the feed concentration increases and follows the same trend as the thermodynamically predicted conversions for sulphate, but remains significantly lower. The increase between sulphate conversions obtained at 8 g/L and 15 g/L was quite significant given that the change in supersaturation values were very small (S_g = 4.2 – 4.8). However, the change in supersaturation from 15 to 35 g/L was significant (S_g = 4.8 – 11.2) but the change in conversion was slight. As the concentration increased, the difference between the theoretical and experimental values for sulphate conversion decreased. Conversions obtained for magnesium closely matched the theoretically predicted values of around 99%. This is because the amount hydroxides are effectively in excess of magnesium. This is in agreement with the findings of Karidakis and co-workers (2005) who also achieved magnesium conversions of around 99% in the treatment of magnesium sulphate with excess calcium hydroxide.

The general increase in sulphate conversion is expected because at higher concentrations there is a higher driving force for crystallization, that is, nucleation and crystal growth. While it is difficult to quantify the effect of supersaturation on these rate processes, the overall rate of crystallization is expected to increase. Figure 5.12 shows the experimental rate of crystallization for the concentration range investigated.

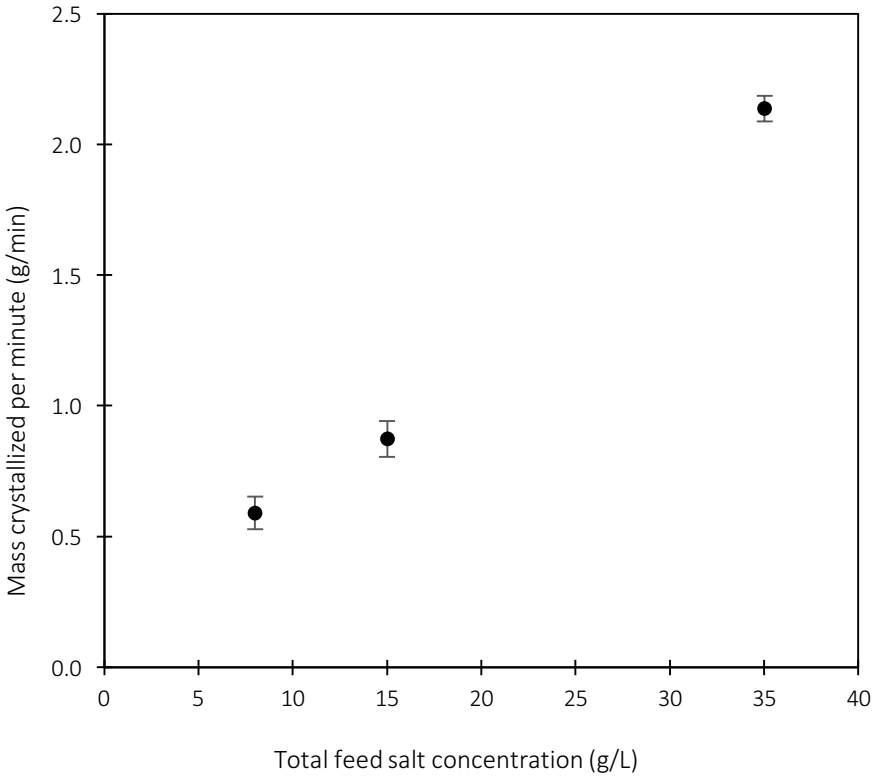

Figure 5.12: Rate of crystallization

The rate of crystallization increased as sulphate concentration increased, however, it should be noted that the residence time across the concentration range decreased slightly because the amount of calcium hydroxide suspension fed into the reactor increased and thus increased the fluid velocity in the column. These results are in agreement with what is expected, however, they do not account for the significant increase in conversion between similar levels of supersaturation and the slight increase between large supersaturation differences. The change in conversion would not be expected to increase significantly if the theoretical conversion was being reached, however, in this case gypsum conversion at 35 g/L remained significantly lower than the theoretical conversion suggesting that the system was limited kinetically and not because of thermodynamically.

Failure to reach theoretical sulphate conversions was attributed to an insufficient residence time, given the size of the reactor used in this study. To test this, a sample of filtered effluent was left for a period of time and a precipitate was visually observed on the walls of the test tube. It is important to note that gypsum requires an induction time before nucleation (Smith and Sweett, 1971; Liu and Nancollas, 1973; Klepetsanis and

Koutsoukos, 1991; Uchymiak et al., 2008), which is a function of supersaturation and may lag the nucleation process further, even in the presence of seeds (Mullin, 2001).

Another reason for this discrepancy between theoretical and experimental conversions is that calcium hydroxide may not dissolve fast enough. In the case of magnesium conversion, hydroxyl ions, which react to form magnesium hydroxide, is fed in excess with respect to magnesium ions and yielded high conversions (> 98%). This indicates that an excess of calcium to sulphate ratio may improve sulphate conversions. The excess in hydroxide ions arises as a result of calcium hydroxide being fed in stoichiometric amounts with respect to sulphates in the system, with the amount of sulphates being more than the amount of magnesium present in the stream. In order to determine if the dissolution of calcium hydroxide was responsible for the low sulphate conversions, a best fit equation, based on literature experiments on the dissolution rate of calcium hydroxide was used to predict possible dissolution times of the calcium hydroxide reagent.

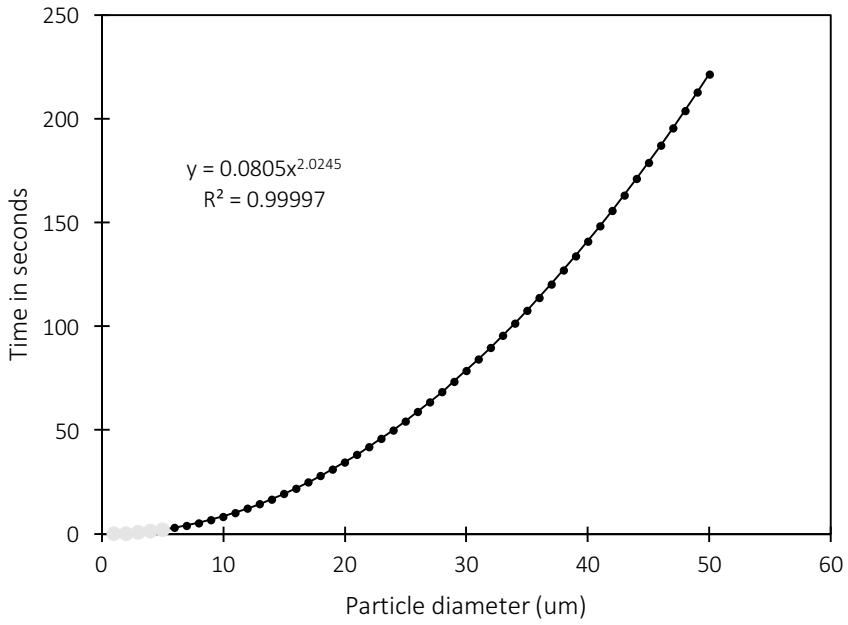

Figure 5.13: Extrapolated dissolution time of a calcium hydroxide particle (adapted from Kadambi et al., 1998)

The calcium hydroxide suspension used had a d50 of 5 μm and d97 of 50 μm, and would thus require between 2 and 221 seconds to completely dissolve according to Figure 5.13. The residence time, with respect to the bed height, was approximately 175 seconds or less, which would be insufficient to dissolve all the calcium hydroxide. It should be noted that the dissolution of calcium hydroxide is motivated by the consumption of hydroxyl ions in the reaction with magnesium, creating a reactive dissolution effect. However, since magnesium is in excess of sulphates, once the reaction involving magnesium has completed, reactive dissolution ceases.

It should be noted that conditions within the reactor for each concentration differ significantly. Higher feed concentrations require more calcium hydroxide reagent, and thus higher flowrates, to meet the

stoichiometric requirement for sulphate conversion. The increase in solids may increase mixing efficiencies in the column. In addition to the extra calcium hydroxide, newly precipitated solids, which provide a larger surface area in the reactor, are expected to increase rates of crystallization.

5.4.3 Recovery efficiency of the fluidised bed crystallizer

The recovery efficiency is a measure of how efficiently gypsum product is retained in the fluidised bed reactor. The recovery efficiency of a fluidised bed crystallizer couples the residual species in solution and inefficiencies due to fines being elutriated. The difference between the recovery efficiency and the conversion is the presence of fines in the system. Figure 5.14 shows the sulphate recovery efficiency for concentrations within the feasible operating region. The corresponding magnesium and sulphate conversions are presented in Figure 5.11.

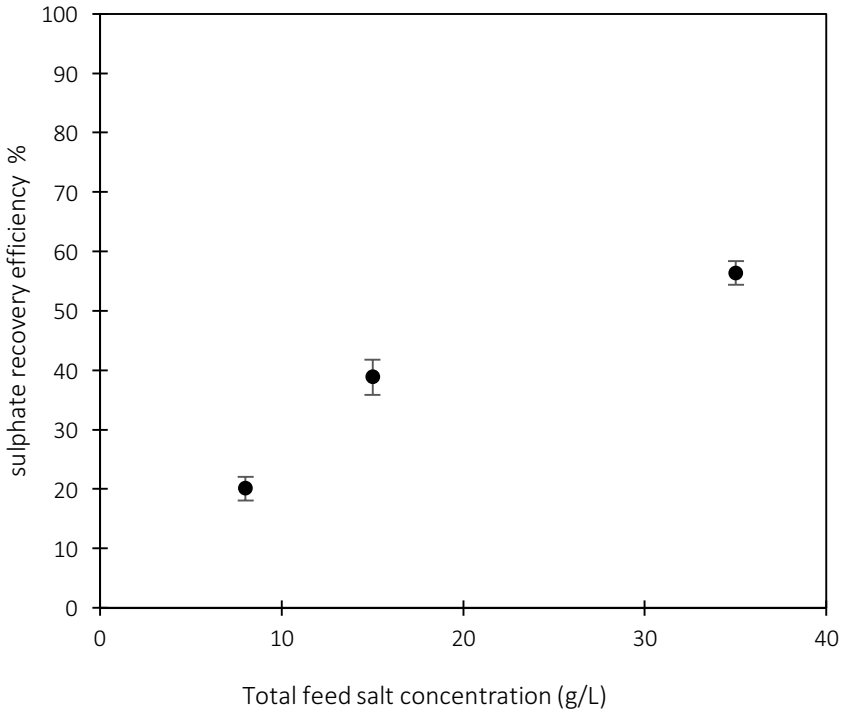

Figure 5.14: Sulphate removal efficiency

Figure 5.14 shows that the recovery efficiency increases as concentration increases. This is not in agreement with the study by Seckler (1994), who found that the recovery efficiency of phosphate in fluidised beds using a calcium hydroxide suspension decreased with increasing concentration. This is because at higher concentrations more fines are expected to be generated, even though conversions are expected to be higher. However, higher concentrations promote conditions for agglomeration and growth, resulting in larger particles that are too heavy to be elutriated which improves recovery. This, coupled with the faster rate of crystallization at higher concentrations increases the overall mass in the reactor and may trap particles that would otherwise be elutriated. It is possible to increase the recovery of products by including post precipitation solid-liquid separation steps such as filtration, centrifugation or thickening steps that can deal with fines (Guillard, 2001).

The maximum allowable sulphate concentration for discharged wastewater is between 200-600 ppm, depending on location regulations (Meays and Nordin, 2013). Table 5.1 shows the residual sulphate concentrations obtainable if maximum sulphate conversions were achieved and experimentally obtained sulphate levels.

Table 5.1: Equilibrium and experimentally obtained residual sulphate concentrations

	Equilibrium residual sulphate (ppm)	Experimental residual sulphate (ppm)
8 g/L	2200	2300
15 g/L	2800	4000
35 g/L	1400	5100

Treatment of this particular waste stream using precipitation only does not yield residual sulphate concentrations within the discharge limit. While residual sulphate concentrations far exceed the discharge limit of 200-600 ppm for the whole concentration range investigated, the equilibrium residual sulphate concentrations show that it is not possible to reach the limit. Given the stream composition, the presence of sodium in the waste stream keeps a significant amount of sulphate in solution through speciation or ion interactions. Alternative treatment methods like cooling crystallization or eutectic freeze crystallization may be able to reduce the sulphate concentration to acceptable levels (Maharaj and Seeparsad, 2014) by removing sodium sulphate and gypsum as a solid.

5.4.4 Crude separation between gypsum and magnesium hydroxide

In an attempt to separate gypsum and magnesium hydroxide products, the relative amounts of each products' fines were quantified against the coated product. Figure 5.15 displays the results obtained for concentrations within the identified operating region.

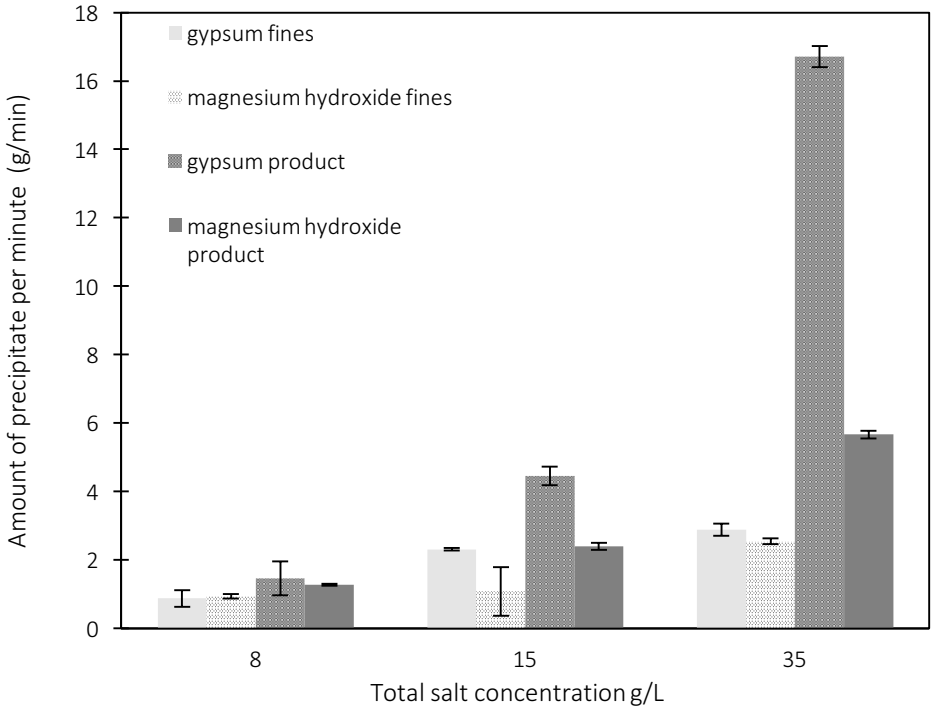

Figure 5.15: Precipitate product and fines distribution

Figure 5.15 shows that a crude separation between magnesium hydroxide and gypsum can be effected in the fluidised bed at 35 g/L. At 8 g/L the amount of gypsum fines to product remaining in the bed is similar and no separation can be effected. However, the amount of gypsum fines compared to the product retained decreased at 15 g/L. The same trend is observed for magnesium hydroxide, which mostly remains in the bed. At 35 g/L the amount of gypsum lost as fines is significantly less than the amount retained as product. The amount of magnesium hydroxide recovered as fines is approximately half the amount lost with the product. The reason for these observations is due to supersaturation effects. At low degrees of supersaturation, gypsum crystals are less likely to agglomerate and effectively attach onto the seed surface and was therefore elutriated. This is in agreement with what has been deduced when considering the morphology of crystals in section 5.3. At 8 g/L, the effluent carried out very small crystals that are most likely prone to elutriation given their size. Crystals formed at 15 g/L and 35 g/L were larger and tended to agglomerate and thus remained in the bed. Magnesium hydroxide crystals, which have the tendency to form agglomerates of nano-sized primary crystals (Henrist et al., 2002), are light enough to be elutriated, however, tend to remain in the bed at higher concentrations because they agglomerate to sizes that may not be elutriated or attach onto product grains. It should also be noted that at higher concentrations, there are more solid interactions which may be the reason magnesium hydroxide is trapped in the bed or tends to form larger agglomerates, which are heavy and thus more difficult to be elutriated.

At low degrees of supersaturation, the growth mechanism is expected to prevail, minimising the formation of fines through nucleation. However, the converse is observed, where low levels of supersaturation result in more fines, due to the presence of seeds. The high ratio of fines to product may be due to the induction time

of gypsum. Even though seeding material is expected to reduce the induction time, it is not clear whether it is completely eliminated altogether. At low degrees of supersaturation, the induction time for gypsum formation is longer. This means that as the supersaturated stream moves through the bed, crystal formation happens in higher regions of the fluidised bed, or above the bed. These crystals remain small because there is not enough supersaturation for crystals to grow to a size that allows them to settle in the bed, and are thus elutriated as fines. However, this is assuming that mixing is instantaneous and supersaturation is achieved in the bed. It is possible that supersaturation is in fact only achieved in higher regions of the reactor, causing fine particles to be formed then, rather than in the bed.

5.4.5 Excess calcium hydroxide

A synthetic solution of 35 g/L total salt concentration was contacted with different ratios of calcium hydroxide in the fluidised bed and the conversion was recorded. Figure 5.16 displays the findings.

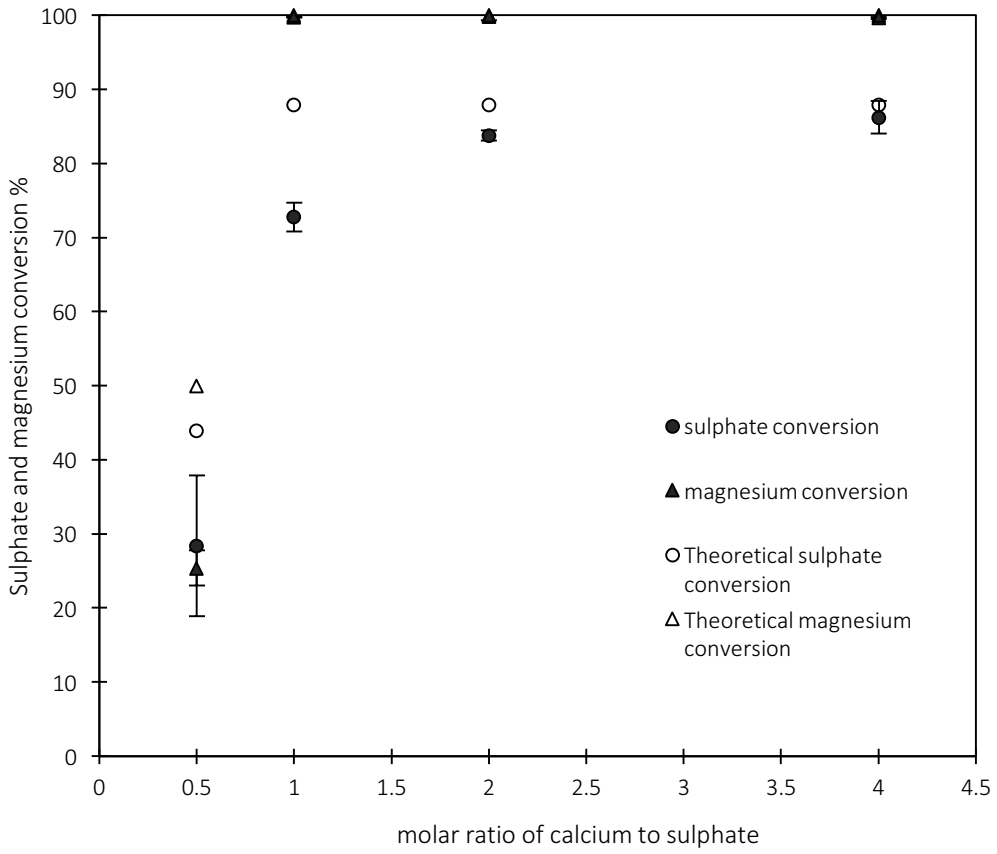

Figure 5.16: Comparison between stoichiometric and excess calcium hydroxide for 35 g/L total salt concentration

The conversion of sulphate increases as the molar ratio of calcium hydroxide to sulphates in the feed increases, and reaches the predicted equilibrium sulphate conversion at an excess molar ratio of four calcium to sulphate ions for the particular suspension used. This is in agreement with Seckler's (1994) findings in phosphate removal, in which calcium supply above stoichiometric amounts result in higher efficiencies. Zang and co-workers (2013) also found that sulphate conversions increased with higher concentrations of calcium hydroxide in their study of gypsum precipitation from sulphuric acid. At stoichiometric amounts of calcium

hydroxide and higher, magnesium conversion is close to the equilibrium conversion. This is because hydroxyl ions are effectively in excess to magnesium ions because the stoichiometric amount of calcium hydroxide is fed to match the sulphates in the system. The excess arises because there are more sulphates than magnesium in the system. Karidakis and co-workers (2005) found that excess amounts of lime increased conversions of sulphates and magnesium in their study of magnesium hydroxide precipitation. The conversion of magnesium and sulphate is significantly lower than the theoretical conversion when insufficient calcium hydroxide was fed, as expected.

The low sulphate conversions at ratios 1 and 2 of calcium hydroxide are essentially due to an insufficient supply of calcium ions in solution to react with sulphate ions, given that the solubility of calcium hydroxide is very low (1.8 g/L). This, coupled with the dissolution kinetics of calcium hydroxide, which is a strong function of particle size and solid content, limits the effective supply of calcium ions. Given that the size distribution of the calcium hydroxide suspension was wide (d50 of 5 μm and d97 of 50 μm), some particles may require longer times for complete dissolution, and have been given sufficient time to dissolve within the residence time of the reactor, resulting in a shortage of calcium ions to reach equilibrium sulphate conversions.

It is also possible for calcium hydroxide solids to serve as sites for gypsum deposition and thus be armoured with a layer that would stop dissolution altogether. It is difficult to ascertain whether armouring of calcium hydroxide does take place, however, it is expected that at larger amounts of solid, armouring effects would be more pronounced and equilibrium conversions would not be obtained. It is therefore expected that dissolution kinetics are responsible for inefficient sulphate conversions.

At a ratio of 4 calcium to sulphate moles, the amount of calcium ions in solution is simply higher than when stoichiometric amounts are fed, and thus improves the amount of ions available for the reaction forming gypsum. A larger amount of small particles that dissolve fast enough are also supplied, which further improves the supply of calcium within the residence time of the reactor. Further to this, the increase in calcium hydroxide solids provide a larger surface area exposed to the bulk solution, which speeds up the dissolution of calcium which would in turn speed up the rate of crystallization. The ratio of 4 times the amount of calcium to sulphates is characteristic of the suspension used and will differ for suspensions with different size distributions.

The presence of more calcium hydroxide solids in the system may further reduce the activation energy for nucleation. This translates to more precipitate forming at a faster rate within the given residence time, thus increasing the conversion. It should be noted that conditions within the reactor for each experiment are not identical. In the case of excess calcium hydroxide, the higher solid content may improve mixing efficiencies and hydrodynamics, resulting in better calcium hydroxide dissolution and better mass transfer of precipitating units.

5.5 Process alternative

The multicomponent stream chosen for this case study has the potential to produce two separate crystalline products, as opposed to the mixed precipitate discussed in the previous section. Since there are limitations to the applicability of the mixed product for re-use, generating two separate products may be economically and practically beneficial. In addition, being able to generate the products separately results in an almost zero waste process, which is of significant importance with rising waste disposal costs. The proposed two-step process sequence is described in the schematic in Figure 5.17.

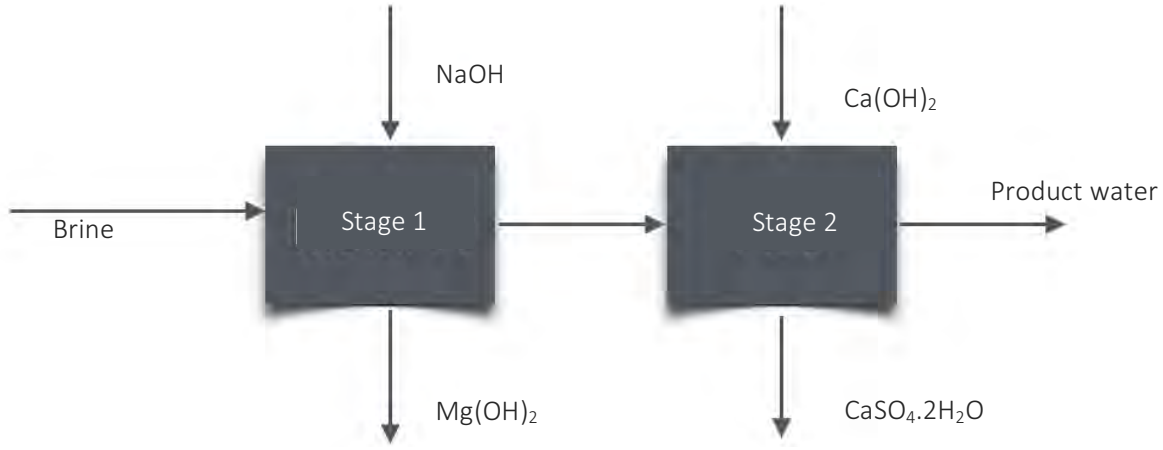

Figure 5.17: Schematic of proposed treatment process

The first step in this process involves precipitation of magnesium hydroxide with caustic soda as the precipitant, since the stream is rich in magnesium sulphate. The next step treats the sodium sulphate generated in the first stage, by forming gypsum when dosed with a calcium hydroxide suspension. This second stage also regenerates caustic soda that could potentially offset reagent costs in the first stage. Mass balances and detailed process flow diagrams of this process, as well as the process explored in previous sections of this report are presented in the appendix.

5.5.1 Thermodynamic modelling and conversion in the two stage process

OLI Systems Stream Analyser ™ was used to model the thermodynamic behaviour of the proposed two-step treatment process. The model was used to determine the type and amount of solids expected in each stage of the process. Figure 5.18 displays the findings for the first stage.

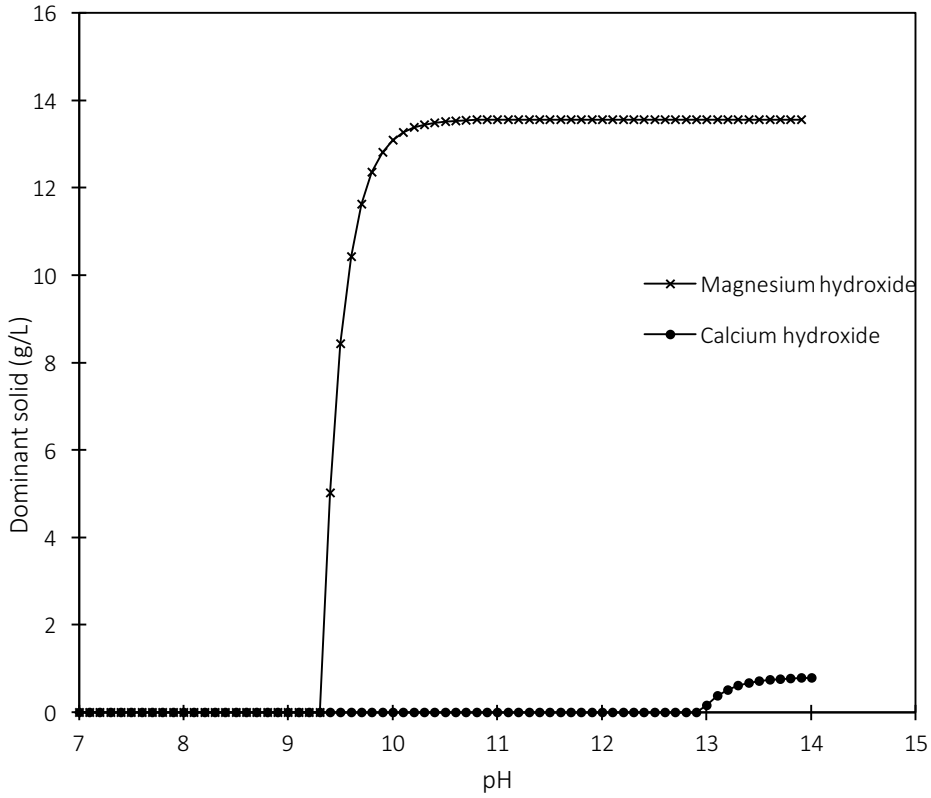

Figure 5.18: Dominant solid as a function of pH (stage one)

Magnesium hydroxide is expected to precipitate out at a pH of 9.3, after which there is a steep increase in the amount precipitated until a pH of around 10.3. This trend is similar to thermodynamic predictions for the one—step process. After a pH of 10.3 the amount of magnesium hydroxide precipitated is constant at 13.6 g/L of synthetic solution containing 35 g/L of total sulphate salts, as presented in Table 4.2. This maximum amount of magnesium hydroxide obtainable corresponds to a 99.5% magnesium conversion. This is comparable with magnesium conversions in the one-step process, which was around 99.8% for the same stream composition. Calcium hydroxide begins to precipitate at a pH of 12.9 as expected.

The type and amount of solids expected in the second stage of the alternative treatment process is presented in Figure 5.19.

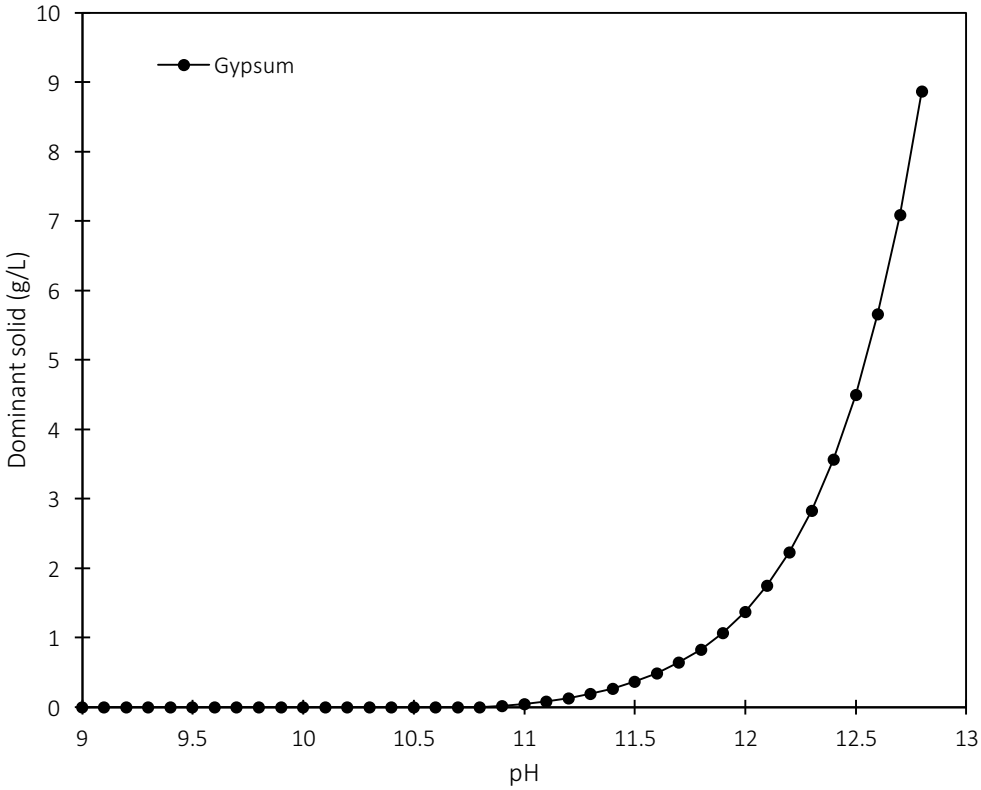

Figure 5.19: Dominant solid as a function of pH (stage two)

In the second stage of the two-step process, gypsum starts precipitating out at a pH of 11, which is slightly higher than the precipitation pH in the one stage process (pH of 9.2). The amount of solid gypsum formed gradually increases from pH 11 to 12, after which there is a steep increase until a pH of 12.7. The maximum amount of gypsum obtainable from this stage is around 8.8 g/L and does not change when additional calcium hydroxide is added into the model (not shown). This maximum amount of gypsum corresponds to a sulphate conversion of 18%, which is substantially lower than the 88% sulphate conversion obtainable in the one step process. This means that residual sulphate levels (9800 ppm) are far above the acceptable minimum sulphate discharge concentration (200-600 ppm). The reason for low sulphate conversions in the second stage is due to the presence of sodium sulphate, which is formed in the preceding stage. Figure 5.20 shows the behaviour of sulphate and calcium activity coefficients in the presence of sodium sulphate.

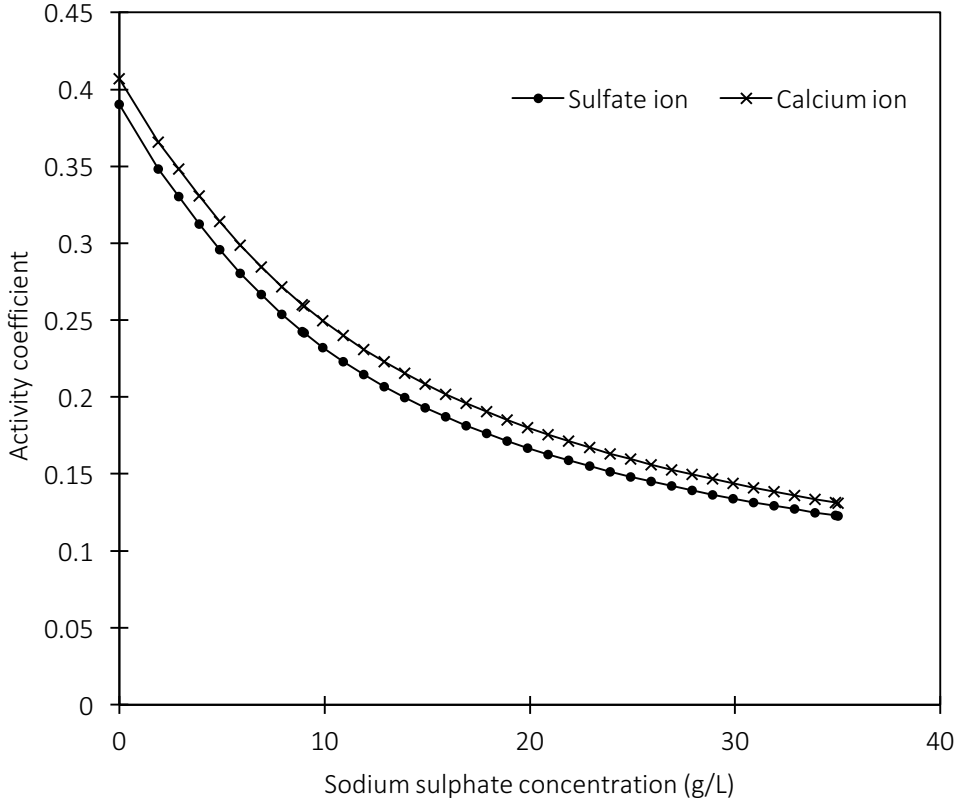

Figure 5.20: Effect of sodium sulphate on sulphate and calcium activity coefficients

The activity coefficients of both calcium and sulphate ions decrease from around 0.4 to 0.1 as the amount of sodium sulphate is increased. This means that the presence of sodium ions decreases the availability of sulphate ions to react to form gypsum, hence the low sulphate conversion of 18%. The decrease in sulphate and calcium activities may be as a result of speciation or complexing, which decreases the amount of ions available to react. OLI Systems Stream Analyser ™ was used to predict the possible ion pairs formed in this system. Table 9.3 in the appendix displays these results. It was found that only trace amounts of ion pairs or complexes are formed and a significant amount of sodium, sulphate and calcium ions remain in solution. It was also predicted that a large portion of calcium hydroxide remained undissolved. The presence of free sulphate, sodium and calcium ions indicate that even though ions are available, the reaction to form gypsum is hindered. As a result of this hindrance, calcium hydroxide is unable to dissolve because calcium ions in solution are not consumed and the solution remains saturated with respect to calcium. In other words, the reaction step in Equation 27 limits the step described in Equation 26.

$$Ca(OH)_2 \leftrightarrow Ca^{2+} + 2OH^- \qquad \text{Equation 26}$$

$$Ca^{2+} + SO_4^{2-} + 2H_2O \leftrightarrow CaSO_4 2H_2O \qquad \text{Equation 27}$$

Calcium and sulphate ions become inactive as a result of shielding effects which is amplified in the presence of sodium, as discussed in section 5.1.1 of this report. Sodium ions are strongly attracted but not bonded to

sulphate ions in solution. The ion pair is then hydrated and becomes shielded from calcium ions. This stops the formation of gypsum and is the reason for the decrease in calcium and sulphate activities observed in Figure 5.20. This effect is corroborated by studies on the effects of sodium ions on the solubility of calcium sulphate (Speigler et al., 1980; Ahuja et al., 2000; Murray, 2004).

6 Conclusion

The aim of this study was to investigate factors that affect the conversion of sulphates and magnesium and the recovery of gypsum and magnesium hydroxide from a multicomponent stream in a fluidised bed crystallizer. The precipitation reaction forming gypsum and magnesium hydroxide was induced by the reaction between a calcium hydroxide suspension and a synthetic solution containing magnesium and sodium sulphate salts.

The seeded fluidised bed crystallizer has been found to be successful in the removal of sulphates and magnesium when treated with calcium hydroxide. The presence of seeds decreased the formation of both gypsum and magnesium hydroxide fines and increased the conversion of gypsum and magnesium by 7 % and 9%, respectively.

It was found that operation of the fluidised bed crystallizer is dependent on feed concentrations of the wastewater to be treated. Concentrations higher than 50 g/L produced precipitate rapidly that hindered fluidisation and carried the bed material out of the reactor.

Conversion of sulphate and magnesium increased as feed concentrations increased from 8 – 35 g/L. The study found that feed concentrations of 35 g/L of total sulphate salts yielded better conversions (± 75%) of sulphates to gypsum compared to 8 g/L (± 30%) due to the higher driving force and thus faster rate of crystallization. A $Ca:SO_4$ molar ratio of 1:1 did not yield equilibrium sulphate conversions, as a result of the incomplete dissolution of calcium hydroxide for the given residence time. However, it was possible to remove 99% of the magnesium in the wastewater stream under these conditions for each concentration investigated, since the Mg:OH molar ratio was effectively in excess. Excess calcium hydroxide (a $Ca:SO_4$ molar ratio greater than 1) improved the supply of calcium ions for reaction and thus sulphate conversions, and the equilibrium conversion of 88% was achieved at four times the amount of calcium to sulphates in the feed stream, based on the characteristic suspension used. Residual sulphate concentrations (2200 ppm at 15 g/L to 1400 ppm at 35 g/L), even after equilibrium conversions were achieved, did not meet the maximum sulphate discharge levels (200-600 ppm).

A crude separation of magnesium hydroxide and gypsum could be initiated in the fluidised bed at 35 g/L. Gypsum crystals formed as needles and progressed to plates at higher feed concentrations. Magnesium hydroxide produced nano-agglomerates that were elutriated out of the bed or were imbedded in the product grain at higher concentrations. Overall the ratio of product, both magnesium hydroxide and gypsum, retained in the bed increased as the concentration increased.

A process alternative to recover gypsum and magnesium hydroxide separately was investigated. Thermodynamic modelling found that a 99% magnesium conversion was obtainable and only 18% sulphate conversion was attainable, due to the electrostatic effects of sodium that shield sulphate ions which would otherwise react with calcium to form gypsum. This shielding effect hindered the consumption of calcium ions which drives the dissolution of calcium hydroxide. This low conversion limits the practicality of this system. Other process alternatives to explore are the use of eutectic freeze crystallization or cooling crystallization which could potentially remover more sulphates than precipitation.

7 Recommendations

This study has found that treatment of high-concentration multicomponent mining effluents using calcium hydroxide is possible in a fluidised bed crystallizer reactor, however, the process may be improved if investigation into the aspects listed below are considered.

7.1 Residence time

The findings in this study indicate that the conversion of the system is dependent on the residence time. For the given reactor, focus was on factors that increased the rate of crystallization, such as an excess feed of calcium hydroxide to sulphates, because the experimental setup used was limited by a short residence time. While this achieved higher conversions, reagent consumption was not efficient. The accelerated rate of crystallization makes control difficult due to the large amount of precipitates formed. A longer residence time in the form of a longer reactor may allow for effective supply of calcium hydroxide without excess quantities being fed into the system. This would eliminate armouring issues, make filtration steps easier, as well as decrease waste disposal costs of the effluent filtrate. A longer reactor may improve the recovery of products since they spend a longer time in the reactor and are thus allowed to grow larger and settle. It would also be beneficial to investigate the effect of mixing on the meso and macro-scale to better understand the implications on calcium hydroxide dissolution.

7.2 Recirculation flow

A possible modification to the experimental setup could be to implement a recycle stream. In previous studies, a recirculation flow was primarily introduced to increase the residence time of the species in the reactor, thereby increasing the conversion (Seckler, 1994; Aldaco, 2005). By combining the recirculation and feed streams, the influent to the reactor becomes dilute, therefore preventing high supersaturation levels (Guillard and Lewis, 2001). In addition, the recirculation flow aids the fluidisation of the bed (Guillard and Lewis, 2001). Seckler (1994) found that by recirculating some of the effluent exiting the reactor, efficiencies in precipitate recovery increased. This is consistent with the findings of other researchers (Peterson et Al., 2002; Zhou et al, 1999; Wilms et Al., 1988, Aldaco, 2007; Villa Gomez, 2013). The recirculation stream could also be modified to recycle fine particles suspended above the bed. Reintroducing fine particles to a supersaturated environment will promote agglomeration of fines to larger particles and therefore increase recovery. This is due to more particle collisions, expected in the bed, which will promote cementing of the particles in the reaction zone. However, the implications of a high energy dissipation rate associated with the recirculation flow may cause attrition, that is, further fines formation.

7.3 Calcium hydroxide dissolution

The dissolution of calcium hydroxide, and the rate at which this occurs, is of importance in this system. Given the nature of the precipitation process using a suspension, the formation of one solid while simultaneously dissolving another presents some challenges. Further insight into the dissolution behaviour of calcium hydroxide would be beneficial so that the conversion of sulphates can be achieved more efficiently, that is, at lower amounts of calcium hydroxide.

7.4 Alternative process

Thermodynamic predictions for the alternative process predicted a maximum sulphate conversion of 18%, making it an impractical option. Other process alternatives to explore are the use of eutectic freeze crystallization (EFC) or cooling crystallization which could potentially remove more sulphates than precipitation with calcium hydroxide can. Crystallization methods would be able to recover sodium sulphate as a solid, thereby reducing the amount of residual sulphates.

8 Reference list

Abdel-Aal E., Rashad M. M. and El-Shall H., 2004, "Crystallization of Calcium sulphate dihydrate at different supersaturation ratios and different free sulphate concentrations," *Crystallisation Research Technology*. Vol 39, pp 313-321.

Abdel-Aal A.E., Abdel-Ghafar H.M. and El Anadouli B.E., 2015, "New findings about Nucleation and crystal growth of reverse osmosis desalination scales with and without inhibitor," *Crystal Growth and Design.* Vol. 15, pp5133-5137.

Ahuja L.R., Rojas W.K., Hanson J.D., Shaffer M.J. and Ma J., 2000, "Root zone water quality model: Modelling management effects on water quality and crop production." Water resources publication LLC. ISBN 1-887201-08-4.

Aldaco R., Irabien A. and Luis P., 2005, "Fluidized bed reactor for fluoride removal", *Chemical Engineering Journal*. Vol 107, pp 113-117.

Aldaco R., Garea A., Irabien A., 2007, "Particle growth kinetics of calcium fluoride in a fluidised bed reactor", *Chemical Engineering Science*. Vol 62, pp 2958-2966.

Al-Othman A., 2004, "Gypsum production and hydrochloric acid regeneration by reaction of calcium chloride with sulphuric acid." *Cornell Admin Quarterly*. Vol 22, pp 64-68.

Bates R.G., Bower V.E., Canham R.G., and Prue J.E., 1959. "*The dissociation constant of $CaOH^+$ from 0 to 40 degrees Celsius."* Transactions of the Faraday Society. Vol. 55, pp 2062-2068.

Baysal A., Ozbek N. and Akman S., 2013, "Determination of trace metals in waste water and their removal." I*ntech: Waste water-treatment technologies and recent analytical developments. Pp 145-171. http:/dx.doi.org/10.5772/52025*

Bond R. and Veerapaneni S., 2007, "Zero liquid discharge for inland desalination", *Awwa Research Foundation*, California. ISBN 9781617389696.

Chieng, C. and Nancollas, G., 1982. "The crystallization of magnesium hydroxide, a constant composition study". *Desalination*, Vol. 42. Pp 209-219.

Christoffersen, M.R., Christoffersen, J., Rosmalen, G.M., Weijnen, M.P.C., 1982. "Crystal growth of calcium sulphate dihydrate at low supersaturation." *Journal of Crystal Growth*. Vol.58, pp 585–595.

Costodes, V. and Lewis, A., 2006, "Reactive crystallization of nickel hydroxyl-carbonate in fluidized bed reactor: fines production and column design." *Chemical engineering science,* Vol. 61, pp 1377-1385.

Coulson J.M. and Richardson J.F., 1991, "Chemical engineering", Oxford: Butterworth-Heinemann, 4th edition, Vol. 2.

Ebbing D., 1990. "*General Chemistry 5th Edition*", Boston: Houghton Mifflin Company.

Eckenfelder W., 1966. "*Industrial water pollution control*", New York: McGraw Hill.

Eueler B., Kirschenbaum JL., Ruekberg B., 2000. "Determination of Ksp, delta G, delta H and delta S for the dissolution of calcium hydroxide in water." *Journal of Chemical Education.* Vol. 77, No. 8, pp 1039-1040.

Fajtl J., Tichý, R. and Ledvina, R., 2002, "Gypsum precipitation - A medium to control sulphate pollution of freshwater sediment leachates", *Water, Air, and Soil Pollution*. Vol 135, Pp 141-156.

Geldart D. 1978, "Homogenous Fluidization in Fine Powder Using Various Gases and Pressures", *Powder Technology*. Vol. 19, pp133-136.

Guillard D., 2001. "*Nickel hydroxy-carbonate precipitation in a pellet reactor"*. Master's Thesis, University of Cape Town, Cape Town.

Guillard D., and Lewis A.E., 2001. "Nickel carbonate precipitation in a fluidised-bed reactor". *Industrial and Engineering Chemistry Research.* Vol 40, pp 5564–5569.

Giulietti M., Seckler M. and Dorenzo S., 2001, "Industrial crystallization and precipitation from solution: state of the technique", *Brazilian Journal of Chemical Engineering*. Vol 18, pp 423-428.

Granasy L., Pusztai T., Tegze G., Warren J. and Douglas J., 2005, "Growth and forms of spherulites." *Physical Review E.* Vol.72.

Habashi F., 1997, "Handbook of extractive metallurgy". Germany: Wiley-VCH Vol. 2, ISBN 3-527-28792-2.

Halevy S., Korin E., and Gilron J., 2013, "Kinetics of Gypsum Precipitation for Designing Interstage Crystallizers for Concentrate in High Recovery Reverse Osmosis", *Industrial and Engineering Chemistry Research*. Vol 52, pp 14647-14657.

Hammarstrom J.M., Sibrell P.L. and Belkin E.H., 2003. "Characterisation of limestone reacted with acid mine drainage." *Applied Geochemistry.* Vol.18, pp. 1705-1721.

Hatakka H., Oinas P., Reunanen J. and Palosaari S., 1999, "The effect of supersaturation on agglomeration", http://www.lut.fi/~hhatakka/docit/agglo.html.

He S., Oddo J., Tomson M., 1993, "The nucleation kinetics of calcium sulphate dihydrate in NaCl solutions up to 6 M and 90 degrees celcius" *Journal of colloid and interface science.* Vol. 162, pp297-303.

Heffels S.K. and Kind M., 1999, "*Seeding technology: an underestimated critical success factor for crystallization*", Proceedings of 14th International Symposium on Industrial Crystallization.

Henrist, C., Mathieu, J., Vogels, C., Rulmont, A. and Cloots, R., 2002, "Morphological study of magnesium hydroxide nanoparticles precipitated in dilute aqueous solutions." *Journal of crystal growth*, Vol. 249, pp 321-330.

Hina A., Nancollas G. H. and Grynpas M., 2001. "Surface induced constant composition crystal growth kinetics studies. The brushite-gypsum system". *J. Cryst. Growth* Vol. 223, pp. 213–224.

Hirasawa, I., Toya, Y., 1990. "Fluidized-bed process for phosphate removal by calcium phosphate crystallization". *Crystallization as a Separation Process*. ACS, Washington, DC, pp 355–363.

Howard M and Howard D., 2010, "Introduction to crystallography and mineral crystal systems." Accessed online: 20 January 2019. http://www.rockhounds.com/rockshop/xtal/index.shtml#index.

Jones A. G., 2002, "Crystallization Process Systems", London: Butterworth-Heinemann. ISBN 0 7506 5520 8.

Kadambi J.R., Adler R.J., Prudich M.E., 1998, "Dry scrubbing technologies for flue gas desulphurization." *Springer Business and Science, New York.* ISBN 978-1-4651-2.

Kaksonen A.H., Riekkola-Vanhanen M.L. and Puhakka J.A., 2003. "Optimization of metal sulphide precipitation in fluidised-bed treatment of acidic wastewater". *Water Research*. Vol 37, pp 255–266.

Karidakis T., Agatzini-Leonardou S. and Neou-Syngouna P., 2005, "Removal of magnesium from nickel laterite leach liquors by chemical precipitation using calcium hydroxide and the potential use of the precipitate as a filler material", *Hydrometallurgy*. Vol. 79, Pp 105-114.

Keller Douglas Martin M. R. E. and Hileman, Jr., O. E., 1978a. "Studies on nucleation phenomena occurring in aqueous solutions supersaturated with calcium sulfate". *Can. J. Chem.* Vol. 56, pp. 831–838.

Keller Douglas Martin M. R. E. and Hileman, Jr., O. E., 1978b. 'Studies on nucleation phenomena occurring in aqueous solutions supersaturated with calcium sulfate. II. The induction time". *Can. J. Chem*. Vol. 56, pp 3096–3103.

Keller Douglas Martin, M. R. E. and Hileman, O. E., 1980. "Studies on nucleation phenomena occurring in aqueous solutions supersaturated with calcium sulfate. III. The cation:anion ratio". *Can. J. Chem*. Vol. 58, pp 2127–2131.

Kind M., 1999 "*Precipitation phenomena and their relevance to precipitation technology*", Proceedings of 14th International Symposium on Industrial Crystallization.

Kitamura M., Konno H., Yasui A. and Masuoka H., 2002, "Controlling factors and mechanisms of reactive crystallization of calcium carbonate polymorphs from calcium hydroxide suspensions*". Journal of Crystal Growth*. Vol 236, pp323–332.

Klepetsanis P. G. and Koutsoukos P. G., 1991. 'Spontaneous precipitation of calcium sulfate at conditions of sustained supersaturation'. *J. Colloid Interface Sci*. Vol. 143, pp 299–308.

Klepetsanis P. G., Dalas E. and Koutsoukos P. G., 1999. "Role of temperature in the spontaneous precipitation of calcium sulfate dehydrate". *Langmuir* Vol. 15, pp 1534–1540.

Kubota N. and Fujiwara M., 1990, "Minimum seed crystal size for secondary nucleation of potassium alum in a stirred vessel crystallizer", *Journal of Chemical Engineering Japan*, Vol 23, pp 691-696.

Lancia A., Musmarra D. and Marina P., 1999. "Measuring induction period for calcium sulfate dihydrate precipitation". *AIChE J*. Vol. 45, pp 390–397.

Lash, J.E., Burns, G., 1984. "Heats of crystallization of $CaSO_4$. $2H_2O$". *Bulletin des Societes Chimiques Belges* Vol. 93, pp 271 – 279.

Levenspiel O., 1999, "Chemical Reaction Engineering." 3rd Edition. John Wiley and Sons. ISBN 0-471-25424.

Lewis A., 2010, "Hydroxide and sulphide solubility database."

Lewis, A., Nathoo, J., Seewoo, S., Lacour, S., 2002. "Prevention of Scaling in Mine Waters Using Slurry Precipitation and Recycle Reverse Osmosis (SPARRO)". *15th International Symposium on Industrial Crystallization, Sorrento, Italy*, 15–18th September.

Lewis A., Seckler M., Kramer H. and van Rosmalen G., 2015, "Industrial Crystallization fundamentals and applications" Cambridge University Press. ISBN 978 1 107 05215 4

Linnikov O. D., 1999. "Investigation of the initial period of sulphate scale formation Part 1. Kinetics and mechanism of calcium sulphate surface nucleation at its crystallization on a heat- exchange surface". *Desalination* Vol. 122, pp 1–14.

Liu, S., Nancollas, G.H., 1970. "The kinetics of crystal growth of calcium sulfate dehydrate". *Journal of Crystal Growth* Vol. 6, pp 281 – 289.

Liu, S.T. and Nancollas G. H., 1973 "Linear crystallization and induction-period studies of the growth of calcium sulphate dihydrate crystals". *Talanta* Vol. 20, pp 211–216.

Maharaj C., and Seeparsad T., 2014, "*Comparison of a eutectic freeze crystallization and cycled cooling crystallization- reverse osmosis process for the treatment of reverse osmosis retentate*." University of Cape Town.

Matlock, M.M., Howerton, B.S., Atwood, D.A., 2002 "Chemical precipitation of heavy metals from acid mine drainage", *Water Research*, Vol. 36 (19), pp 4757-4764.

Meays C., Nordin R., 2013, "Ambient Water Quality Guidelines for sulphate." Ministry of Environment. Province of British Colombia.

Merck, 2013, "Calcium cell test, sulphate cell test and magnesiu cell test." *Analystical test kits.*

Mersmann A., 2001, "Crystallization technology handbook." Marcel Dekker, New York. ISBN 0824705289

Miers H.A. and Isaac, F., 1994, "Refractive indices of crystallizing solutions" *Journal of the Chemical Society*. Vol. 89, pp 413-454. In: Mullin, J.W., 2001. "*Crystallisation, 4th Edition*" London: Butterworth-Heinemann.

Mullin J.W., 2001. "*Crystallization*, *4th Edition*". Butterworth-Heinemann, Oxford.

Murray J.W., 2004, "Activity scales and activity corrections." University of Washington.

Neal C. and Stanger G., 1984, "Calcium and magnesium hydroxide precipitation from alkaline ground waters in Oman, and their significance to the process of serpentinization." *Mineralogical magazine*. Vol 48, pp 237-241.

Nielsen A. E, 1979, *Industrial Crystallisation*, Amsterdam: Jong and Jancic.

Nienow A.W., Harnby N. and Edwards M.F., 1997, "*Mixing in the Process Industries."* Butterworth- Heinemann.

OLI Analyser Studio, 2015, OLI systems Inc.

Othmer D.F., 1956, *Fluidisation*, New York: Reinbold, pp 213.

Packter A., 1974. "The precipitation of calcium sulphate dihydrate from aqueous solution: induction periods, crystal numbers and final size". *Journal of Crystal Growth* Vol. 21, pp 191–194.

Peterson K., van Hille R., Lewis A., 2002, "*Copper sulphide precipitation in a fluidised bed reactor*." Master's Thesis, University of Cape Town, Cape Town.

Peng X., Wang Y., Chai L., Shu Y., 2009, "Thermodynamic calculation of caso4 -$Ca(OH)_2$ -H_2O system phase equilibriums" *Transactions of non-ferrous ions, Society of China: English Edition.* Vol 2, pp 71-79.

Perry R.H. and Green D., 1997, "Perry's chemical engineer's handbook", Singapore: McGraw-Hill Book Company, 7th Edition., ISBN: 0-07049-841-5

Popovic D., Stupar G., Milanindonic J., Todorovic M., and Zrilic M., 2011. "Solubility in the ternary system $CaSO_4$-Na_2SO_4-H_2O at 298.15K. Russian Journal of physical chemistry A. Vol. 85, pp.2349-2353.

Pritchard G., 1998, "Plastics Additives: An A-Z reference." Polymer science and technology: Springer science and business media. 1st Edition., ISBN 978-94-011-5862-6.

Prisciandaro M., Lancia A. and Musmarra D., 2001. "Calcium sulfate dihydrate nucleation in the presence of calcium and sodium chloride salts". *Ind. Eng. Chem. Res.* Vol. 40, pp 2335–2339.

Pritzel C. and Trettin R., 2011. "Influencing the morphology of gypsum." *Proceedings of the 10th International Congress for Applied Mineralogy.* pp541

Rademacher S., and Johannsen K., 1999, "Modelling the kinetics of calcium hydroxide dissolution in water." *Acta Hydrochim. Hydrobiol. Vol. 27, No.2 pp 72-78.*

Randal, D., 2010. Development of a brine treatment protocol using eutectic freeze crystallization. PhD Thesis University of Cape Town.

Randolph A. D., and Larson M. A., 1998, "Theory of particulate processes: analysis and techniques of continuous crystallisation", San Diego: Academic Press, 2nd Edition., ISBN 0125796528.

Reznik I.J., Ganor J., Gruber C., and Gavrieli I., 2012, "Towards the establishment of a general rate law for gypsum nucleation", *Geochimica et Cosmochimica Act*, Vol 85, pp 75-87.

Rhodes M., 1998. "Introduction to Particulate Technology", University of Monash, Australia ISBN 0-471-98482-5

Seckler M.M., 1994, "*Calcium phosphate precipitation in a fluidized bed*", Doctoral thesis, Delft University of Technology, The Netherlands.

Seewoo S., Van Hille R., and Lewis A., 2004. "Aspects of gypsum precipitation in scaling waters." *Journal of Hydrometallurgy. Vol. 75, pp 135-146.*

Seider W.D., Deadar J.D., Lewin D.R., and Widagdo S., 2010. "Product and process design principles: synthesis, analysis and evaluation. 3rd ed. Danvers: John Wiley and Sons.

Shih, W., Rahardianto, A., Lee, R. and Cohen Y., 2005. "Morphometric characterization of calcium sulphate dehydrate scale on reverse osmosis membranes." *Journal of Membrane science.* Vol. 252. Pp253-263.

Smith, B. R. and Sweett F., 1971. "The crystallization of calcium sulfate dihydrate." *Journal of Colloid Interface Sci*. Vol. 37, pp 612–618.

Söhnel O. and Garside J., 1992, "Precipitation, basic principles and industrial application", Oxford: Butterworth Heinemann, ISBN 0 7506 1107 3.

Sohnel O. and Mullin J.W., 1987 "Agglomeration in batch precipitated suspensions", AIChE Symposium, series no. 284. Vol. 87, pp 182-188.

Spiegler K.S. and Laird A.D.K., 1980, "Principles of Desalination." Academic Press.

Sunagawa I., 2005. "Crystals: Growth, morphology and perfection." Cambridge University Press.

Tai Y.C., Chen C.Y., Chien C.W., 1999, "Crystal Growth Kinetics of Calcite in a dense fluidised bed crystallizer", *AIChE Journal,* Vol 45, pp 1605-1614.

Tai, C.Y., Hsu, H.P., *2001.* "Crystal growth kinetics of calcite and its comparison with readily soluble salts". *Powder Technology.* Vol. 121 (1), pp 60–67.

Theonen T., 1999, "Pitfalls in the use of solubility limits for radioactive waste disposal", *Nuclear Technology,* Vol. 126, pp 75-87

Torbacke M. and Rasmuson A.C., 2001, "Influence of different scales of mixing in reaction crystallisation", *Chemical Engineering Sci*ence, Vol 56(7), pp 2459-2473.

Toyokura K., Tanaka H. and Tanahashi J., 1973 "Size distribution of crystals from classified bed type crystallizer", *J.Chem. Eng. Jap.,* Vol. 6, pp. 325-331.

Tunay O., Tasli R. and Orhon D., 1992, "Factors affecting the performance of hydroxide precipitation of metals", *Proc. Ind. Waste Conf*., 46th.

Turton R., Bailie R.C., Whiting W.B. and Shaeiwitz J.A., 2009. "Analysis, synthesis and design of chemical processes. 3rd Ed. Upper saddle river: Prentice Hall.

Uchymiak M., Lyster E., Glater J. and Cohen Y., 2008. "Kinetics of gypsum crystal growth on a reverse osmosis membrane". *J. Membr. Sci*. Vol. 314, pp 163–172.

Uhl W.V. and Gray J.B., 1966, "*Mixing: theory and practice"*, New York: Academic Press.

van Dijk J.C., Wilms D., and Scholler M., 1987 "Recovery of metals by crystallization in the pellet reactor", *Envir. Tech., Prod. Env. Conf*, Vol 2, pp 294-303.

van Dijk J.C*.,* Van Ammers M., Graveland A. and Nuhn P.A.N.M., 1986, "State of the art of pellet softening in the Netherlands", *Water Supply*, Vol 4, pp 223-235.

van Hille R., Peterson K. and Lewis A., 2005, "Copper sulphide precipitation in a fluidised bed reactor." *Chemical Engineering Science*, Vol 60, pp 2571-2578.

Villa Gomez D. and Denys K., 2013, "Simultaneous sulphate reduction and metal precipitation in an inverse fluidized bed reactor", *Masters thesis*, Delft University of Technology, The Netherlands.

Wang Y. and Anderson P.R., 1992, "Effect of the surface characteristics of seed on copper precipitation", *Water Science Technology,* Vol. 26, No. 9-11, pp 2141-2143.

Wilms D., Buildeo Rai P., van Dijk J., Schöller M., 1988. "Recovery of nickel by crystallization of nickel carbonate in a fluidised bed reactor." Proceedings of the VVT Symposium on Non-Waste Technology, Espoo, Finland

Wojcik J.A., 1999, "Modelling of fluidised bed crystallizers", Proceedings of 14th International Symposium on Industrial Crystallization.

Wu, J., Du, J. and Gao, Y., 2014. "Crystal growth morpholgy of magnesium hydroxide." *Turkish Journal of Chemistry*, Vol. 38, pp 402-412.

Zhang Y., Deng L., Chen F., 2013, "Reactive crystallization of calcium sulphate dihydrate from acidic wastewater and lime." *Chinese Journal of Chemical Engineering*. Vol 21, pp 1303-1312.

Zhou P., Huang J.C., Li A.W.F. and Wei S., 1999, "Heavy metal removal from wastewater in fluidized bed reactor", *Water Research*, Vol. 33, pp 1918-1924.

9 Appendix A-results

Section 1: Methodology

Table 9.1: Composition of silica seeding material

Component	%
SiO_3	99.75
Al_2O_3	0.07
Fe_2O_3	0.023
TiO_3	0.024
ZrO_2	0.005
CaO	0.003
MgO	Traces
L.O.I	0.12

Section 2: Thermodynamic modelling

Table 9.2: Speciation predicted by OLI

species in	Liquid 1 Species	Vapor Species	Solid Species
H_2O	H_2O	H_2O	H_2O
$CaSO_4$	OH^{-1}	H_2SO_4	$Ca(HSO_4)_2.2H_2SO_4$
$MgSO_4$	H_3O^{+1}	SO_3	$Ca(HSO_4)_2$
Na_2SO_4	Ca^{+2}		$Ca(OH)_2$ (Portlandite)
$Ca(OH)_2$	$CaOH^{+1}$		CaO (Lime)
	$CaSO_4$		$CaSO_4.0.5H_2O$ (Bassanite)
	H_2SO_4		$CaSO_4.2H_2O$ (Gypsum)
	HSO_4^{-1}		$CaSO_4$ (Anhydrite)
	SO_3		$Mg(HSO_4)_2.2H_2SO_4$
	SO_4^{-2}		$Mg(HSO_4)_2.2H_2O$
	Mg^{+2}		$Mg(OH)_2$ (Brucite)
	$MgOH^{+1}$		MgO (Periclase)
	$MgSO_4$		$MgSO_4.12H_2O$
	$Na_2SO_4.NaHSO_4$		$MgSO_4.1H_2O$ (Kieserite)
	$NaOH.Na_2SO_4$		$MgSO_4.4H_2O$ (Starkeyite)
	Na^{+1}		$MgSO_4.5H_2O$ (Pentahydrite)
	NaOH		$MgSO_4.6H_2O$ (Hexahydrite)
			$MgSO_4.7H_2O$ (Epsomite)
			MgSO4
			$Na_2SO_4.5CaSO_4.3H_2O$
			$Na_2SO_4.CaSO_4$ (Glauberite)
			$Na_2SO_4.10H_2O$ (Mirabilite)
			Na_2SO_4 (Thenardite)
			$Na_2SO_4.NaHSO_4$

			$2Na_2SO_4.CaSO_4.2H_2O$ (Eugsterite)
			$2NaOH.3Na_2SO_4$
			$NaHSO_4.H_2SO_4.1H_2O$
			$NaHSO_4.H_2SO_4$
			$NaHSO_4.2H_2SO_4$
			$NaHSO_4.1H_2O$ (Matteuccite)
			$NaHSO_4$
			$NaOH.1H_2O$
			$NaOH.2H_2O$
			$NaOH.3.5H_2O$
			$NaOH.4H_2O$
			$NaOH.5H_2O$
			$NaOH.7H_2O$
			NaOH

Table 9.3: Supersaturation calculation for magnesium hydroxide

	$[Mg^{2+}]$ mol/l	$[OH^-]$ mol/l	$k_{sp(Mg(OH)2)}$ (mol/dm^3)	Activity $coeff_{Mg2+}$	Activity $coeff_{OH-}$	Supersaturation
1,5	0,01	0,02	1,80E-11	0,46	0,82	6,85E+04
8	0,05	0,02	1,80E-11	0,43	0,70	2,49E+05
15	0,10	0,02	1,80E-11	0,38	0,70	4,15E+05
35	0,23	0,02	1,80E-11	0,29	0,70	7,35E+05
50	0,33	0,02	1,80E-11	0,27	0,70	9,80E+05
120	0,80	0,02	1,80E-11	0,17	0,60	1,08E+06

Table 9.4: Supersaturation calculation for gypsum

	$[Ca^{2+}]$mol/l	$[SO_4^{2-}]$mol/l	$k_{sp(CaSO4.2H20)}$ (mol/dm^3)	Activity $coeff_{Ca2+}$	Activity $coeff_{SO42-}$	Supersaturation
1,5	0,02	0,01	3,14E-05	0,45	0,45	1,7
8	0,03	0,06	3,14E-05	0,26	0,25	4,2
15	0,03	0,12	3,14E-05	0,20	0,20	4,8
35	0,03	0,28	3,14E-05	0,20	0,20	11
50	0,03	0,40	3,14E-05	0,20	0,20	16
120	0,03	0,97	3,14E-05	0,15	0,15	21

Section 3: Batch experiments

pH investigation

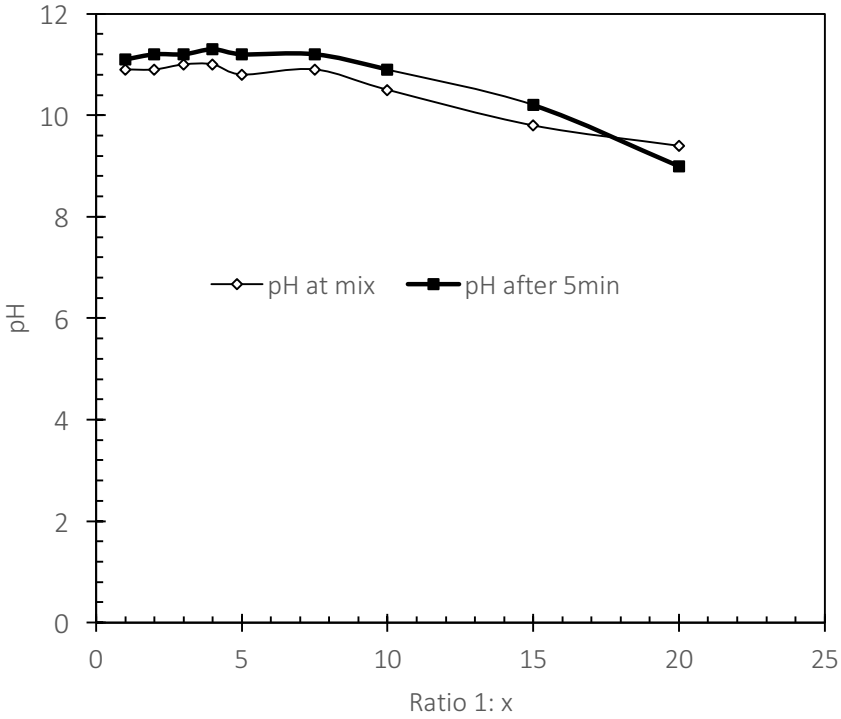

Figure 9.1: pH as a function of calcium hydroxide to synthetic solution ratio

Gypsum fluidisation

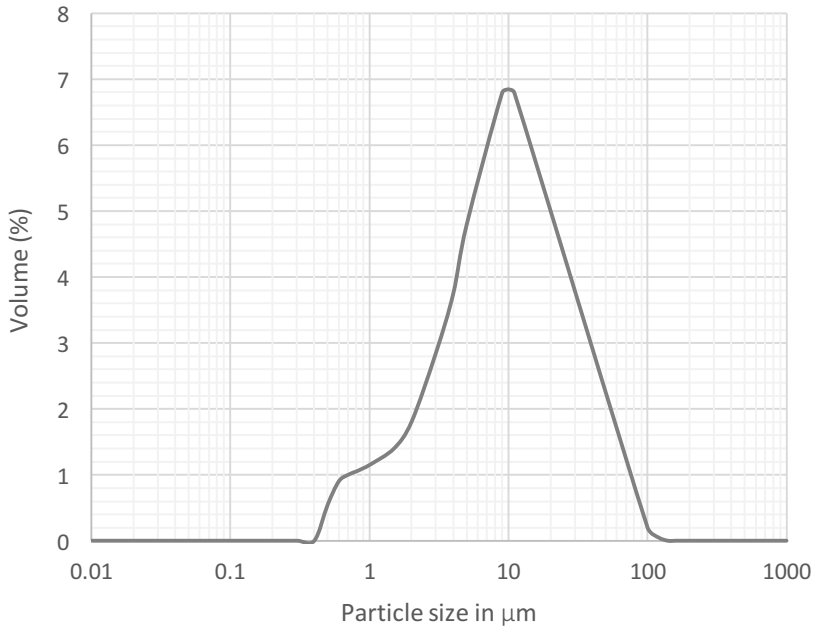

Figure 9.2: Particle size distribution of analytical grade gypsum by volume %

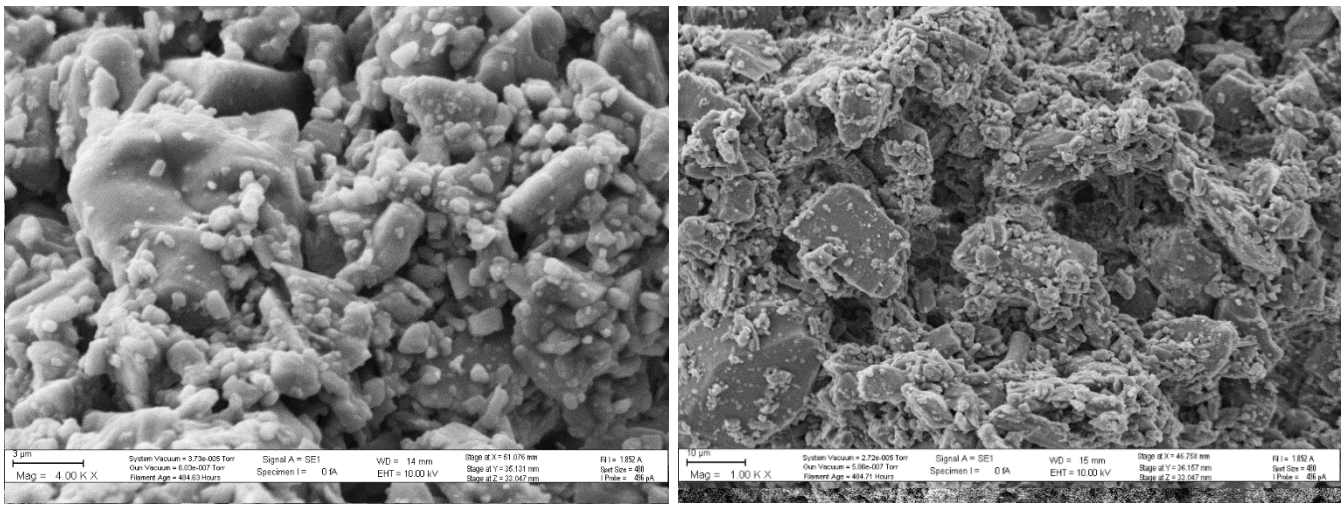

Figure 9.3: SEM images of gypsum seeds

Figure 9.4: Fluidised bed crystallizer containing gypsum seeds

Figure 9.5: Channelling observed in fluidised bed crystallizer with gypsum seeds

Figure 9.6: Partial fluidisation of a bed using gypsum seeds

Silica fluidisation

Figure 9.7: First experimental run using silica seeds. Left to right a) lower region of column. b) Region of 2nd calcium hydroxide inlet c) Region above 2nd calcium hydroxide inlet d) Higher region of column.

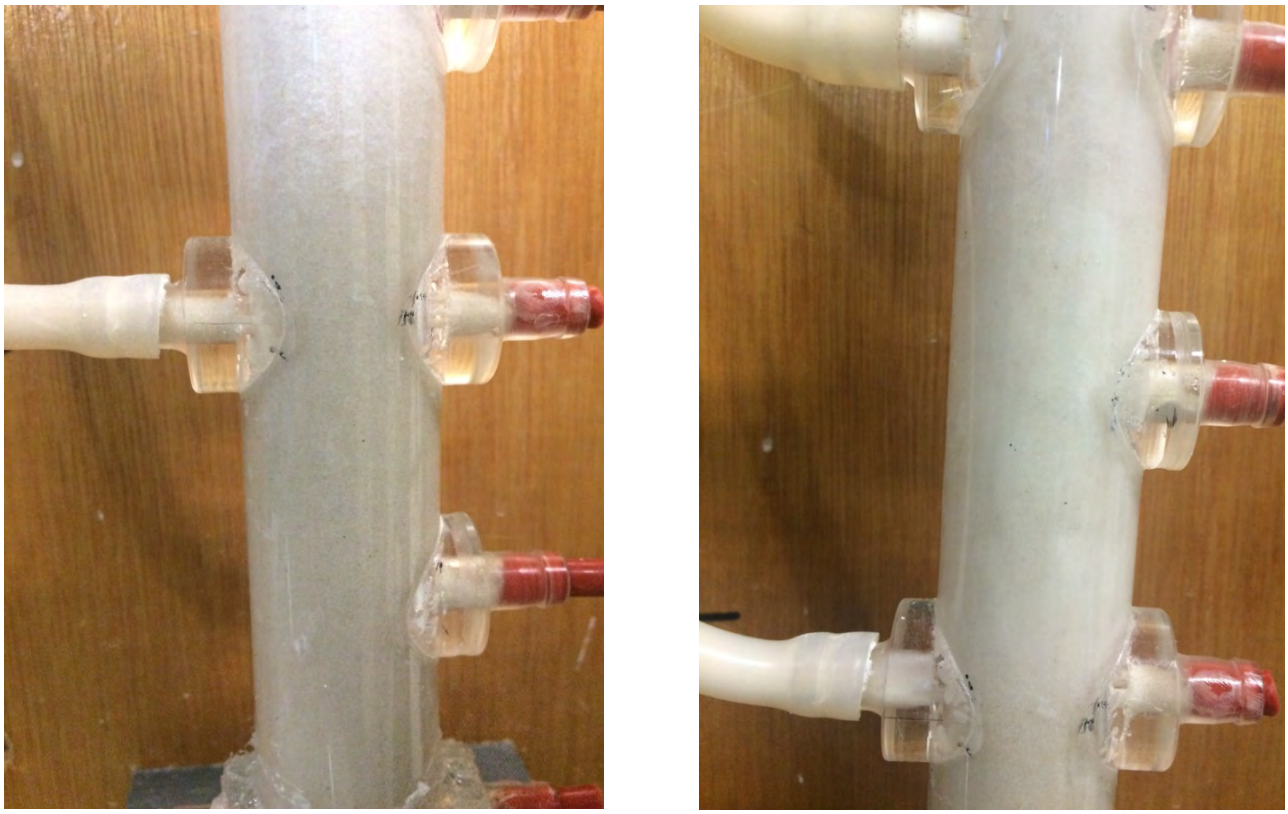

Figure 9.8: Fluidised bed crystallizer with silica seeds

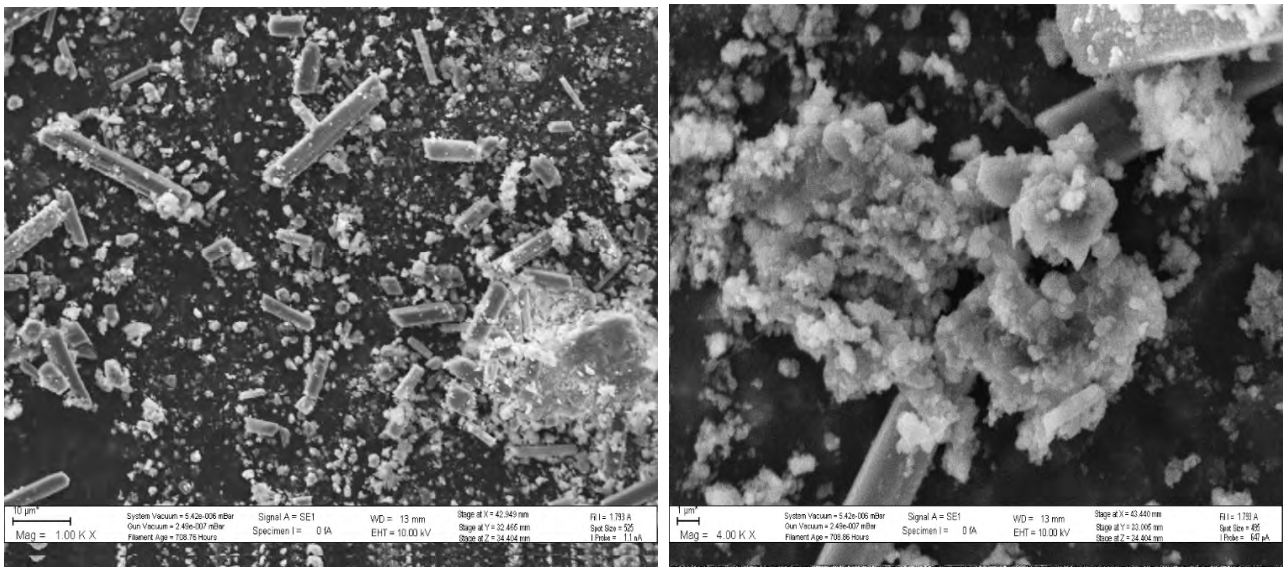

Figure 9.9: SEM Images of solids from effluent suspension with continuous calcium hydroxide flow

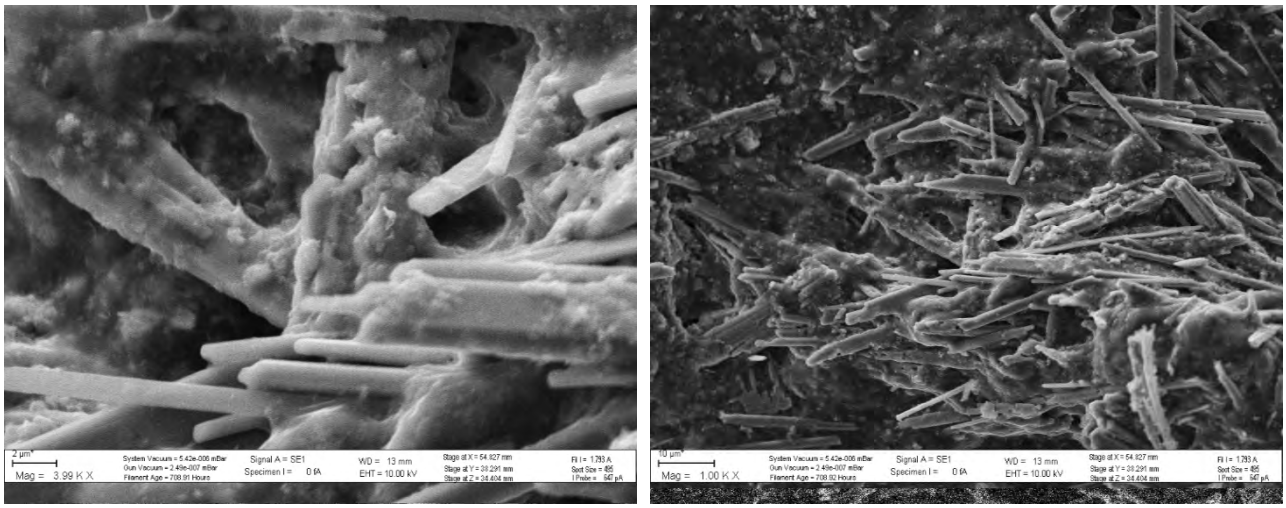

Figure 9.10: SEM images of coated silica product

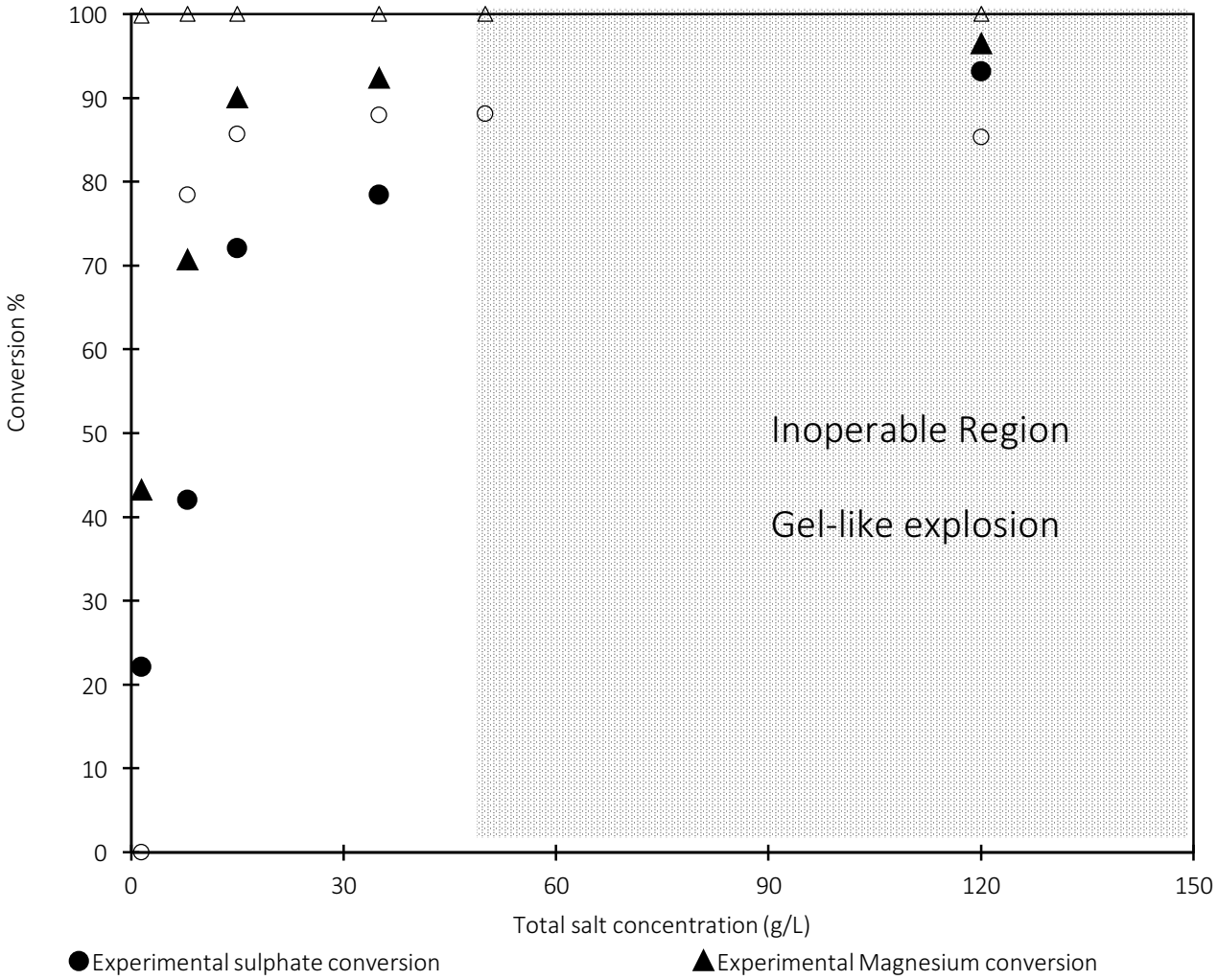

Figure 9.11: Operating region

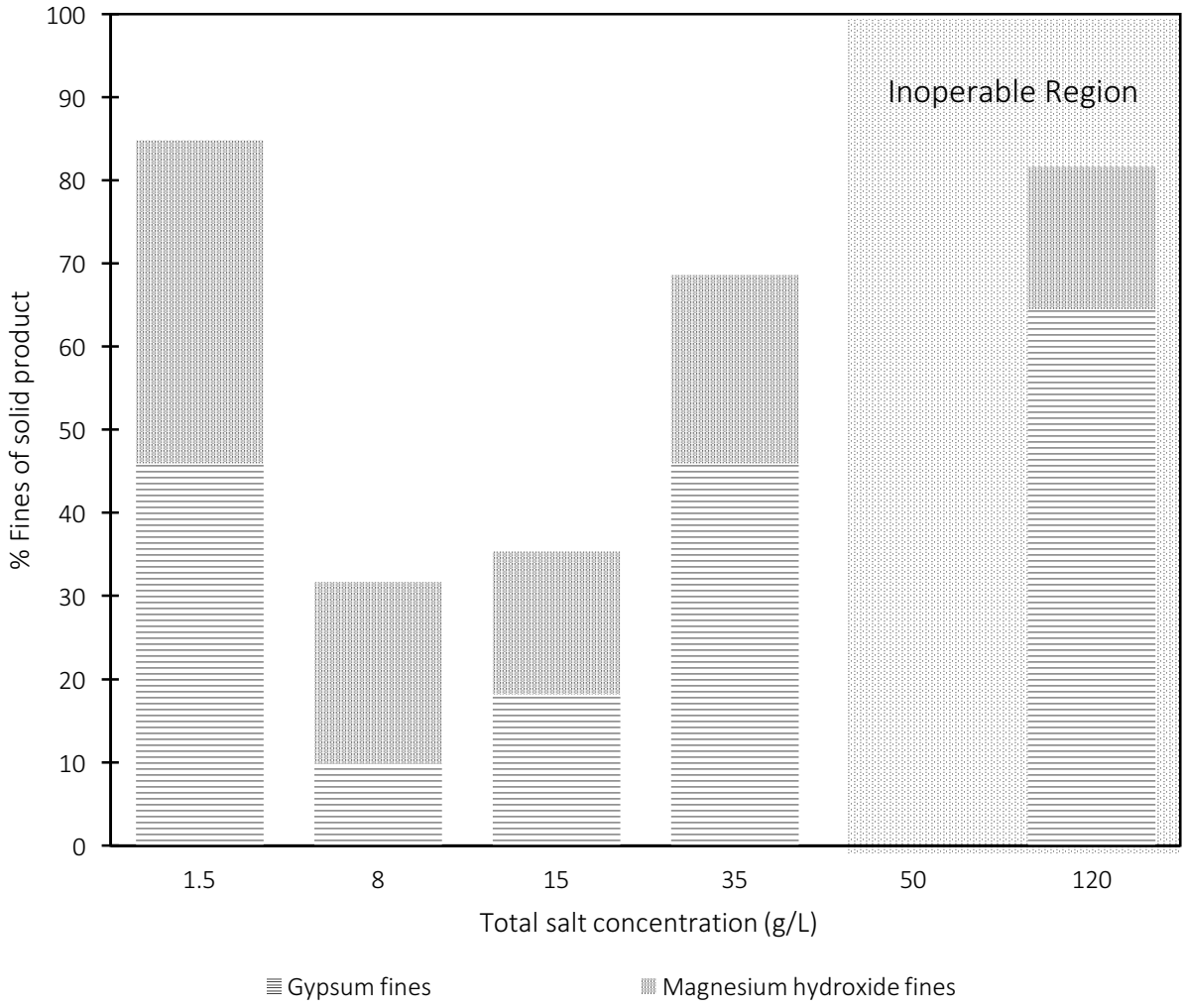

Figure 9.12: Fines produced in batch experiments

Section 4: Morphology

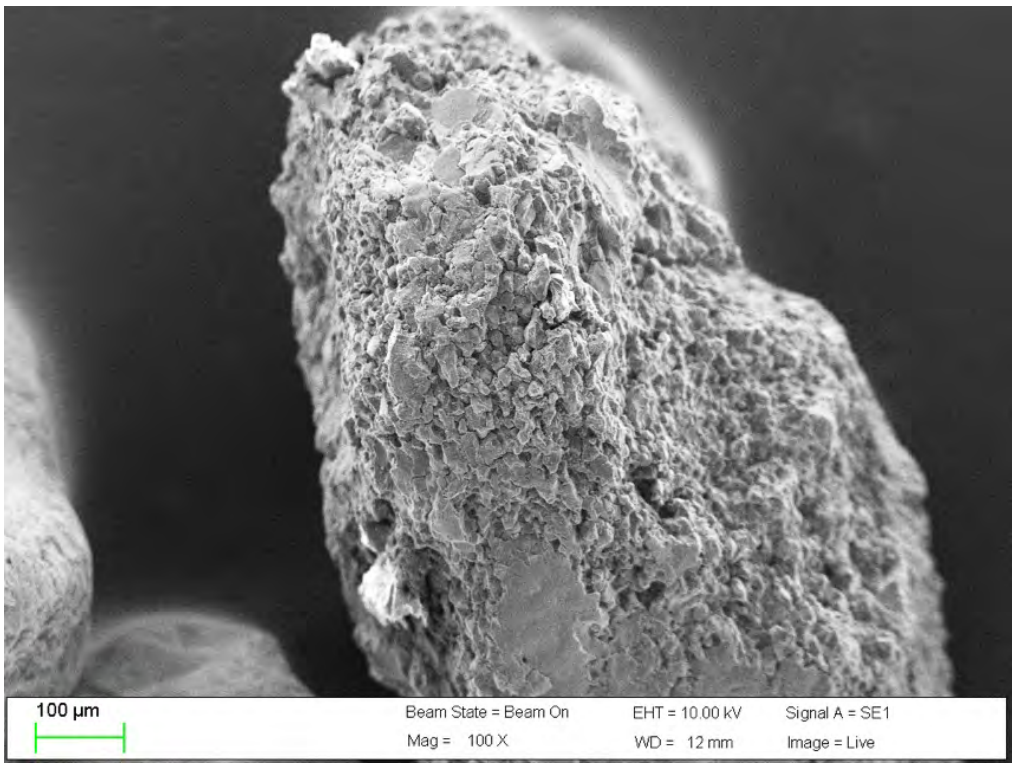

Figure 9.13: SEM image of silica surface

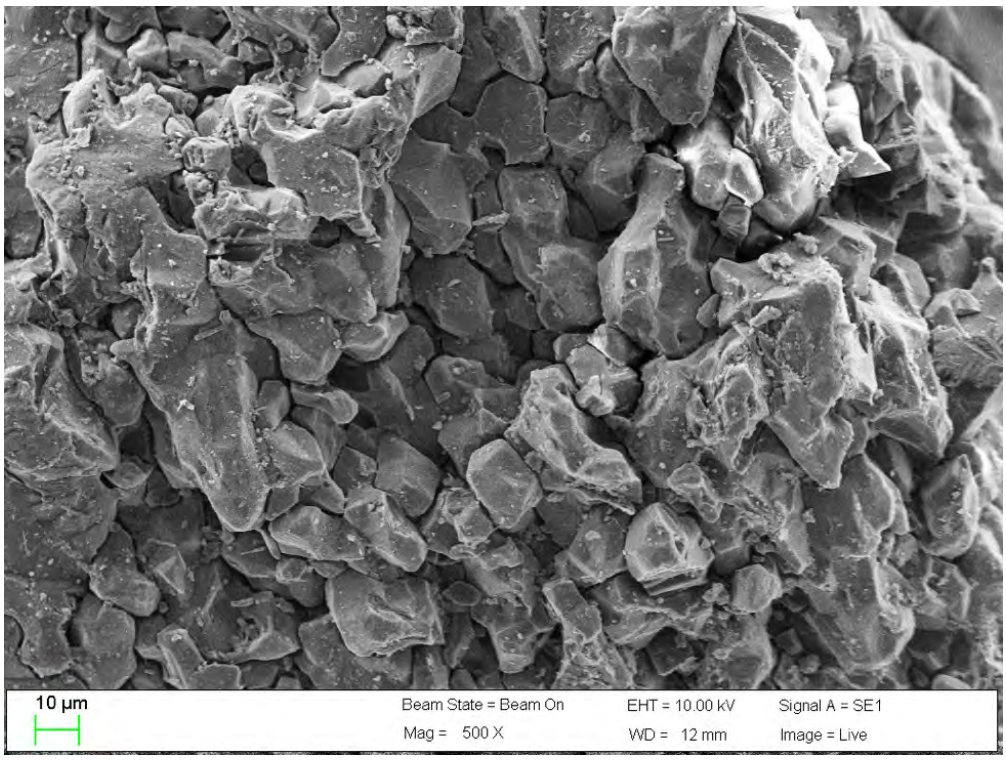

Figure 9.14: SEM image of silica surface (Close up)

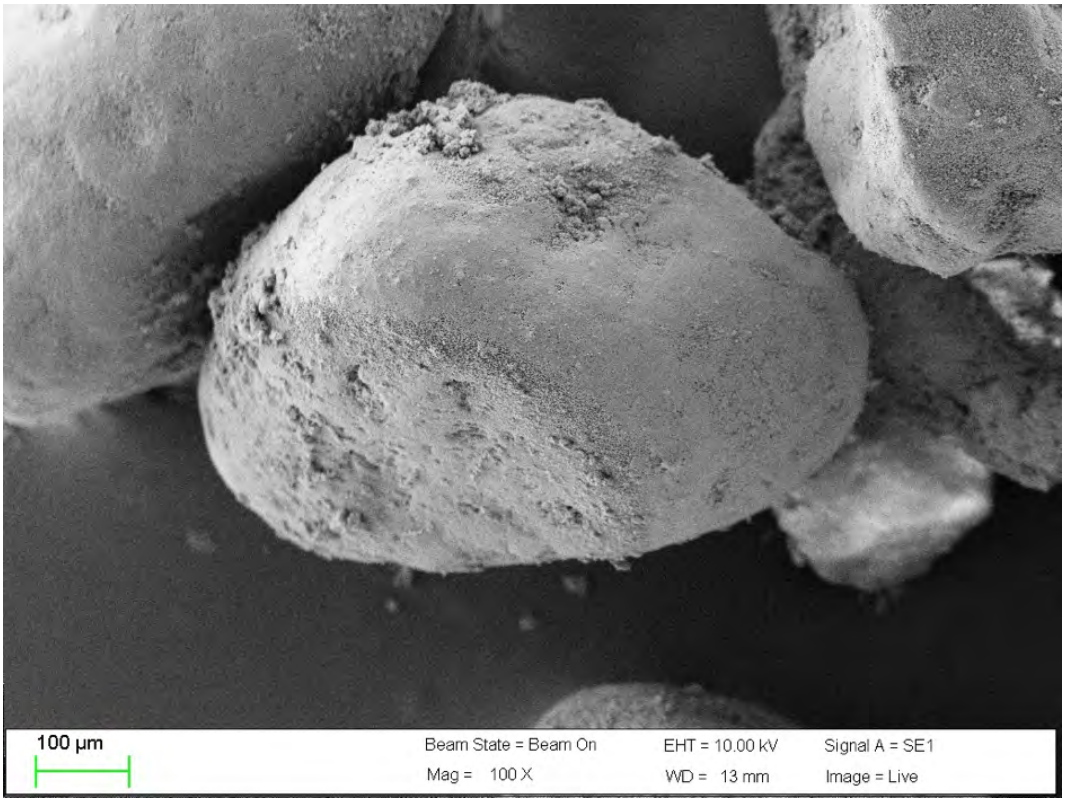

Figure 9.15: SEM image of 8 g/l product

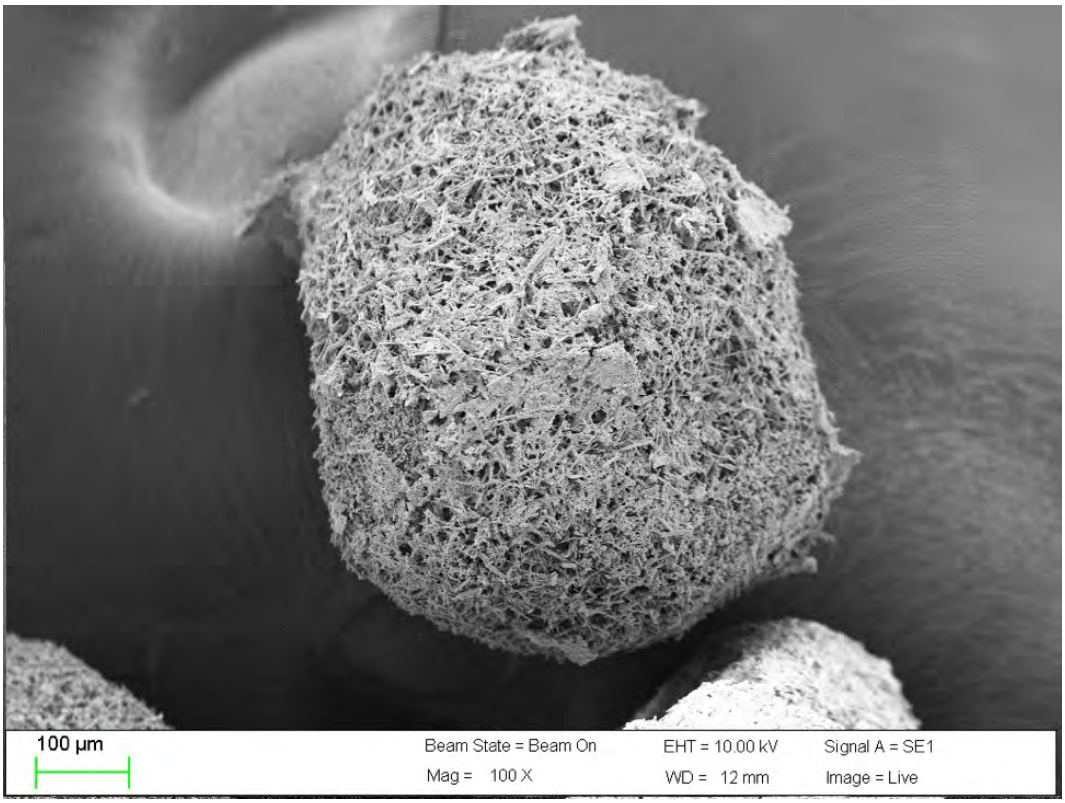

Figure 9.16: SEM image of 15 g/L product

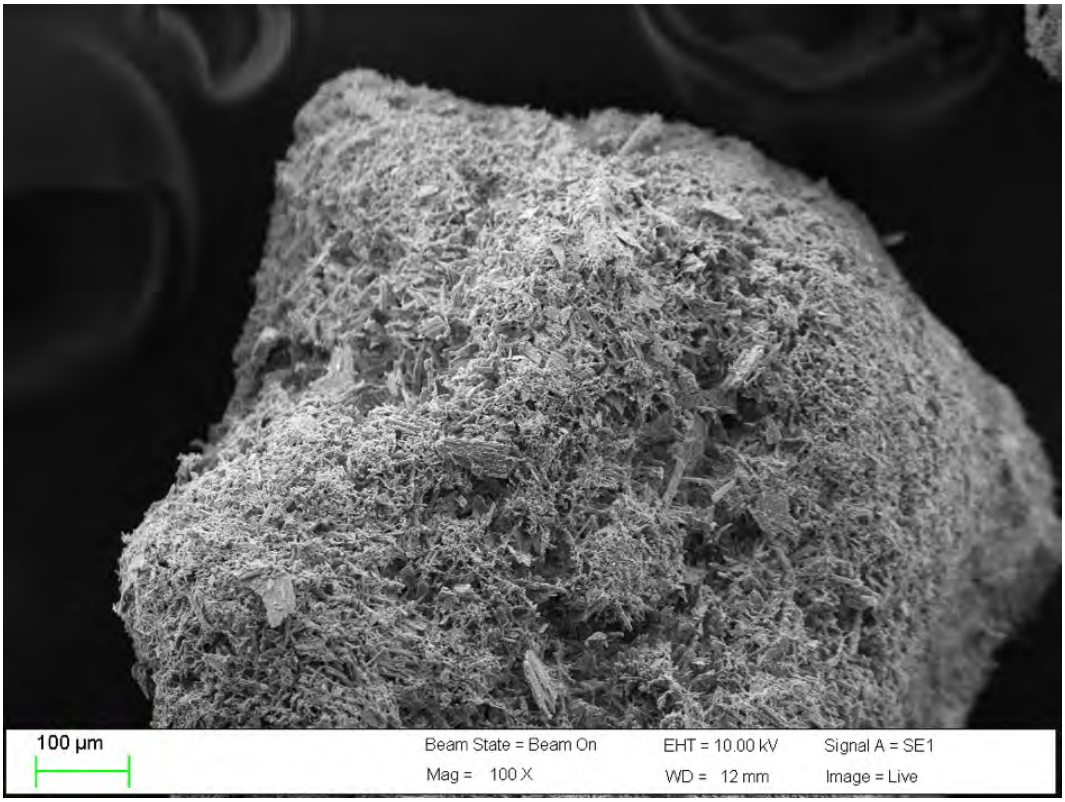

Figure 9.17: SEM image of 35g/L product

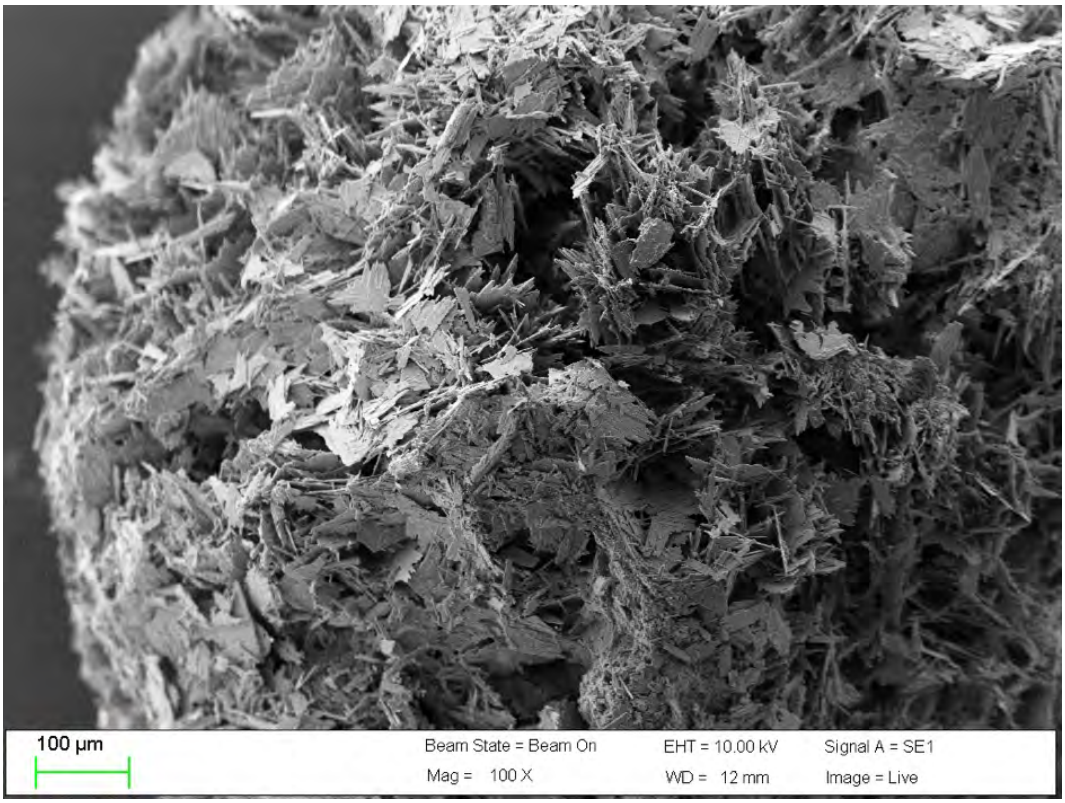

Figure 9.18: SEM image of 120g/L product

Section 5: Alternative process

One stage process mass balance

Fines		Aqueous	
Compound	Flowrate (g/min)	Compound	Flowrate (g/min)
$Mg(OH)_2$	4.6	$MgSO_4$	0.9
$CaSO_4.2H_2O$	9.4	$CaSO_4$	2.5
$Ca(OH)_2$	0.4	$*Na_2$	0.7
		H_2O	621
		$Ca(OH)_2$	1.06
Total	14.4	Total	626

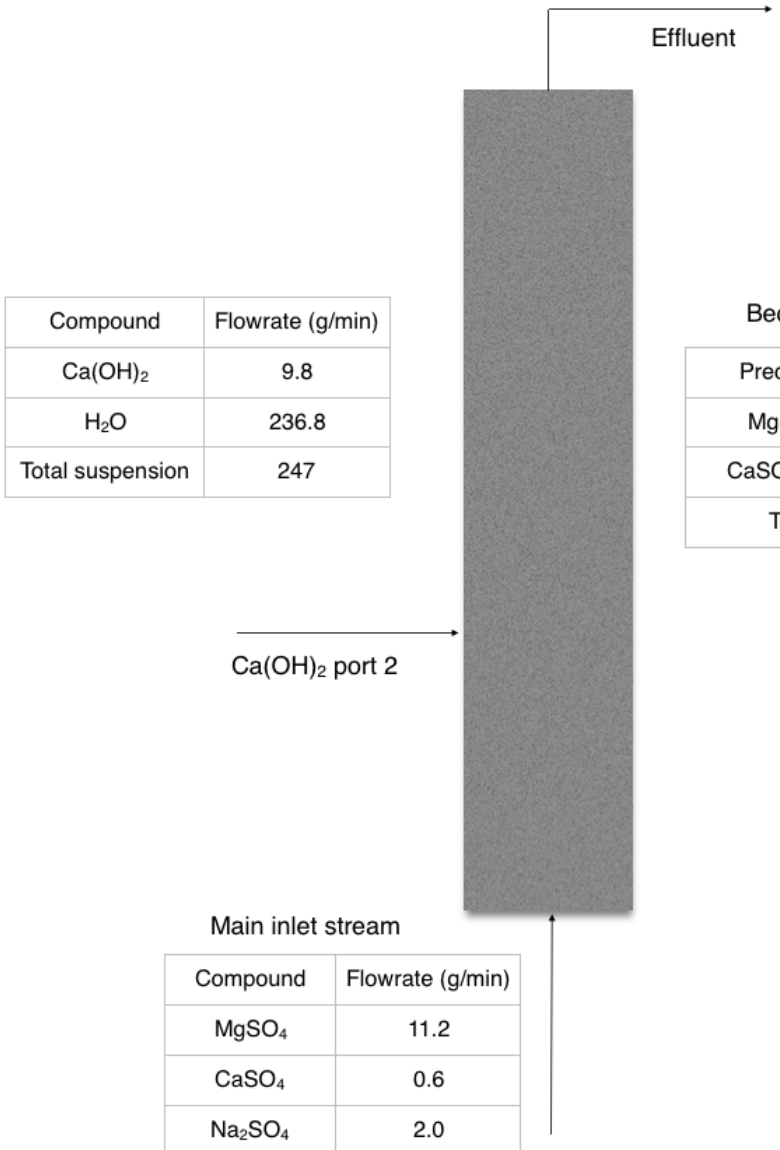

Compound	Flowrate (g/min)
$Ca(OH)_2$	9.8
H_2O	236.8
Total suspension	247

Bed accumulation

Precipitate	Rate
$Mg(OH)_2$	0.2
$CaSO_4.2H_2O$	3.3
Total	3.5

Compound	Flowrate (g/min)
$MgSO_4$	11.2
$CaSO_4$	0.6
Na_2SO_4	2.0
H_2O	386
Total	400

Element	Error g/min
Mg^{2+}	0.06
Ca^{2+}	1.0
SO_4^{2-}	0.3
OH^-	0.5

Two stage process mass balance

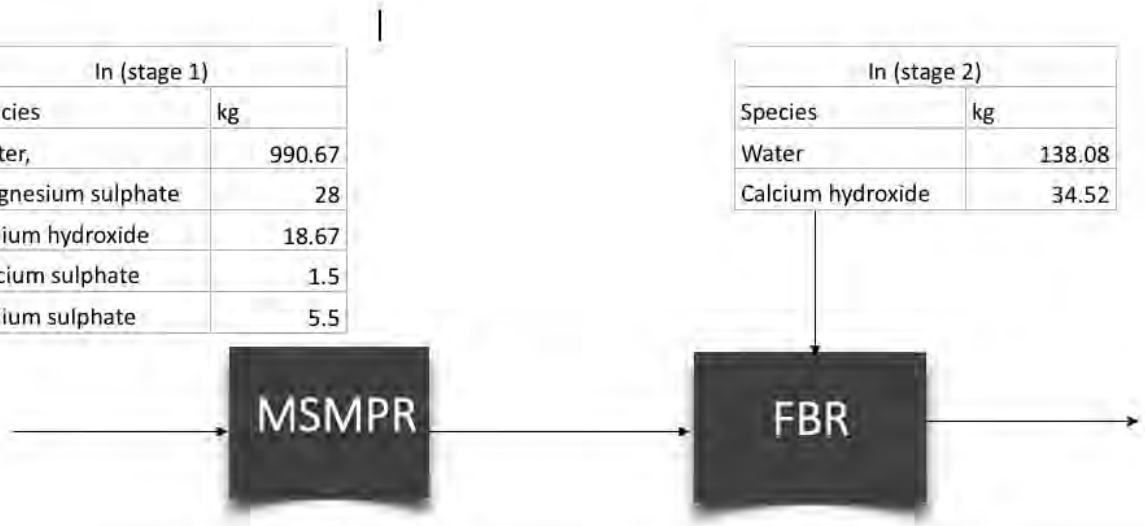

In (stage 1)	
Species	kg
Water,	990.67
Magnesium sulphate	28
Sodium hydroxide	18.67
Calcium sulphate	1.5
Sodium sulphate	5.5

In (stage 2)	
Species	kg
Water	138.08
Calcium hydroxide	34.52

Out (stage 1) fed to stage 2	
Species	kg
Water	9.91E+02
Hydroxide ion(-1)	2.92E-02
Sulphuric(VI) acid	5.57E-26
Bisulphate(VI) ion (-1)	4.27E-09
Magnesium ion(+2)	2.04E-03
Magnesium hydroxide ion(+1)	1.42E-04
Magnesium sulfate	3.93E-06
Sulphur trioxide	4.86E-40
Sulphate ion(-2)	2.23E+01
Sodium ion(+1)	1.07E+01
Hydronium ion(+1)	3.30E-10
Sodium sulphate bisulphate	5.10E-12
NA_3OHSO_4	5.55E-06
Sodium hydroxide	9.53E-09
Magnesium hydroxide (solid)	1.36E+01
Total	1.04E+03

Out (stage 2)	
Species	kg
Water	1.10E+03
Hydroxide ion(-1)	1.98E+00
Sulphuric(VI) acid	1.09E-29
Bisulphate(VI) ion (-1)	4.36E-11
Sodium ion(+1)	1.07E+01
Sulphur trioxide	9.59E-44
Sulphate ion(-2)	1.78E+01
Calcium ion(+2)	3.01E-01
Calcium hydroxide ion(+1)	4.41E-01
Calcium sulfate	8.47E-01
Hydronium ion(+1)	5.36E-12
Sodium sulphate bisulphate	1.73E-14
NA_3OHSO_4	2.32E-04
Sodium hydroxide	6.33E-07
Calcium hydroxide (solid)	2.99E+01
Gypsum	7.14E+00
Total	1.17E+03

Table 9.5: Thermodynamically predicted species for second stage in the alternative treatment process

	total	aqueous	solid
	g/L	g/L	g/L
Water	1052.11	1052.11	
Hydronium ion(+1)	5.06E-12	5.06E-12	
Hydroxide ion(-1)	1.94849	1.94849	
Sulphuric(VI) acid	1.04E-29	1.04E-29	
Bisulphate(VI) ion (-1)	5.21E-11	5.21E-11	
Sodium sulphate bisulphate	4.45E-14	4.45E-14	
NA3OHSO4	2.69E-04	2.69E-04	
Sodium ion(+1)	10.9411	10.9411	
Sodium hydroxide	6.48E-07	6.48E-07	
Sulphur trioxide	9.10E-44	9.10E-44	
Sulphate ion(-2)	18.3162	18.3162	
Calcium ion(+2)	0.288748	0.288748	
Calcium hydroxide ion(+1)	0.318987	0.318987	
Calcium sulphate	0.810701	0.810701	
Calcium hydroxide	21.5486		21.5486
Calcium sulphate dihydrate (Gypsum)	9.01304		9.01304
Total (by phase)	1115.3	1084.74	30.5617

Section 6: Preliminary findings

Figure 9.19: Top region of the bed showing settling particles

Figure 9.20: Gypsum sticking onto the reactor walls

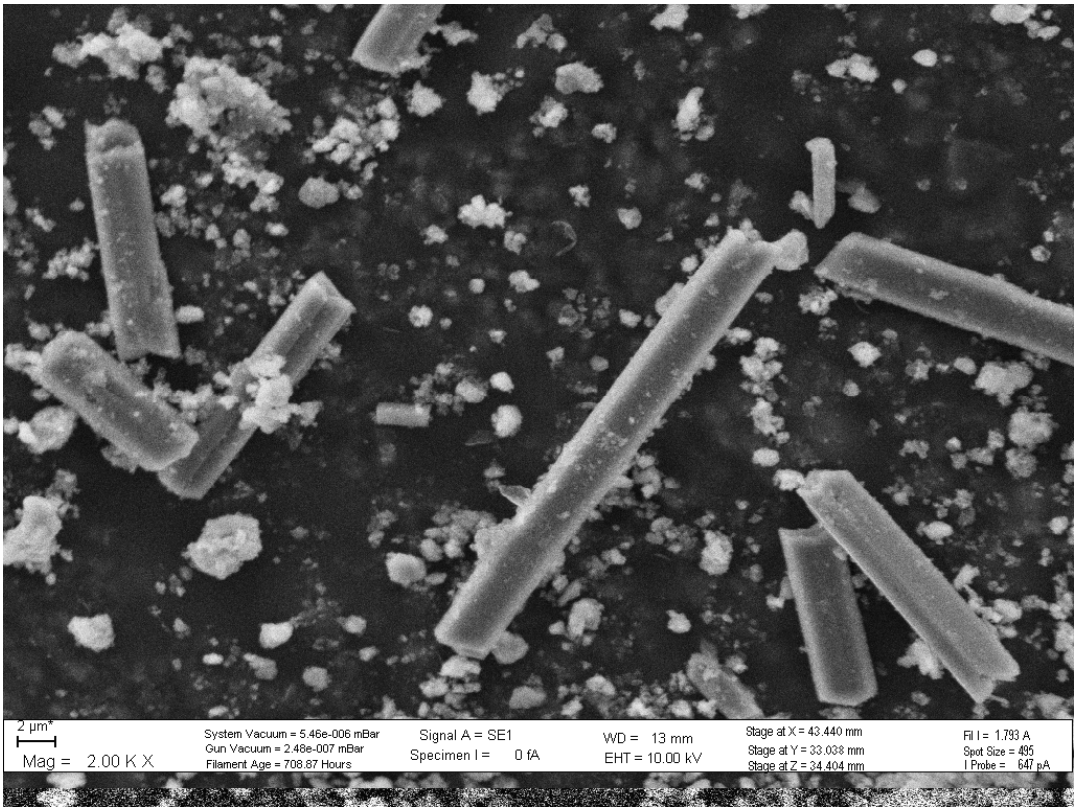

Figure 9.21: SEM images of solids from effluent suspension with continuous calcium hydroxide flow

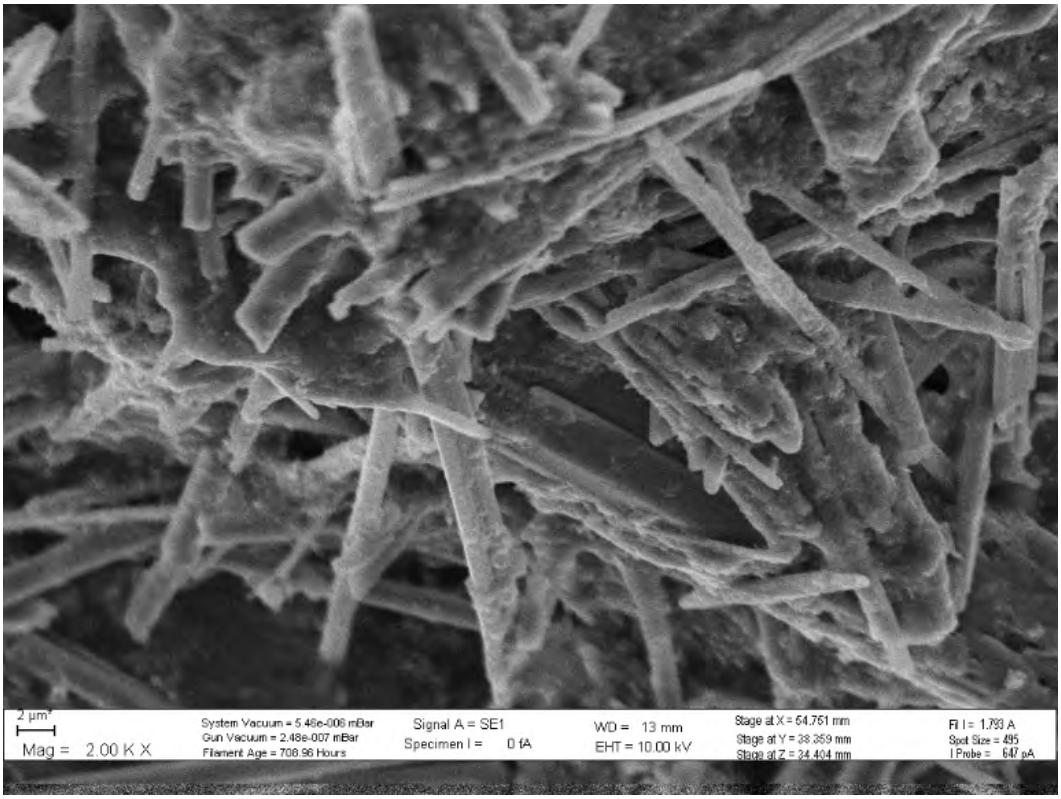

Figure 9.22: SEM image of solid from effluent suspension after calcium hydroxide flow was discontinued

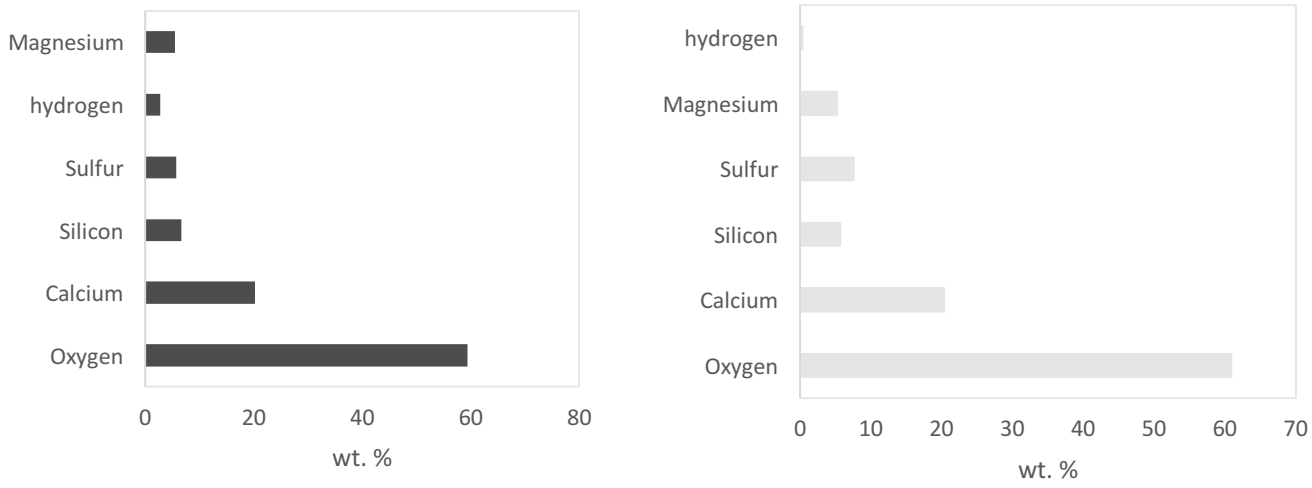

Figure 9.23: Elemental analysis of product composition from SEM- a) top region of the reactor (left) and b) lower region of the reactor (right)

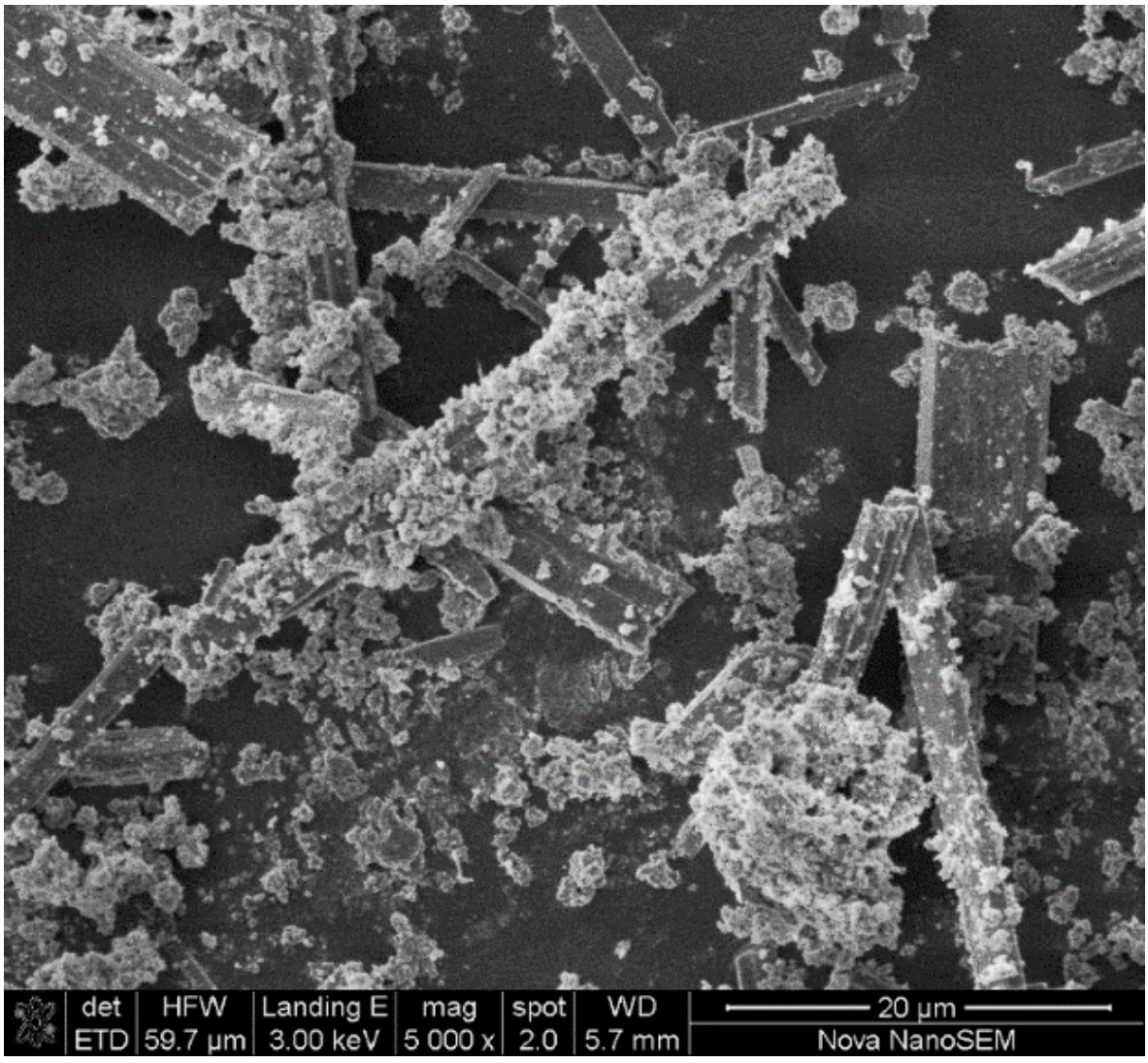

Figure 9.24: SEM image of the obtained image from higher region of reactor

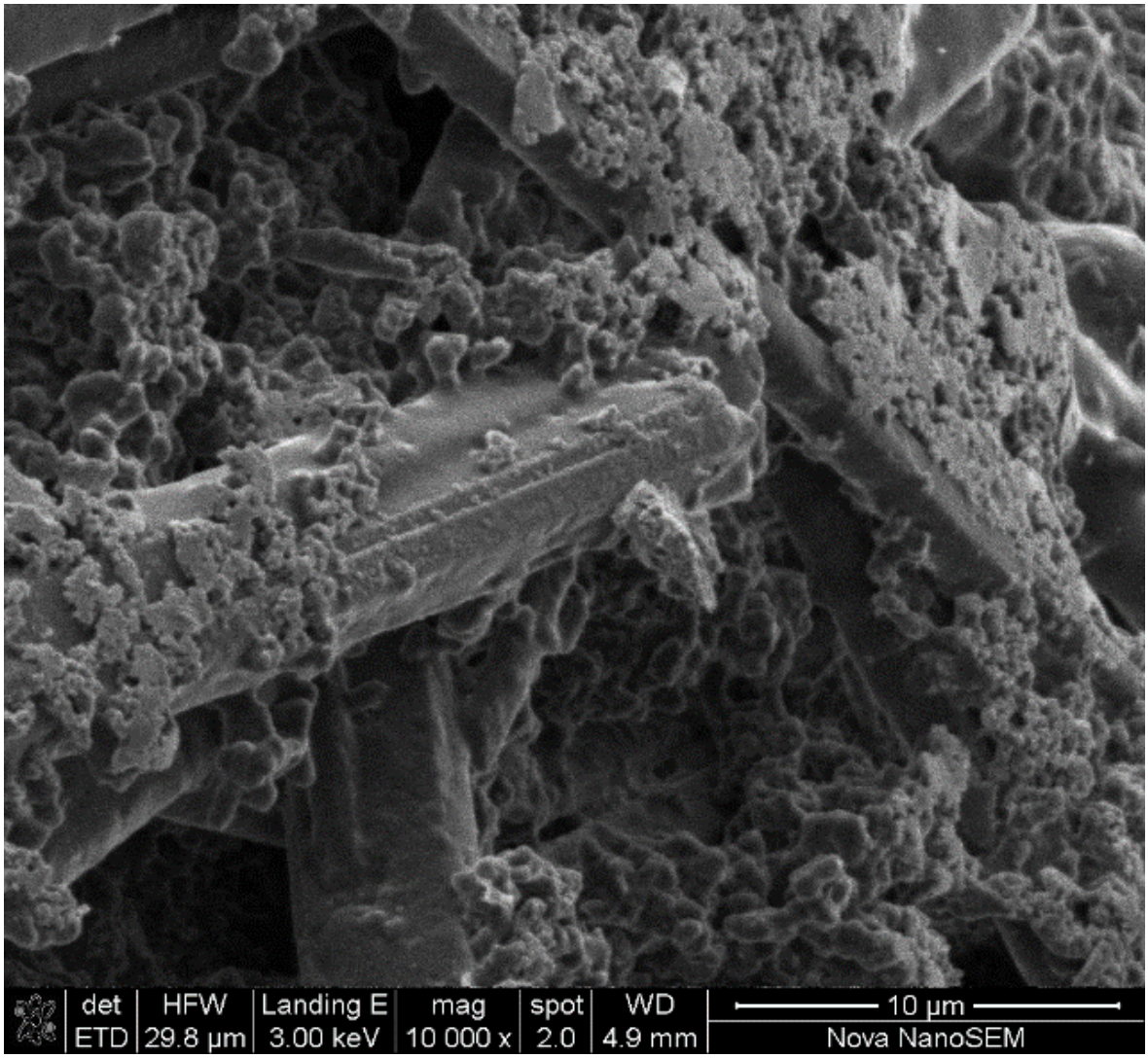

Figure 9.25: SEM image of the obtained product

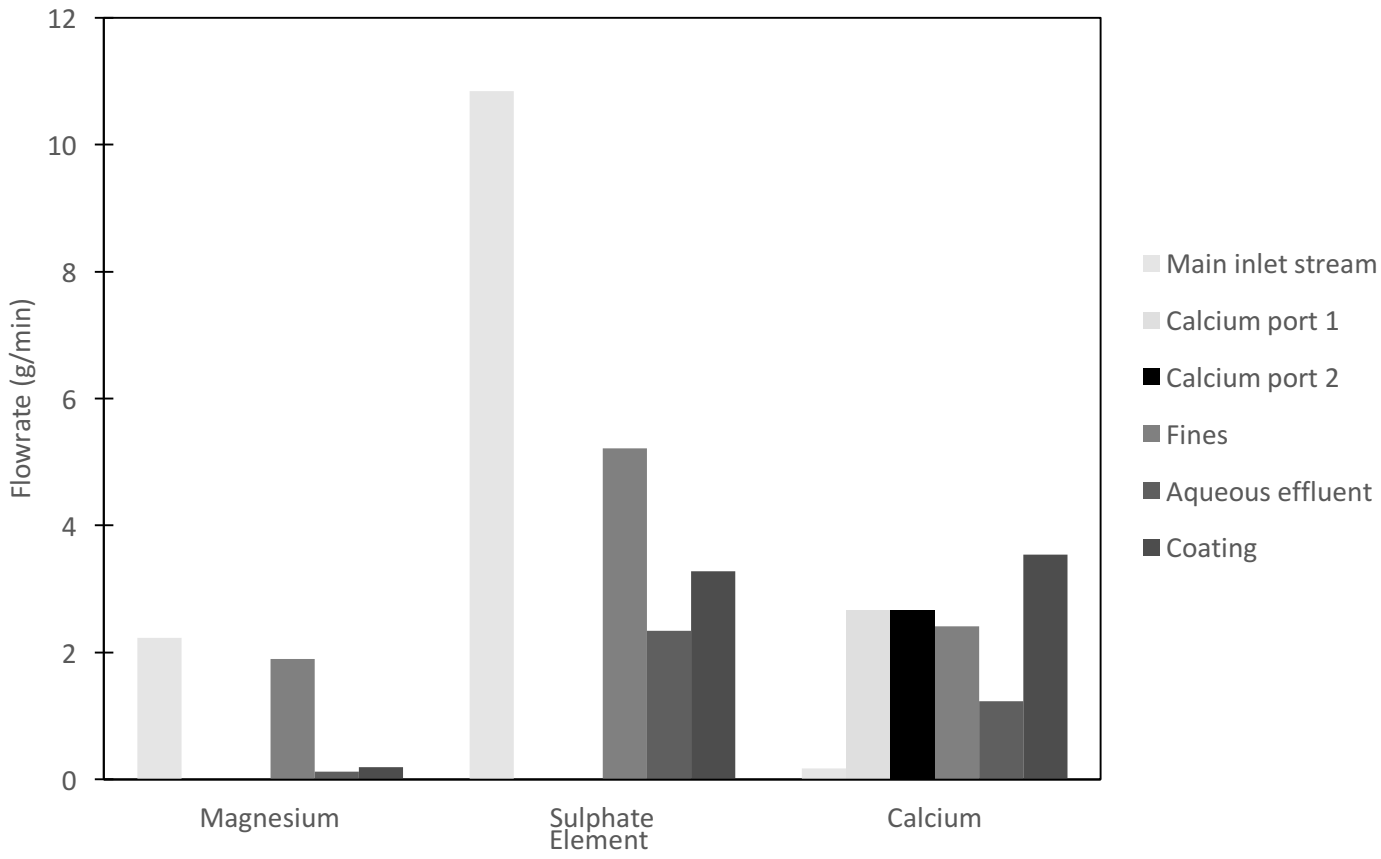

Figure 9.28: Elemental mass balance for 35g/L total salt solution

EBE Faculty: Assessment of Ethics in Research Projects

Any person planning to undertake research in the Faculty of Engineering and the Built Environment at the University of Cape Town is required to complete this form before collecting or analysing data. When completed it should be submitted to the supervisor (where applicable) and from there to the Head of Department. If any of the questions below have been answered YES, and the applicant is NOT a fourth year student, the Head should forward this form for approval by the Faculty EIR committee: submit to Ms Zakiya Chikte (Zakiya.chikte@uct.ac.za); New EBE Building, Ph 021 650 5739).

Please note – It is important to keep a signed copy of this form as students must include a copy of the completed form with the dissertation/thesis when it is submitted for examination.

Name of Principal Researcher/Student: Chiara Maharaj **Department:** Chemical Engineering

If a Student: **Degree:** Msc Eng (Chem Eng) **Supervisor:** Alison Lewis

If a Research Contract indicate source of funding/sponsorship: HOIST

Research Project Title: Treatment of a multicomponent mining effluent using milk of lime in a fluidized bed reactor

Overview of ethics issues in your research project:

Question 1: Is there a possibility that your research could cause harm to a third party (i.e. a person not involved in your project)?	YES	~~NO~~ X
Question 2: Is your research making use of human subjects as sources of data? If your answer is YES, please complete Addendum 2.	YES	~~NO~~ X
Question 3: Does your research involve the participation of or provision of services to communities? If your answer is YES, please complete Addendum 3.	YES	~~NO~~ X
Question 4: If your research is sponsored, is there any potential for conflicts of interest? If your answer is YES, please complete Addendum 4.	YES	~~NO~~ X

If you have answered YES to any of the above questions, please append a copy of your research proposal, as well as any interview schedules or questionnaires (Addendum 1) and please complete further addenda as appropriate.

I hereby undertake to carry out my research in such a way that

- there is no apparent legal objection to the nature or the method of research; and
- the research will not compromise staff or students or the other responsibilities of the University;
- the stated objective will be achieved, and the findings will have a high degree of validity;
- limitations and alternative interpretations will be considered;
- the findings could be subject to peer review and publicly available; and
- I will comply with the conventions of copyright and avoid any practice that would constitute plagiarism.

Signed by:

	Full name and signature	Date
Principal Researcher/Student: Chiara Maharaj		12-02-2016

This application is approved by:

Supervisor (if applicable): Alison Lewis		
HOD (or delegated nominee): Final authority for all assessments with NO to all questions and for all undergraduate research.	C VAN STEEN	16-2-16
Chair : Faculty EIR Committee For applicants other than undergraduate students who have answered YES to any of the above questions.		

ADDENDUM 1:
Please append a copy of the research proposal here, as well as any interview schedules or questionnaires:

ADDENDUM 2: To be completed if you answered YES to Question 2:

It is assumed that you have read the UCT Code for Research involving Human Subjects (available at http://web.uct.ac.za/depts/educate/download/uctcodeforresearchinvolvinghumansubjects.pdf) in order to be able to answer the questions in this addendum.

2.1 Does the research discriminate against participation by individuals, or differentiate between participants, on the grounds of gender, race or ethnic group, age range, religion, income, handicap, illness or any similar classification?	YES	NO
2.2 Does the research require the participation of socially or physically vulnerable people (children, aged, disabled, etc) or legally restricted groups?	YES	NO
2.3 Will you not be able to secure the informed consent of all participants in the research? (In the case of children, will you not be able to obtain the consent of their guardians or parents?)	YES	NO
2.4 Will any confidential data be collected or will identifiable records of individuals be kept?	YES	NO
2.5 In reporting on this research is there any possibility that you will not be able to keep the identities of the individuals involved anonymous?	YES	NO
2.6 Are there any foreseeable risks of physical, psychological or social harm to participants that might occur in the course of the research?	YES	NO
2.7 Does the research include making payments or giving gifts to any participants?	YES	NO

If you have answered YES to any of these questions, please describe how you plan to address these issues (append to form):

ADDENDUM 3: To be completed if you answered YES to Question 3:

3.1 Is the community expected to make decisions for, during or based on the research?	YES	NO
3.2 At the end of the research will any economic or social process be terminated or left unsupported, or equipment or facilities used in the research be recovered from the participants or community?	YES	NO
3.3 Will any service be provided at a level below the generally accepted standards?	YES	NO

If you have answered YES to any of these questions, please describe how you plan to address these issues (append to form)

ADDENDUM 4: To be completed if you answered YES to Question 4

4.1 Is there any existing or potential conflict of interest between a research sponsor, academic supervisor, other researchers or participants?	YES	NO
4.2 Will information that reveals the identity of participants be supplied to a research sponsor, other than with the permission of the individuals?	YES	NO
4.3 Does the proposed research potentially conflict with the research of any other individual or group within the University?	YES	NO

If you have answered YES to any of these questions, please describe how you plan to address these issues(append to form)